جمهورية العراق

وزارة التعليم العالي والبحث العلمي

جامعة بابل

حسابات انتقال الحرارة للجريان الطبائقي المستقر المتطوّر بين صفيحتين متوازيتين

رسالة مقدمة إلى كلية الهندسة في جامعة بابل وهي جزء من متطلبات نيل درجة الماجستير علوم في الهندسة الميكانيكية

من قبل المهندس

أحمد علي شاكر

م٢٠٠٦ هـ١٤٢٧

Republic of Iraq
Ministry of Higher Education
And Scientific Research
University of Babylon

بسم الله الرحمن الرحيم

HEAT TRANSFER CHARACTERISTICS IN NON-DEVELOPED STEADY LAMINAR FLOW BETWEEN PARALLEL PLATES

A thesis

Submitted to the College of Engineering

University of Babylon in Partial Fulfillment of the Requirements for The degree of Master of Science in Mechanical Engineering

By

AHMED ALI SHAKER

(B. Sc)

١٤٢٧ HIJRI ٢٠٠٦ AC

Abstract

In the present work, developing laminar flow of a Newtonian incompressible fluid and heat transfer in the entrance region of a two parallel plate channel were investigated. The continuity, x-momentum, and energy equations were solved as a steady state in two dimension equations. The dimensionless technique was used. These equations have been represented by finite difference technique. This model has been solved by using the new method of implicit scheme, which would minimize the solution errors.

A computer program in QuickBasic Language was built to perform the numerical solution for constant wall temperature, and constant wall heat flux boundary conditions. The Gaussian elimination method which is to be used, eliminates the need to assume the shape of the velocity and temperature profiles. This approach provides a picture of the variation of the velocity and temperature within the entire channel.

The study was made for five values of Reynolds number (Re=١٠٠, Re=٥٠٠, Re=١٠٠٠, Re=١٥٠٠ and Re=٢٠٠٠) and for four values of Prandtl number (Pr=٠.٧, Pr=١, Pr=١.٢ and Pr=٦) for parallel plate channel, and for both case: Constant Wall Temperature and Constant Heat Flux respectively. The effects of heat conduction, body force, free convection, heat generation and viscous dissipation within the fluid are neglected. The study was made for the upper part of duct only because of the symmetry and a regular computational grid (ΔX = ΔY = constant) was used.

The shape of the velocity and temperature profiles seem to be consistent with available theoretical results. The velocity profile becomes fully developed at approximately $\frac{L_e}{2a} = 0.05\,\mathrm{Re}$, and the temperature distribution becomes fully developed at approximately $\frac{L_{et}}{2a} = 0.05\,\mathrm{Re}.\mathrm{Pr}$, as expected. The shape of the fully developed dimensionless temperature distribution θ(X,Y) differs according to whether a constant wall temperature or heat flux is maintained. The computational algorithm is able to calculate all the hydrodynamic properties such as velocities. Also the computational algorithm is able to predict all the thermal properties such as the temperature, bulk temperature, and local Nusselt number. The validity of thermal results for constant wall temperature and constant wall heat flux is verified and shows that there is a good agreement between the results of the present numerical solution and the correlation related to it.

ACKNOWLEDGMENTS

(In The Name of Allah, The Gracious and Merciful)

First of all, I would like to express my deep thanks and gratitude to my supervisors, Dr. Tahseen A. Al-Hattab & Dr. Adil A. Al-Moosawy for their great support, guidance, advice and assistance throughout the various stages of the present work.

I would like also to thank all staff of mechanical engineering department for their kind help and invaluable advice.

I record my sincere gratitude to my family and to my friends for their encouragement and support during the period of preparing this work.

Finally, I am grateful to all those who have helped me in carrying out this research.

A.A.Shaker

٢٠٠٦

الخلاصة

يتضمن البحث الحالي دراسة نظرية للجريان الطبائقي غير تام التطوّر لمائع غير قابل للانضغاط (يخضع لقوانين نيوتن) وانتقال الحرارة لمنطقة النمو (Entrance Region) خلال مجرى متكون من صفيحتين متوازيتين. تم الحل لمعادلة الاستمرارية و معادلة الزخم باتجاه المحور السيني و معادلة الطاقة للحالة المستقرة ذات البعدين. تم استخدام تقنية الحل اللابعدي (Dimensionless). هذه المعادلات مُثلت بتقنية الفروقات المحددة (Finite Difference Technique). هذا النموذج حُلَّ باستخدام طريقة جديدة (implicit scheme), التي تقلل من أخطاء الحل.

تم بناء برنامج بإستخدام لغة (QuickBasic) لإنجاز الحل العددي لحالتين من الشروط الحدودية الحرارية: حالة بثبوت درجة حرارة الجدار و الأخرى بثبوت الفيض الحراري للجدار. تم استعمال طريقة (Gaussian elimination) حيث لا نحتاج لفرض شكل توزيع السرع و درجات الحرارة ضمن المجرى (لا نحتاج لإعطاء قيم أولية للشبكة العقدية الداخلية). علاوة على ذلك هذا الأسلوب يعطينا صورة لاختلاف السرع و درجات الحرارة ضمن كامل المجرى.

أجريت الدراسة لخمس قيم من أرقام رينولدز (Re=١٠٠, Re=٥٠٠, Re=١٠٠٠, Re=١٥٠٠, Re=٢٠٠٠) و لأربع قيم من أرقام برانتل (Pr=٠.٧, Pr=١, Pr=١.٢, Pr=٦) للمجرى المتكون من صفيحتين متوازيتين ولحالتين من الشروط الحدودية: حالة بثبوت درجة حرارة الجدار والأُخرى بثبوت الفيض الحراري للجدار. تم إهمال تأثير كل من انتقال الحرارة بالتوصيل و قوة الجسم (body force) و انتقال الحرارة بالحمل الحر و الحرارة المتولدة و تشتت اللزوجة للمائع. أجريت الدراسة للجزء العلوي من المجرى فقط بسبب التناظر وقد تم استعمال شبكة عقدية متساوية بكلا الاتجاهين.

شكل السرع و درجات الحرارة تبدو متفقة مع النتائج النظرية المتوفرة. شكل توزيع السرع يصبح كامل النمو عند حوالي ($\frac{L_e}{2a} = 0.05\,\mathrm{Re}$) وشكل توزيع درجات الحرارة يصبح كامل النمو عند حوالي ($\frac{L_{et}}{2a} = 0.05\,\mathrm{Re}.\mathrm{Pr}$), كما متوقع. شكل توزيع درجات الحرارة (اللابعدية) في منطقة النمو الكامل تختلف باللأعتماد على الشرط الحدي إذا بثبوت درجة حرارة السطح أو بثبوت الفيض الحراري للسطح. إمكانية الحل العددي تتضمن حساب جميع الصفات الهيدروديناميكية مثل منحنيات السرعة, و كذلك تتضمن إمكانية الحل العددي القدرة على تنبؤ جميع الصفات الحرارية مثل توزيع درجات الحرارة

و متوسط درجة الحرارة و رقم نسلت الموضعي. تم التأكد من صحَّة

النتائج الحرارية لحالة التسخين بثبوت درجة حرارة الجدار و ثبوت الفيض الحراري للجدار حيث كان هنالك توافق جيد بين الحل العددي الحالي والعلاقات التجريبية و النظرية المتعلقة به لباحثين سابقين.

THE COMMITTEE CERTIFICATE

We certify that we have read this thesis, entitled **"Heat Transfer Calculation Non-Developed Steady Laminar Flow Between Parallel Plates",** and as examining committee, examined the student *"***Ahmed Ali Shaker***"* in its contents and in what is connected with it, and that in our opinion it meets the standard of a thesis for the degree of Master of Science in Mechanical Engineering.

Signature:
Name: Assist Professor
Dr. Majid H. Majeed
(Member)
Date: / /٢٠٠٦

Signature:
Name: Lecture
Dr. **Falah Kaify Matlowb**
(Member)
Date: / /٢٠٠٦

Signature:
Name: Assist Professor
Dr**. Tahseen A. Al-Hattab**
(Supervisor)
Date: / /٢٠٠٦

Signature:
Name: Assist Professor
Dr**. Adil A. Al-Moosawy**
(Supervisor)
Date: / /٢٠٠٦

Signature:
Name: Assist Professor
Dr. **Haroun A.K. Shahad**
(Chairman)
Date: / /٢٠٠٦

Approval of the Mechanical Engineering Department.
Head of the Mechanical Engineering Department
Signature:
Name: Assist Professor
Dr. **Adil A. Al-Moosawy**

Approval of the Deanery of the College of Engineering.
Dean of the College of Engineering
Signature:
Name: Professor
Dr. **Abd Al-Wahid K. Rajih**
Date: / /٢٠٠٦

Date: / /٢٠٠٦

Certification

We certify that this thesis entitled "**Heat Transfer Calculation Non-Developed Steady Laminar Flow Between Parallel Plates**" which is prepared by "**Ahmed Ali Shaker**" had been carried out completely under our supervision at Babylon University in partial fulfillment of the requirements for the degree of Master of Science in Mechanical Engineering.

Signature: Signature:

Name: Asst. Prof. Name: Asst. Prof.

Dr. Tahseen A. Al-Hattab Dr. Adil A. Al-Moosawy

Date: / /٢٠٠٦ Date: / /٢٠٠٦

LIST OF CONTENTS

LIST OF SYMBOLS

The following symbols are used generally throughout the text. Other are defined as when used.

Symbol	Definition	Unit
a	The Distance Between Centerline and Wall of Duct	*m*
C.H.F	Constant Heat Flux	——
C.W.T	Constant Wall Temperature	——
d	The Distance Between Two Parallel Plate Channel	*m*
D	Diameter of Circular Duct	*m*
h	Heat Transfer Coefficient	W/m^2K
k	Thermal Conductivity	*W/mK*
L	Length of Channel	*m*
L_e	Hydrodynamic Entry Length	*m*
L_{et}	Thermal Entry Length	*m*
m	Number of Grid Nodes in the Axial Direction	——
n	Number of Grid Nodes in the Vertical Direction	——
Nu	Nusselt Number	——
Nu_x	Local Nusselt Number	——
p	Pressure	N/m^2
P	Dimensionless Pressure	——
Pr	Prandtl Number	——
Q	Heat Transfer Rate	*W*
$q_s^{"}$	Heat Flux	W/m^2
r	Radial Direction of Circular Duct	*m*
Re	Reynolds Number	——
T	Temperature	^oc
T_b	Bulk Temperature	^oc
θ	Dimensionless Temperature	——
θ_b	Dimensionless Bulk Temperature	——
u	Velocity in Axial Direction	*m/s*
U	Dimensionless Velocity in Axial Direction	——
v	Velocity in Vertical Direction	*m/s*
V	Dimensionless Velocity in Vertical Direction	——
x	Axial Direction of the Duct	*m*
X	Dimensionless Axial Direction of the Duct	——
Δx	The Distance Between Two Nodal Points in the Axial Direction	*m*
ΔX	The Dimensionless Distance Between Two Nodal	____

	Points in the Axial Direction	
y	Vertical Direction of the Duct	*m*
Y	Dimensionless Vertical Direction of the Duct	——
Δy	The Distance Between Two Nodal Points in the Vertical Direction	*m*
ΔY	The Dimensionless Distance Between Two Nodal Points in the Vertical Direction	——

Greek Symbols

Symbol	Definition	Unit
α	Thermal Diffusivity	m^2/s
ν	Kinematic Viscosity	m^2/s
μ	Dynamic Viscosity	$N.s/m^2$
ρ	Density of Fluid	kg/m^2
c_p	Specific Heat at Constant Pressure	*J/kg.K*
δ	Hydrodynamic Boundary Layer Thickness	*m*
δ_t	Thermal Boundary Layer Thickness	*m*

Subscripts

Symbol	Definition	Unit
i, j	The Index Increment Along the Axial and Vertical Direction	——
o	Inlet	——
w	Refers to Wall	——
s^1	Refers to First Surface	——
s^2	Refers to Second Surface	——

APPENDIX -A

SOLUTION FOR A SET OF LINEAR ALGEBRAIC EQUATIONS HAVING A TRIDIAGONAL MATRIX OF COEFFICIENTS

The matrix of coefficients of a set of linear algebraic equations is classified as tridiagonal if it consists of a band of nonzero elements centered on the main diagonal and three elements wide, and if the remaining elements of the matrix are zero. A set of equations of this type may be written as

$$\begin{vmatrix} 1 & 2 & 2 & 2 & 2 & 2 & 0 \\ \beta_0 & \Omega_0 & & & & & 1/\Delta X \\ \varepsilon_1 & \beta_1 & \Omega_1 & & & & 1/\Delta X \\ & \varepsilon_2 & \beta_2 & \Omega_2 & & & 1/\Delta X \\ & & \varepsilon_3 & \beta_3 & \Omega_3 & & 1/\Delta X \\ & & & \varepsilon_4 & \beta_4 & \Omega_4 & 1/\Delta X \\ & & & & \varepsilon_5 & \beta_5 & 1/\Delta X \end{vmatrix} \times \begin{vmatrix} U_{i+1,0} \\ U_{i+1,1} \\ U_{i+1,2} \\ U_{i+1,3} \\ U_{i+1,4} \\ U_{i+1,5} \\ P_{i+1} \end{vmatrix} = \begin{vmatrix} S \\ \Phi_0 \\ \Phi_1 \\ \Phi_2 \\ \Phi_3 \\ \Phi_4 \\ \Phi_5 \end{vmatrix} \quad \ldots(A.١)$$

Before continuing with the specific case of a tridiagonal set of equations, we will briefly discuss in general the Gaussian elimination method which is to be used.

The objective of Gaussian elimination, which is a commonly employed and highly efficient method of solving sets of linear equations, is to transform the matrix of coefficients of the set into an upper triangular form (i.e., a form in which all elements below the main diagonal are zero). This may be accomplished by the operations of multiplying or dividing any equation by a constant and adding or subtracting any equation from any other equation. This upper triangular set has the form

$$\begin{vmatrix} R_{11} & R_{12} & R_{13} & R_{14} & R_{15} & R_{16} & R_{17} \\ & R_{22} & R_{23} & R_{24} & R_{25} & R_{26} & R_{27} \\ & & R_{33} & R_{34} & R_{35} & R_{36} & R_{37} \\ & & & R_{44} & R_{45} & R_{46} & R_{47} \\ & & & & R_{55} & R_{56} & R_{57} \\ & & & & & R_{66} & R_{67} \\ & & & & & & R_{77} \end{vmatrix} \times \begin{vmatrix} U_{i+1,0} \\ U_{i+1,1} \\ U_{i+1,2} \\ U_{i+1,3} \\ U_{i+1,4} \\ U_{i+1,5} \\ P_{i+1} \end{vmatrix} = \begin{vmatrix} Z_1 \\ Z_2 \\ Z_3 \\ Z_4 \\ Z_5 \\ Z_6 \\ Z_7 \end{vmatrix} \quad \ldots(A.٢)$$

The last equation may then be solved directly for ($P_{i+١}$), the next to the last for ($U_{i+١,٥}$) once ($P_{i+١}$) has been found, etc… continuing the back substitution until the top equation is finally solved for (U_o) .

Equations of the form (A.١) are particularly easy to put into the form (A.٢). A number of the necessary operations will be performed on equation (A.١) to illustrate the method and then generalized to a recurrence scheme highly suitable for a digital computer. First, $\beta_0 R_1 - R_2$

Where R١=first row and R٢=second row

$$\begin{vmatrix} 1 & 2 & 2 & 2 & 2 & 2 & 0 \\ 0 & A_1 & B_1 & B_1 & B_1 & B_1 & D_1 \\ \varepsilon_1 & \beta_1 & \Omega_1 & & & & 1/\Delta X \\ & \varepsilon_2 & \beta_2 & \Omega_2 & & & 1/\Delta X \\ & & \varepsilon_3 & \beta_3 & \Omega_3 & & 1/\Delta X \\ & & & \varepsilon_4 & \beta_4 & \Omega_4 & 1/\Delta X \\ & & & & \varepsilon_5 & \beta_5 & 1/\Delta X \end{vmatrix} \times \begin{vmatrix} U_{i+1,0} \\ U_{i+1,1} \\ U_{i+1,2} \\ U_{i+1,3} \\ U_{i+1,4} \\ U_{i+1,5} \\ P_{i+1} \end{vmatrix} = \begin{vmatrix} S \\ E_1 \\ \Phi_1 \\ \Phi_2 \\ \Phi_3 \\ \Phi_4 \\ \Phi_5 \end{vmatrix} \quad \ldots(A.٣)$$

where

$$A_1 = 2\beta_0 - \Omega_0$$

$$B_1 = 2\beta_0$$

or $D_1 = -C \; D_1 = -1/\Delta X$

$$E_1 = S\beta_0 - \Phi_0$$

second, $\varepsilon_1 R_1 - R_3$

Where R ١=first row and R ٣=third row

$$\begin{vmatrix} & \textbf{A-٢} & 2 & 2 & 2 & 2 & 0 \\ 0 & A_1 & B_1 & B_1 & B_1 & B_1 & D_1 \\ 0 & f_1 & g_1 & q_1 & q_1 & q_1 & h_1 \\ & \varepsilon_2 & \beta_2 & \Omega_2 & & & 1/\Delta X \\ & & \varepsilon_3 & \beta_3 & \Omega_3 & & 1/\Delta X \\ & & & \varepsilon_4 & \beta_4 & \Omega_4 & 1/\Delta X \\ & & & & \varepsilon_5 & \beta_5 & 1/\Delta X \end{vmatrix} \times \begin{vmatrix} U_{i+1,0} \\ U_{i+1,1} \\ U_{i+1,2} \\ U_{i+1,3} \\ U_{i+1,4} \\ U_{i+1,5} \\ P_{i+1} \end{vmatrix} = \begin{vmatrix} S \\ E_1 \\ w_1 \\ \Phi_2 \\ \Phi_3 \\ \Phi_4 \\ \Phi_5 \end{vmatrix} \quad \text{...(A.٣)}$$

where

$$f_1 = 2\varepsilon_1 - \beta_1$$

$$g_1 = 2\varepsilon_1 - \Omega_1$$

or $h_1 = -C \; h_1 = -1/\Delta X$

$$w_1 = S\varepsilon_1 - \Phi_1$$

third, $f_1 R_2 - A_1 R_3$

Where R ٢=second row and R ٣=third row

$$\begin{vmatrix} 1 & 2 & 2 & 2 & 2 & 2 & 0 \\ 0 & A_1 & B_1 & B_1 & B_1 & B_1 & D_1 \\ 0 & 0 & A_2 & B_2 & B_2 & B_2 & D_2 \\ & \varepsilon_2 & \beta_2 & \Omega_2 & & & 1/\Delta X \\ & & \varepsilon_3 & \beta_3 & \Omega_3 & & 1/\Delta X \\ & & & \varepsilon_4 & \beta_4 & \Omega_4 & 1/\Delta X \\ & & & & \varepsilon_5 & \beta_5 & 1/\Delta X \end{vmatrix} \times \begin{vmatrix} U_{i+1,0} \\ U_{i+1,1} \\ U_{i+1,2} \\ U_{i+1,3} \\ U_{i+1,4} \\ U_{i+1,5} \\ P_{i+1} \end{vmatrix} = \begin{vmatrix} S \\ E_1 \\ E_2 \\ \Phi_2 \\ \Phi_3 \\ \Phi_4 \\ \Phi_5 \end{vmatrix} \quad \text{...(A.٤)}$$

where

$$A_2 = f_1 B_1 - A_1 g_1$$

$$B_2 = f_1 B_1 - A_1 q_1$$

$$D_2 = f_1 D_1 - A_1 h_1$$

$$E_2 = f_1 E_1 - A_1 w_1$$

These operations may be repeated for all equations, and the resulting set is of the form

$$\begin{vmatrix} 1 & 2 & 2 & 2 & 2 & 2 & 0 \\ A_1 & B_1 & B_1 & B_1 & B_1 & D_1 \\ 0 & A_2 & B_2 & B_2 & B_2 & D_2 \\ 0 & 0 & 0 & A_3 & B_3 & B_3 & D_3 \\ 0 & 0 & 0 & 0 & A_4 & B_4 & D_4 \\ 0 & 0 & 0 & 0 & 0 & A_5 & D_5 \\ 0 & 0 & 0 & 0 & 0 & 0 & D_6 \end{vmatrix} \times \begin{vmatrix} U_{i+1,0} \\ U_{i+1,1} \\ U_{i+1,2} \\ U_{i+1,3} \\ U_{i+1,4} \\ U_{i+1,5} \\ P_{i+1} \end{vmatrix} = \begin{vmatrix} S \\ E_1 \\ E_2 \\ E_3 \\ E_4 \\ E_5 \\ E_6 \end{vmatrix} \quad \ldots(A.٥)$$

The last equation of (A-٥) is

$$P_{i+1} = \frac{E_6}{D_6} \quad \ldots(A.٦)$$

Back substitution into the next to last equation yields

$$U_{i+1,5} = \frac{E_5 - D_5 * P_{i+1}}{A_5} \quad \ldots(A.٧)$$

All of the remaining equations yield a similar relation.

If the order just discussed is followed, then the method has the great advantage that all of the initially zero elements off of the tridiagonal band in (A.١) remain zero throughout all operations. As a result, these elements do not require storage space on a digital computer; thus, the only storage space required is for the tridiagonal band and the unknown and right side column vectors. The total storage space required is therefore (٥n-٢) locations rather

than the ($n^{۲}+۲n$) required for a complete matrix representation. In addition, the diagonals (ε_j , β_j), and (Ω_j) may be represented as vectors rather than as elements of a matrix. This eliminates the necessity of using matrix subscripts, which with many algebraic programming systems requires additional operations and hence, additional computer time. The most important time saving with this method, however, is brought about by the fact that the number of necessary operations is of б(n), whereas for the usual Gaussian elimination for a filled matrix, the number of operations is of б($n^{۳}$).

With the relatively well-conditioned sets of equations which result from finite difference representations, sets of equations with n of the order of several hundred may be readily and accurately handled using this method.

References

[A-١] Hornbeck, R.W., "Numerical Marching Techniques for Fluid Flows with Heat Transfer", National Aeronautics and Space Administration, Washington, ١٩٧٣.

APPENDIX -B

A-٥

FINITE DIFFERENCE REPRESENTATIONS

The foundation of all numerical analysis, and particularly of finite difference methods, is the Taylor series. A function ***H***(x) may be expanded in a Taylor series near $x=x_o$ if ***H*** and all of its derivatives exist and are finite near $x=x_o$. The infinite series expression is

$$H(x) = H(x_0) + (x - x_0)\frac{dH}{dx}\bigg|_{x=x_0} + \frac{(x - x_0)^2}{2!}\frac{d^2H}{dx^2}\bigg|_{x=x_0} + \frac{(x - x_0)^3}{3!}\frac{d^3H}{dx^3}\bigg|_{x=x_0} + \ldots\ldots$$

...(B.١)

The results may be directly extended to functions of many variables. The following notation will be employ:

$$\left.\begin{aligned} x - x_o &= \Delta x \\ H(x) = H(x_o + \Delta x) &= H_{i+1} \\ H(x_o) &= H_i \\ \left.\frac{dH}{dx}\right|_{x_o} &= \left.\frac{dH}{dx}\right|_i, etc. \end{aligned}\right\} \quad \text{...(B.٢)}$$

Equation (B.١) may then be rewritten as

$$\text{...(B.٣)}\ H_{i+1} = H_i + \Delta x \left.\frac{dH}{dx}\right|_i + \frac{(\Delta x)^2}{2!}\left.\frac{d^2H}{dx^2}\right|_i + \frac{(\Delta x)^3}{3!}\left.\frac{d^3H}{dx^3}\right|_i + \text{.....}$$

Can be obtain an expression for $\left.\frac{dH}{dx}\right|_i$ by solving equation (B.٣) for this quantity:

$$\text{...(B.٤)}\ \left.\frac{dH}{dx}\right|_i \quad \text{B-١} \quad \text{ـ٤} \quad \frac{-H_i}{} - \frac{\Delta x}{2!}\left.\frac{d^2H}{dx^2}\right|_i - \frac{(\Delta x)^2}{3!}\left.\frac{d^3H}{dx^3}\right|_i + \text{.....}$$

If only values of ***H*** are known, but not any of its derivatives, then equation (B.٤) provides an approximation to $\left.\frac{dH}{dx}\right|_i$ if neglect all terms involving higher derivatives of ***H*** . Since Δx is small and the derivatives of ***H*** are finite (but unknown), the dominant error term in equation (B.٤) will presumably be $\frac{\Delta x}{2}\left.\frac{d^2H}{dx^2}\right|_i$. Since the only part of the term which is under our control is Δx.

$$\text{...(B.٥)}\ \left.\frac{dH}{dx}\right|_i = \frac{H_{i+1} - H_i}{\Delta x} + \sigma(\Delta x)$$

where б(Δx) is interpreted as of order Δx. The term (H_{i+1}-H_i)/Δx is called a forward difference representation of $\left.\frac{dH}{dx}\right|_i$ of error order Δx .

By define

$$H_{i-1} = H(x_o - \Delta x) \quad \text{...(B.٦)}$$

and express H_{i-1} by a Taylor series expansion around x_o , obtain

$$H_{i-1} = H_i - \Delta x \left.\frac{dH}{dx}\right|_i + \frac{(\Delta x)^2}{2!}\left.\frac{d^2H}{dx^2}\right|_i - \frac{(\Delta x)^3}{3!}\left.\frac{d^3H}{dx^3}\right|_i + \ldots.. \quad \text{...(B.٧)}$$

Solving this equation for $\left.\frac{dH}{dx}\right|_i$ gives

$$\left.\frac{dH}{dx}\right|_i = \frac{H_i - H_{i-1}}{\Delta x} + \frac{\Delta x}{2!}\left.\frac{d^2H}{dx^2}\right|_i - \frac{(\Delta x)^2}{3!}\left.\frac{d^3H}{dx^3}\right|_i + \ldots.. \quad \text{...(B.٨)}$$

$$\text{or} \quad \left.\frac{dH}{dx}\right|_i = \frac{H_i - H_{i-1}}{\Delta x} + \sigma(\Delta \text{ג}, \quad \text{...(B.٩)}$$

The expression (H_i-H_{i-1})/Δx is called the backward difference expression of error order Δx for $\left.\frac{dH}{dx}\right|_i$

If equation (B.٧) is subtracted from equation (B.٣), obtain

$$H_{i+1} - H_{i-1} = 2(\Delta x)\left.\frac{dH}{dx}\right|_i + \frac{2(\Delta x)^3}{3!}\left.\frac{d^3H}{dx^3}\right|_i + \ldots.. \quad \text{...(B.١٠)}$$

Solving for $\left.\frac{dH}{dx}\right|_i$

$$\left.\frac{dH}{dx}\right|_i = \frac{H_{i+1} - H_{i-1}}{2(\Delta x)} - \frac{(\Delta x)^2}{3!}\left.\frac{d^3H}{dx^3}\right|_i - \frac{(\Delta x)^4}{5!}\left.\frac{d^5H}{dx^5}\right|_i + \ldots\ldots \quad \text{...(B.١١)}$$

or $$\left.\frac{dH}{dx}\right|_i = \frac{H_{i+1} - H_{i-1}}{2(\Delta x)} + \sigma((\Delta x)^2) \quad \text{...(B.١٢)}$$

The expression (H_{i+1}-H_{i-1})/٢(Δx) is called a central difference expression of error order $(\Delta x)^2$ for $\left.\frac{dH}{dx}\right|_i$. Since Δx is small, the central difference expression (B.١٢) is more accurate than either the forward (B.٥) or backward (B.٨) difference expressions for $\left.\frac{dH}{dx}\right|_i$, assuming a fixed Δx .

The solving require only one type of difference expression for the second derivative. This may be found by equating the expressions for $\left.\frac{dH}{dx}\right|_i$

from equations (B.٤) and (B.٨):

$$\frac{H_{i+1} - H_i}{\Delta x} - \frac{\Delta x}{2!}\left.\frac{d^2H}{dx^2}\right|_i - \frac{(\Delta x)^2}{3!}\left.\frac{d^3H}{dx^3}\right|_i - \frac{(\Delta x)^3}{4!}\left.\frac{d^4H}{dx^4}\right|_i + \ldots\ldots\ldots$$

$$= \frac{H_i - H_{i-1}}{\Delta x} + \frac{\Delta x}{2!}\left.\frac{d^2H}{dx^2}\right|_i - \frac{(\Delta x)^2}{3!}\left.\frac{d^3H}{dx^3}\right|_i + \frac{(\Delta x)^3}{4!}\left.\frac{d^4H}{dx^4}\right|_i + \ldots\ldots \quad \text{...(B.١٣)}$$

Solving for $\left.\frac{d^2H}{dx^2}\right|_i$ gives

$$\left.\frac{d^2H}{dx^2}\right|_i = \frac{H_{i+1} - 2H_i + H_{i-1}}{(\Delta x)^2} - \frac{(\Delta x)^2}{12}\left.\frac{d^4H}{dx^4}\right|_i + \ldots\ldots\ldots + \sigma(\Delta x)^4 \quad \text{...(B.١٤)}$$

or $$\left.\frac{d^2H}{dx^2}\right|_i = \frac{H_{i+1} - 2H_i + H_{i-1}}{(\Delta x)^2} + \sigma((\Delta x)^2) \quad \text{...(B.١٥)}$$

The expression $(H_{i+1}-2H_i+H_{i-1})/(\Delta x)^2$ is called a second central difference expression of error order $(\Delta x)^2$ for $\left.\frac{d^2H}{dx^2}\right|_i$.

The central difference expressions will be used for derivatives in the transverse (nonmarching) directions. (This was usually not possible for the continuity equation). When boundary conditions are required on the first transverse derivative of a function (as in heat flux problems), it is important that the error order in the expression for the gradient at the boundary be the same as that of the central difference expressions used in the interior of the region. Since the central differences discussed here are of error order $(\Delta x)^2$, it is necessary that the derivative exp**B-4**s at the boundary also be of order $(\Delta x)^2$. Central differences cannot be directly applied at the boundary, since a point outside the region of interest would have to be employed. An imaginary point exterior to the region can be utilized, but it is generally the author's preference to employ forward or backward differences of order $(\Delta x)^2$ and thus express the derivatives entirely in terms of points interior to the region of interest and the boundary points.

First consider forward differences. The $H(x_o+2(\Delta x))=H_{i+2}$ will be find by a Taylor Series expansion around x_o:

$$\text{...(B.16)}\quad H_{i+2} = H_i + 2(\Delta x)\left.\frac{dH}{dx}\right|_i + 2(\Delta x)^2\left.\frac{d^2H}{dx^2}\right|_i + \frac{4(\Delta x)^3}{3}\left.\frac{d^3H}{dx^3}\right|_i + \ldots..$$

Now multiply equation (B.3) by 4 and subtract equation (B.16):

$$\text{...(B.17)}\quad 4H_{i+1} - H_{i+2} = 3H_i + 2(\Delta x)\left.\frac{dH}{dx}\right|_i - \frac{2}{3}(\Delta x)^3\left.\frac{d^3H}{dx^3}\right|_i + \ldots..$$

Solving for $\left.\frac{dH}{dx}\right|_i$ gives

$$\left.\frac{dH}{dx}\right|_i = \frac{-H_{i+2}+4H_{i+1}-3H_i}{2(\Delta x)} + \frac{(\Delta x)^2}{3}\left.\frac{d^3H}{dx^3}\right|_i + \ldots\ldots \quad \text{...(B.١٨)}$$

or $$\left.\frac{dH}{dx}\right|_i = \frac{-H_{i+2}+4H_{i+1}-3H_i}{2(\Delta x)} + \sigma((\Delta x)^2) \quad \text{...(B.١٩)}$$

The expression $(-H_{i+٢}+٤H_{i+١}-٣H_i)/٢(\Delta x)$ is called a forward difference representation of error order $(\Delta x)^٢$ for $\left.\frac{dH}{dx}\right|_i$

In an entirely analogous wav. the $H_{i-٢}$ will be find by a Taylor series expansion and proceed to find

$$\left.\frac{dH}{dx}\right|_i = \frac{3H_i-4H_{i-1}+H_{i-2}}{2(\Delta x)} + \sigma((\Delta x)^2) \quad \text{...(B.٢٠)}$$

where the expression $(٣H_i-٤H_{i-١}+H_{i-٢})/٢(\Delta x)$ is called a backward difference representation of error order $(\Delta x)^٢$ for $\left.\frac{dH}{dx}\right|_i$

Now summarize the results obtained thus far:

Derivative	Difference representation	Type	Error order
$\left.\frac{dH}{dx}\right\|_i$	$\frac{H_{i+1}-H_i}{\Delta x}$	Forward	(Δx)
$\left.\frac{dH}{dx}\right\|_i$	$\frac{H_i-H_{i-1}}{\Delta x}$	Backward	(Δx)
$\left.\frac{dH}{dx}\right\|_i$	$\frac{H_{i+1}-H_{i-1}}{2(\Delta x)}$	Central	$(\Delta x)^٢$

$\left.\frac{dH}{dx}\right\|_i$	$\frac{-H_{i+2}+4H_{i+1}-3H_i}{2(\Delta x)}$	Forward	$(\Delta x)^{٢}$
$\left.\frac{dH}{dx}\right\|_i$	$\frac{3H_i-4H_{i-1}+H_{i-2}}{2(\Delta x)}$	Backward	$(\Delta x)^{٢}$
$\left.\frac{d^2H}{dx^2}\right\|_i$	$\frac{H_{i+1}-2H_i+H_{i-1}}{(\Delta x)^2}$	Central	$(\Delta x)^{٢}$

References

[B-١] Hornbeck, R.W., "Numerical Marching Techniques for Fluid Flows with Heat Transfer", National Aeronautics and Space Administration, Washington, ١٩٧٣.

Chapter One

INTRODUCTION

١.١ GENERAL

When considering external flow, it is necessary to ask only whether this flow is laminar or turbulent. However, for an internal flow, must also concerned with the existence of entrance and fully developed regions.

The laminar flow in a duct is illustrated in figure (١-١), where fluid enters the duct with a uniform velocity profile at section (١). As the fluid makes contact with the surface, viscous effects become important and a boundary layer develops with increasing x. This development occurs at the expense of a shrinking inviscid flow region and concludes with boundary layer merger at the centerline. Following this merger, viscous effects extend over the entire section and the velocity profile no longer changes with increasing x. The flow is then said to be fully developed, section (٢), and the distance from the entrance at which this condition is achieved is termed the hydrodynamic entry length, L_e. As shown in figure (١-١), the fully developed velocity profile is parabolic for laminar flow in a circular pipe. For turbulent flow, the profile is flatter due to turbulent mixing in the radial direction [١].

When dealing with internal flows, it is important to be cognizant of the extent of the entry region, which depends on whether the flow is laminar or turbulent. In a fully developed flow, the critical Reynolds number corresponding to the onset of turbulence is Re ≈ ٢٣٠٠, although much larger Reynolds numbers (Re ≈ ١٠,٠٠٠) are needed to achieve fully turbulent conditions. The transition to turbulence is likely to begin in the developing boundary layer of the entrance region [١].

For laminar flow (Re ≤ ٢٣٠٠) the hydrodynamic entry length may be expressed as:

$$\frac{L_e}{D} = 0.05\,\mathrm{Re} \quad \ldots(١.١)$$

This expression is based on the presumption that fluid enters the tube from a rounded converging nozzle and is hence characterized by a nearly uniform velocity profile at the entrance (Figure ١-١). Although there is no satisfactory general expression for the entry length in turbulent flow, it has known that it is approximately independent of Reynolds number and that, as a first approximation

$$10 \le \left(\frac{L_e}{D} \right) \le 60 \quad \ldots(١.٢)$$

For the purposes of this work, it has been assumed that the flow fully developed turbulent [١].

An important feature of hydrodynamic conditions in the fully developed region is that both the radial velocity component v and the gradient of the axial velocity component $\left(\frac{\partial u}{\partial x} \right)$ are everywhere zero.

$$v = 0 \quad \ldots(١.٣)$$

and

$$\frac{\partial u}{\partial x} = 0 \quad \ldots(١.٤)$$

Hence, the axial velocity component depends only on r, $u(x,r) = u(r)$ [١].

If fluid enters the tube of figure (١-٢) at a uniform temperature $T(r,0)$ that is less than the surface temperature, convection heat transfer occurs and a thermal boundary layer begins to develop. Moreover, if the tube surface condition is fixed by imposing either a uniform temperature (T is constant) or

a uniform heat flux ($q_s^{"}$ is constant), a thermal fully developed condition is eventually reached. The shape of the fully developed temperature profile $T(r,x)$ differs according to whether a uniform surface temperature or heat flux is maintained. For both surface conditions. However, the amount by which fluid temperatures exceed the entrance temperature increases with increasing x [١].

For laminar flow the thermal entry length may be expressed as:

$$\frac{L_{et}}{D} = 0.05\,\mathrm{Re}\,.\,\mathrm{Pr} \quad \ldots(١.٥)$$

Since the existence of convection heat transfer between the surface and the fluid dictates that the fluid temperature must continue to change with x, one might legitimately question whether fully developed thermal conditions can ever be reached. The situation is certainly different from the hydrodynamic case, for which $\left(\frac{\partial u}{\partial x} = 0\right)$ in the fully developed region. In contrast, if there is heat transfer $\left(\frac{\partial T_m}{\partial x}\right)$, as well as $\left(\frac{\partial T}{\partial x}\right)$ at any radius r, is not zero. Accordingly, the temperature profile T(r) is continuously changing with x, and it would seem that a fully developed condition could never be reached. This apparent contradiction may be reconciled by working with a dimensionless form of the temperature [١].

Analyses have often been simplified by working with dimensionless temperature differences, as for transient conduction and the energy conservation equation. Introducing a dimensionless temperature difference of the form $(T_s - T)/(T_s - T_m)$, conditions for which this ratio becomes

independent of x are known to exist. That is, although the temperature profile T(r) continues to change with x, the relative shape of the profile no longer changes and the flow is said to be thermally fully developed. The requirement for such a condition is formally stated as:

$$\frac{\partial}{\partial x}\left[\frac{T_s(x)-T(r,x)}{T_s(x)-T_m(x)}\right]=0 \quad \ldots(١.٦)$$

where T_s , is the tube surface temperature, T is the local fluid temperature, and T_m is the mean temperature of the fluid over the cross section of the tube [١].

If (Pr > ١), the hydrodynamic boundary layer develops more rapidly than the thermal boundary layer (L_e < L_{et}), while the inverse is true for (Pr < ١).[١]

Heat transfer in the combined entry region of non-circular ducts is of particular interest in the design of compact heat exchangers. In these applications passages are generally short and usually composed of cross-sections such as triangular or rectangular geometries in addition to the circular tube or parallel plate channel. Also, due to the wide range of applications, fluid prandtl numbers usually vary between (٠.١ < Pr < ١٠٠٠), which covers a wide range of fluids encompassing gases and highly viscous liquids such as automotive oils.

Closed form solutions do not exist for the problem, hydrodynamically and thermally developing laminar flow between two parallel plates. Thus, this problem can be solved by using numerical methods. A numerical solution is obtained by considering the momentum and energy equations and the continuity equation. The solution presented here is an attempt to provide a

complete picture of the hydrodynamic and thermal variation in the flow within the entire channel.

In the present work, developing steady laminar flow and heat transfer in the entrance region of parallel plate channel as shown in figure (١-٣), will be studied. The governing continuity, x-momentum and energy equations will be numerically solved by using the Finite Difference Method. Two heating boundary conditions will be applied, Constant Wall Temperature and Constant Heat Flux. QuickBasic program is used to compute all the required fluid flow and heat transfer features.

١.٢ LAYOUT OF THESIS

This thesis is organized in six chapters:-

١. Presents the mathematical analysis for Partial Differential Equations which describe developing laminar fluid flow and heat transfer in parallel plate channel. This has been dealt within chapter three.

٢. Presents the details of the theoretical consideration of the suggested technique for two types of thermal boundary conditions, Constant Wall Temperature and Constant Heat Flux, and how to be executed to obtain the general case for laminar fluid flow through parallel plate channel. This has been dealt within chapter four.

٣. Presents the results of the suggested technique such that the dimensionless velocity profile, dimensionless temperature distribution, dimensionless bulk temperature, and local Nusselt number. This has been dealt within chapter five.

٤. Gives a summary of the conclusions which can be drawn from this study and the suggestions for further related works. This has been dealt within chapter six.

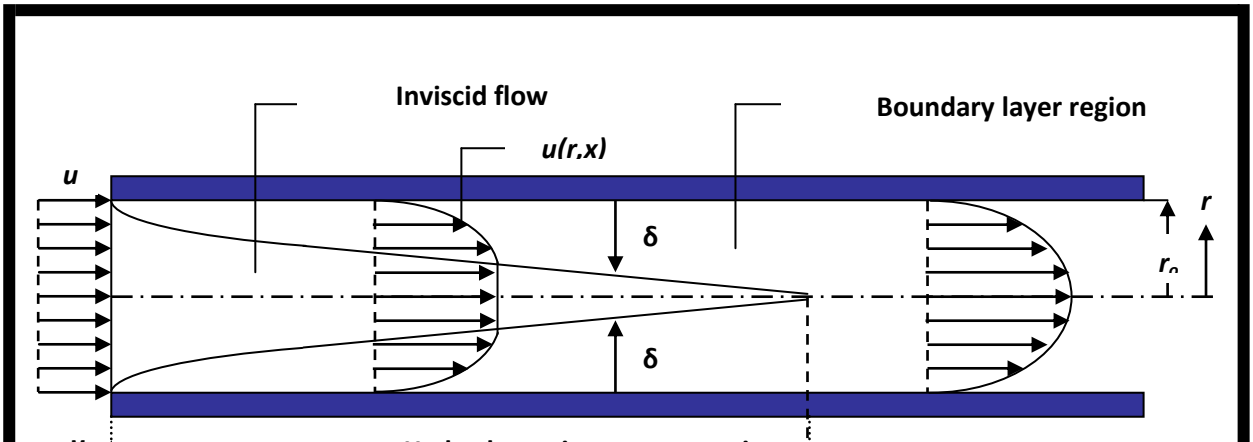

FIGURE (١-١): Laminar, hydrodynamic boundary layer development in a circular tube. Ref. [١].

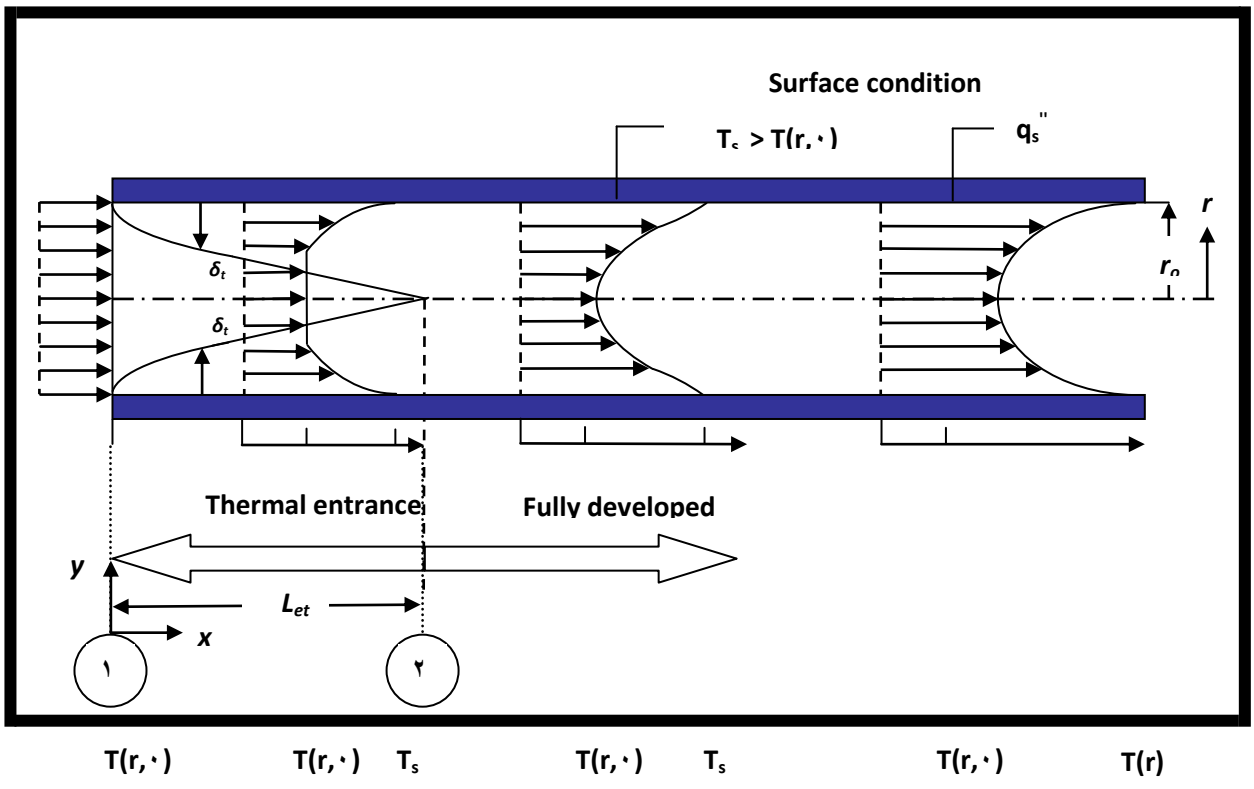

FIGURE (١-٢): Thermal boundary layer development in a heated circular tube. Ref. [١].

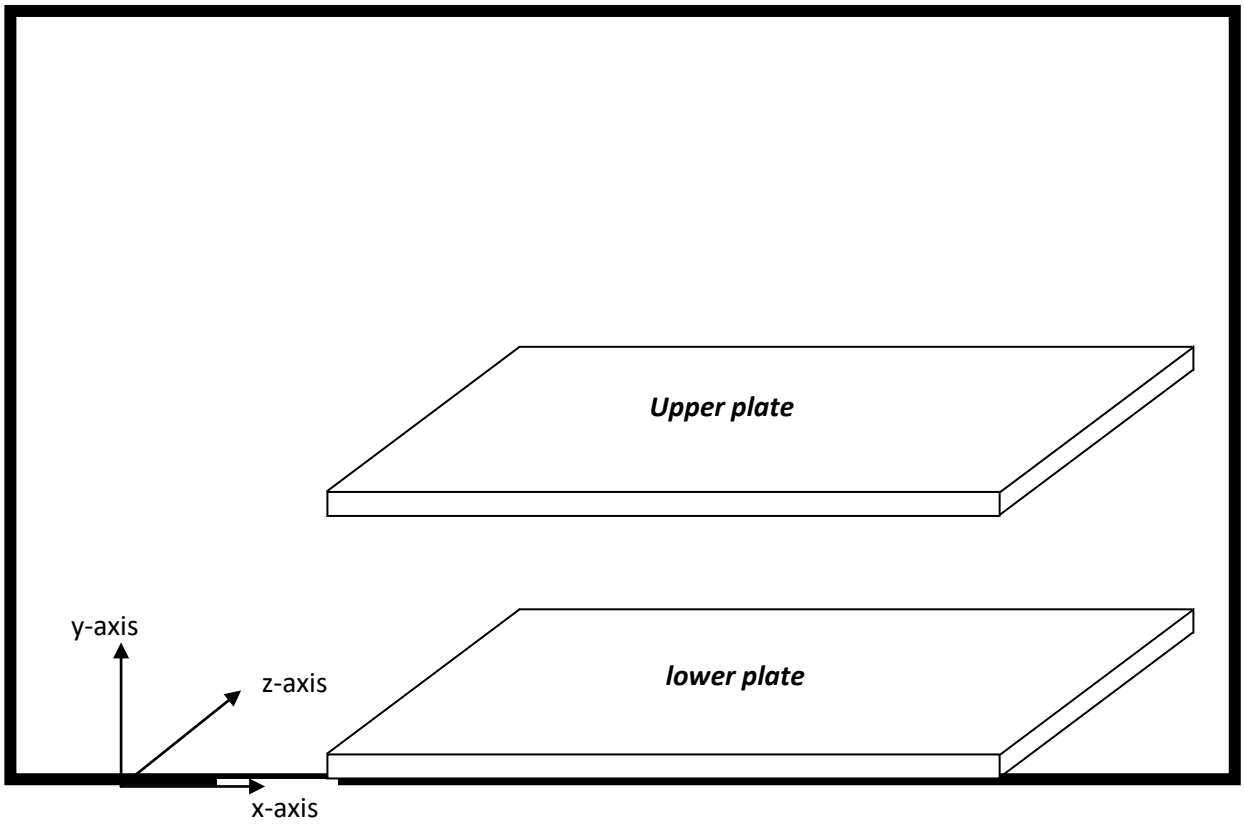

Chapter Two

LITERATURE SURVEY

FIGURE (١-٣): Parallel plate channel

The performance of the numerical work in predicting the velocity field of some industrial problems has become increasingly important. The flow in ducts occurs in many industrial applications, such as compact heat exchangers, nuclear reactors and gas turbine cooling systems. However, the flow in these cooling passage is considered turbulent. Many fundamental studies of the flow in straight ducts can be found. The researchers in these studies emphasis on the velocity and temperature fields, hydraulic parameters such as Nusselt number, Reynolds number.

Schmidt and **Zeldin** [٢], investigated numerically the case for the evaluation of the rate of heat transfer in the thermal entrance region of ducts with axial conduction. The velocity profile is fully developed and flow in a tube and between parallel plates is studied. Local and average Nusselt numbers and mixing temperatures are presented as a function of the peclet number. A criterion is also established which proves usefulness for predicting the conditions under which axial conduction may be ignored.

Emery and **Gessner** [٣], computed the velocity and temperature profiles for turbulent flow, both in the entrance region and the fully developed state in a duct with heated parallel plates. They started the calculations at the duct

inlet and used a finite difference technique and a three- dimensional mixing length originally defined for corner flows, so it was possible to predict an axial flow behavior and the non-asymptotic approach to fully developed flow with and without associated heat transfer. The boundary conditions used were ($u(0,y)=u_{in}$, $u(x,0)=0$, $v(x,0)=0$ for x≥ ٠).

Babus'haq [٤], studied the local heat transfer characteristics for air flowing turbulently inside a smooth heat transfer pipe of ٢٩.١mm. inside diameter and length equal to ١٧٩.١cm. (x/D=٦١.٥) have been determined experimentally over a range of Reynolds numbers from ١٢٠٠٠ to ٥٦٠٠٠. A wall boundary heating condition of uniform heat flux was imposed. The entrance configurations investigated included a long calming section (x/D=٦٩) and four short calming sections (x/D=٥٠, ٣٠ and ١٥) for which previous data are limited.

Emery, **Neighbors,** and **Gessner** [٥], computed velocity and temperature profiles for developing steady turbulent flow in a square duct with Constant Wall Temperature, Constant Heat Flux or asymmetric heating. The computations utilized an explicit numerical differencing scheme and an algebraic closure model based upon a three dimensional mixing length. The computed local and fully-developed shear stresses and heat transfer were shown to be in a good agreement with measured data and with predictions using the $k-\varepsilon$ closure model. The equations of the system were effected by means of the inlet conditions, $u(0,y,z)=u_{in}$ and $v(0,y,z)=w(0,y,z)=0$, with all Reynolds stress components equal to zero at the inlet and with the boundary conditions at the wall of $u=v=w=0$ and either $T_w=0$ for Constant Wall Temperature , or $-k\frac{\partial T}{\partial n}=q_w$ for Constant Heat Flux. The law of the wall, in conjunction with the seventh power law velocity profile was applied at all axial

positions to determine the wall shear stress which was then used in evaluating the axial velocity at the first nodal point from the wall.

Ching and **Jenq** [٦], studied laminar and turbulent heat transfer in pipe flow for liquid metals. Three flow regions, namely fully-developed, developing thermal, and developing thermal and velocity regions were considered. The Van Driest mixing length hypothesis was adapted to model the turbulent shear stress, and the Cebeci model was extended to model the turbulent thermal conductivity of liquid metal flows. The thermal damping constant was redetermined in the study for the fully-developed region as well as other developing regions. Correlation for heat transfer calculation was given for boundary conditions at Constant Heat Flux and Constant Wall Temperature. The effect of the variation of physical properties was also studied. Coefficient of heat transfer calculation when the property is variable was given in a simple form of a liquid sodium eutectic.

Emery and **Gessner** [٧], made comparisons between experimental data and numerical predictions based on a three-dimensional length-scale model applicable to developing turbulent flow in rectangular duct of arbitrary aspect ratio. There was an underproduction in the friction factor behavior calculation at Reynolds numbers (Re<٥٠,٠٠٠) and overproduction in the axial centerline velocity calculation when (x/Dh≥٣٠) for the same previous range of Re. The cause of these discrepancies was probably attributable to the length-scale model.

Lawal [٨], studied entrance region non-isothermal flow and heat transfer to power-law fluids with rectangular coordinates transformed into new orthogonal coordinates and the finite difference technique for arbitrary cross-section ducts.

Al-Ali and **Selim [٩],** studied developing laminar flow and heat transfer in the entrance region of a parallel plate channel with uniform surface temperature by a new integral method. Unlike earlier Karman-Pohlhausen analyses, the new analysis provides solutions which are free from jump discontinuities in the gradients of the velocity and temperature distributions throughout and at the end of the entrance region. The hydrodynamic and thermal results from the present analysis therefore join smoothly and asymptotically to their fully- developed values. The heat transfer results obtained are further found to agree well with previously published numerical solutions.

Szilagyi and **Susan-Resiga** [١٠], investigated four different kinds of laminar flows between two parallel plate by using the Lattice Boltzmann Method (LBM). The LBM accuracy is estimated in two cases using numerical fits of the parabolic velocity profiles and the kinetic energy decay curves, respectively. The error relative to the analytical kinematic viscosity values was found to be less than one percent in both cases. The LBM results for the unsteady development of the flow when one plate is brought suddenly at a constant velocity, are found in an excellent agreement with the analytical solution. Because the classical Schlichting's approximate solution for the entrance-region flow is not valid for small Reynolds numbers, a Finite Element Method solution was used in order to check the accuracy of the LBM results in this case.

Lakovic, Stefanovic, Ilic, and **Stojiljkovic** [١١], investigated convective heat and mass transfer in the part of hydrodynamic stabilization of the flow through the channel formed of two parallel plates. The solution is given for the boundary conditions of the first kind. The similarity method between this

problem and corresponding potential flow is applied, in order to obtain the solution.

Inaoka, Yamamoto, and **Suzuki** [١٢], studied numerically a flat plate laminar boundary layer disturbed by a square rod. Flow becomes unsteady when the space between the rod and the wall is increased. Heat transfer enhancement was obtained on the flat plate downstream of the square rod while skin friction is deteriorated, thus, dissimilarity between the momentum transfer and heat transfer can be generated. The mechanism of this dissimilarity is strongly related to the behavior of the Karman-like vortex, i.e. wavering motion of the separation vorticity layers formed from both sides of the square rod periodically produces an isolated vortex island from the lifted tip of the wall vorticity layer. This isolated vortex induces the clockwise fluid motion which supplies cold fresh fluid of the main stream region into the near wall region from the downstream side and generates the dissimilarity there.

Silva, Guerrero, and **Cotta** [١٣], studied the boundary layer equations for steady incompressible laminar channel flow by integral transform method, adopting the stream function-only formulation of the governing equations, instead of the more commonly used primitive variables formulation. This hybrid numerical-analytical approach provides benchmark results under user-prescribed accuracy targets and is recognized in the validation of purely numerical schemes. The relative merits of the stream function formulation are illustrated through numerical results for the convergence behavior in the case of a plane Poiseuille flow.

Benhamou, Galanis, and **Laneville** [١٤], studied numerically the transient developing laminar flow of a Newtonian incompressible fluid in a straight horizontal pipe oscillating around the vertical diameter at its entrance. The

impulsive start of the latter generates a transient pulsating flow, whose duration increases with the axial distance. In any cross-section, this flow consists of a pair of symmetrical counter-rotating vortices which are alternatively clockwise and anti-clockwise. The circumferentially averaged friction factor and the axial pressure gradient fluctuate with time and are always larger than the corresponding values for a stationary pipe. On the other hand, local axial velocities and local wall shear stress can be smaller than the corresponding stationary pipe values during some part of the pipe oscillation. The fluctuation amplitude of these local variables increases with the axial distance and can be as high as ٥٠٪ of the corresponding stationary pipe value, even at short distances from the pipe entrance. Eventually, the flow field reaches a periodic regime that depends only on the axial position. The results show that the transient flow field depends on the pipe oscillation pattern (initial position and/or direction of initial movement).

Barber and **Emerson** [١٥], investigated the effects of the Reynolds number on the hydrodynamic development lengths in circular and parallel plate ducts. The study was conducted using **THOR-٢D**- a two- dimensional finite-volume Navier-Stokes solver developed by the Computational Engineering Group at **CLRC** Dares bury Laboratory. The solver was specifically adapted for the simulation of non-continuum flows by the inclusion of appropriate tangential slip-velocity boundary conditions at the solid perimeter walls. However, in the case of the parallel plate geometry, entrance development lengths in the slip-flow regime are approximately ٢٥٪ longer than the corresponding continuum solution.

Shariff and **Greywall** [١٦], studied a new algorithm to compute paralyzed axisymmetric flows with heat transfer. These computations require

using **χ**, distance along the centerline of the duct, and **ξ**, the stream function, as the independent variables. The dependent variables used are **U(χ,ξ),** the streamwise velocity, **T(χ,ξ),** the temperature, and **R(χ,ξ),** the cross-stream coordinate of the stream surface **ξ.** Sample computations were carried out for the flow of the standard air, through a pipe of constant diameter, with a hydrodynamically fully developed flow condition at the entrance. Results of the computations are in a close agreement with the available analytical results.

Zhang and **Niu** [١٧], investigated the laminar flow in ducts of irregular cross-sectional shapes which is of important to heat recovery heat exchangers. In this article, heat transfer and pressure drop characteristics in corrugated sinusoidal duct with arc lower boundaries are studied for a hydro dynamically fully developed, thermally developing flow under uniform temperature conditions. The numerical method is of high-order accuracy, numerically implicit, and unconditionally stable. The cross-derivative term is treated as a source term and is solved by iterations in which a varying axial step size ensures a fast convergence without sacrificing details near the inlet of the thermal entry region. This method allows for the simulation of unevenly distributed nodes on boundaries, in combination with the transformation of the special duct geometry to a rectangular computational domain. The detailed finite difference discretization of the governing momentum and energy equations is provided. The local and mean Nusselt numbers are calculated for different aspect and bending ratios. The velocity and temperature profiles are plotted.

Barber and **Emerson** [١٨], studied microfluidic modeling techniques and examines the role of the Reynolds number on the hydrodynamic development length at the entrance to circular and parallel plate micro-channels. The results

suggest that rarefaction has only a marginal effect on the development length in circular pipes. However, in the case of the parallel-plate geometry, entrance development lengths at the upper limit of the slip-flow regime are shown to be almost ٢٥٪ longer than the corresponding continuum solution.

Adachi and **Uehara** [١٩], investigated the correlation between heat transfer and pressure drop in channels with periodically grooved parts along the streamwise direction for various channel configurations by assuming two-dimensional and periodically fully developed flow and temperature fields. Streamwise periodic variations of the cross-section induce the bifurcation from steady-state flow to oscillatory one. Heat transfer is enhanced significantly after the bifurcation with the increase of pressure drop. An efficiency defined as the ratio of the heat transfer enhancement to the increase of pressure drop is considered. It is found that the channels with expanded grooves perform efficiently while the channels with contracted grooves inefficiently.

Patnaik, Gowda, Ravisankar, Narayana, and **Seetharamu** [٢٠], investigated enumerates finite-element based prediction of internal flow problems with heat transfer. The present numerical simulations employ a velocity correction algorithm, with a Galerkin weighted residual formulation. Two problems each in laminar and turbulent flow regimes are investigated, by solving full Navier-Stokes equations. Flow over a backward-facing step is studied with extensive validations. The robustness of the algorithm is demonstrated by solving a very complex problem viz. a disk and doughnut baffled heat exchanger which has several obstructions in its flow path. The effect of wall conductivity in turbulent heat transfer is also studied by performing a conjugate analysis. Temporal evolution of flow in a channel due to circular, square and elliptic obstructions is investigated to simulate the

vortex dynamics. Flow past an in-line tube bank of a heat exchanger shell is numerically studied. Resulting heat and fluid flow patterns are analyzed. Important design parameters of interest such as the Nusselt number, skin friction coefficient, pressure drop etc. are obtained. It is successfully demonstrated that the velocity correction approach with a Galerkin weighted residual formulation is able to effectively simulate a wide range of fluid flow features.

Mahulikar and **Tso** [٢١], investigated the thermal development of the fluid flow in a circular tube under laminar forced convection, it is possible to define a thermal development ratio which leads with the identification of four different conditions of flow within the laminar regime. These different flow conditions subsequently lead to ١٢ possible ways of classifying changes in the thermal development of flow. Central to the concept is the proposed universally applicable description of thermal undevelopment of flow. The refined classification is shown to better describe several practical cases encountered in heat transfer applications, as well as in fluid flow near a changing boundary.

Uzun [٢٢], investigated the numerical solutions for laminar heat transfer of a non-Newtonian fluid in the thermal entrance region for triangular, square, sinusoidal, etc. ducts for Constant Wall Temperature. The continuity equation and parabolic forms of the energy and momentum equations in Cartesian coordinates are transformed by the elliptic grid generation technique into new non-orthogonal coordinates with the boundary of the duct coinciding with the coordinate surface. The effects of an axial heat conduction, viscous dissipation and thermal energy sources within the fluid are neglected. The transformed equations are solved by the finite difference technique. As an application of

the method, flow and heat transfer results are presented for ducts with triangular, square, sinusoidal, and four-cusped cross sections and square cross section with four indented corners.

Barber and **Emerson** [٢٣], studied the role of the Reynolds number on the hydrodynamic development length at the entrance to parallel plate micro-channels. The entrance development region is almost ٢٥٪ longer than that predicted using continuum flow theory.

Sahin and **Ben-Mansour** [٢٤], investigated the numerical solution to the entropy generation in a circular pipe. Radial and axial variations are considered. Navier-Stokes equations in cylindrical coordinates are used to solve the velocity and temperature fields. Uniform wall heat flux is considered as the thermal boundary condition. The distribution of the entropy generation rate is investigated throughout the volume of the fluid as it flows through the pipe. Engine oil is selected as the working fluid. In addition, water and Freon are used in a parametric study. The total entropy generation rate is calculated by integration over the various cross-sections as well as over the entire volume.

Erbay, Ercan, Sulus, and **Yalcin** [٢٥], investigated the two dimensional numerical analysis of entropy generation during transient convective heat transfer for laminar flow between two parallel plate. The fluid is incompressible and Newtonian and the flow is the hydrodynamically and thermally developing. The plates are held at constant equal temperatures higher than that of the fluid. The bottom plate moves in either parallel or in inverse direction to the flow. The governing equations of the transient convective heat transfer are written in two-dimensional Cartesian coordinates and solved by the finite volume method with SIMPLE algorithm. The solutions

are carried for Reynolds numbers of ١٠٢, ٥*١٠٢ and ١٠٣ and Prandtl number of ١. After the flow field and the temperature distributions are obtained, the entropy values and the sites initiating the entropy generation are investigated. The lowest average number of the entropy generation on the bottom plate is obtained in parallel motion. The corners of the channel plates at the entrance play the role of active sites where the generation of entropy is triggered.

Oyumi, S.M. [٢٦], studied the continuity equation and the simplified version of the time dependent boundary layer momentum and energy equations simultaneously for flow between two parallel plates, using an explicit numerical procedure. Solving the three equations simultaneously eliminates the need to assume the shape of the velocity and temperature profiles. Furthermore, this approach provides a picture of the variation of the velocity and temperature within the entire channel. The steady-state solution is obtained by letting time become very large. The shape of the velocity and temperature profiles seem to be consistent with theoretical expectations. The velocity and temperature profiles become fully developed at approximately x/a = ٠.٠٥ Re for Pr = ١, as expected. The average Nusselt number Nu in the fully developed region is computed to be ٧.٣٥ for the case of constant surface temperature and ٧.٩٣ for the case of the constant heat flux.

Muzychka and **Yovanovich** [٢٧], studied a new model for predicting Nusselt numbers in the combined entrance region of non-circular ducts and channels are developed. This model predicts both local and average Nusselt numbers and is valid for both isothermal and isoflux boundary conditions. The model is developed by using the asymptotic results for convection from a flat plate, thermally developing flows in non-circular ducts, and fully developed flow in non-circular ducts. Through the use of a novel characteristic length

scale, the square root of cross-sectional area, the effect of duct shape on Nusselt number is minimized. Comparisons are made with several existing models for the circular tube and parallel plate channel and with numerical data for several non-circular ducts.

Hooman K., Ranjbar-Kani, and **Hooman F.** [٢٨], studied the perturbation solution for flow in a porous saturated channel bounded by two isothermal parallel plates. It is considered that the flow is affected by an internal source term to be heated or cooled. The Brinkman flow model is employed to find fully developed velocity distribution. This solution permits a uniform solution for the energy equation to find the temperature distribution as well as the Nusselt number.

Haddad, Abuzaid, and **Al-Nimr** [٢٩], investigated numerically the entropy generation due to steady laminar forced convection fluid flow through parallel plate microchannel. The effect of Reynolds, Prandtl, and the nondimensional temperature difference on entropy generation within the microchannel is discussed. The entropy generation within the microchannel is found to increase as Reynolds, Prandtl and the nondimensional temperature difference increase.

Demartini, Vielmo, and **Moller** [٣٠], investigated the numerical and experimental analysis of the turbulent flow of air inside a channel of rectangular section, containing two rectangular baffle plate. This is an important problem in the scope of heat exchangers where the characterization of the flow, pressure distribution, as well as the existence and the extension of possible recirculation's need to be identified. The differential equations that describe the flow were integrated by the Finite Volumes Method, in two dimensions, employing the Fluent software with the k-ε model to describe the

turbulence. The mesh is structured, with rectangular volumes. Several boundary conditions were explored. The more realistic results obtained by prescribing the inlet velocity field and atmospheric pressure at the exit. The obtained results are compared with experimental data, analyzed and commented the deviations. The velocity field was measured with a hot wire anemometer and the pressure field with an electronic manometer. The largest variations in the pressure and velocity fields occur in the regions near to the deflectors, as expected.

Ibrahim, A.N. [٣١], studied numerically the developing turbulent flow and heat transfer through rectangular and circular duct have been studied numerically. The study includes the numerical solution of the continuity, momentum, and energy equations together with the two equations of the (k-ε) turbulence model. The clustering of the grid in the radial direction near walls for each duct was used in the numerical solution. A computer program in FORTRAN ٩٠ was built to perform the numerical solution for each duct.

The results showed that, Thermal Entry Length lies between, x/D(١.٤-١.٦) for the two ducts which means that the development of thermal boundary layer is so fast because the very high heat transfer coefficients which are resulted from very high velocities near walls and very small selected dimensions of each duct. The very high velocities near walls may result from the use of the wall function with a very small size of spacing between the clustered nodal points especially near walls.

From the above papers a considerable have been concluded in Table (٢-١). While in the present work, the hydrodynamic and thermal boundary layer are considered to develop simultaneously, where this consideration is achieved by assuming uniform velocity and temperature profile at entrance of two

dimensional for two parallel plate channel. The governing continuity, x-momentum and energy equations will be numerically solved by using the Finite Difference Method. Two heating boundary conditions will be applied, Constant Wall Temperature and Constant Heat Flux. QuickBasic language is used to compute all the required fluid flow and heat transfer features.

Table (٢-١)

The Reference	Steady or	Type of Flow	Geometrical Shape	Notes

	Unsteady			
Schmidt and **Zeldin** [٢]	Steady	Laminar	Tube and Parallel Plate Channel	The velocity profile is fully developed.
Emery and **Gessner** [٣]	Steady	Turbulent	Parallel Plate Channel	Three dimensional.
Babus'haq [٤]	Unsteady	Turbulent	Circular Pipe	Experimental work.
Emery, **Neighbors,** and **Gessner** [٥]	Steady	Turbulent	Square Duct	Flow under C.W.T & C.H.F boundary condition. Using K-ε Closure Model.
Ching and **Jenq** [٦]	Steady	Laminar & Turbulent	Circular Pipe	The flow is liquid metals.
Emery and **Gessner** [٧]	Steady	Turbulent	Rectangular Duct	Comparisons between experimental data and numerical predictions.
Lawal [٨]	Steady	Laminar	Rectangular Duct	Studied entrance region non-isothermal flow and heat transfer to power-law fluids.
Al-Ali and **Selim [٩]**	Steady	Laminar	Parallel Plate Channel	Uniform surface temperature. Used a new integral method.

Szilagyi and **Susan-Resiga** [١٠]	Steady	Laminar	Parallel Plate Channel	Used the Lattice Boltzmann Method.
Lakovic, Stefanovic, Ilic, and **Stojiljkovic** [١١]	Steady	Laminar	Parallel Plate Channel	The similarity method between this problem and corresponding potential flow is applied.
Inaoka, Yamamoto, and **Suzuki** [١٢]	Unsteady	Laminar	Flat plate disturbed by a square rod	Used the Karman-like vortex.
Silva, Guerrero, and **Cotta** [١٣]	Steady	Laminar	Parallel Plate Channel	Incompressible flow, used integral transform method.
Benhamou, Galanis, and **Laneville** [١٤]	Steady	Laminar	Straight horizontal pipe	Newtonian incompressible flow.
Barber and **Emerson** [١٥]	Steady	Laminar	Circular and Parallel Plate Ducts	Used **THOR-٢D**- a two- dimensional finite-volume Navier-Stokes solver developed by the Computational Engineering Group at **CLRC** Dares bury Laboratory.
Shariff and	Steady	Laminar	Circular Pipe	Hydrodynamically

Greywall [١٦]				fully developed flow condition.
Zhang and **Niu** [١٧]	Unsteady	Laminar	Irregular Cross-Sectional Shapes	Hydrodynamically fully developed, thermally developing flow under uniform temperature conditions.
Barber and **Emerson** [١٨]	Steady	Laminar	Circular and Parallel Plate micro-channels	A range of Knudsen numbers ٠ ≤ Kn ≤ ٠.١
Adachi and **Uehara** [١٩]	Steady	Laminar	Parallel Plate Channel	Fully developed flow and temperature.
Patnaik, Gowda, Ravisankar, Narayana, and **Seetharamu** [٢٠]	Steady	Laminar & Turbulent	Circular, Square, and Elliptic	Solving full Navier-Stokes equations.
Mahulikar and **Tso** [٢١]	Steady	Laminar	Circular Tube	Used four different conditions.
Uzun [٢٢]	Steady	Laminar	Triangular, Square, Sinusoidal ducts	Non-Newtonian fluid in the thermal entrance region under constant wall temperature boundary condition.

Barber and **Emerson** [٢٣]	Steady	Laminar	Parallel Plate micro-channels	Using continuum flow theory.
Sahin and **Ben-Mansour** [٢٤]	Unsteady	Laminar	Circular Pipe	Uniform wall heat flux.
Erbay, Ercan, Sulus, and **Yalcin** [٢٥]	Steady	Laminar	Two Parallel Plate Channel	The fluid is incompressible and Newtonian and the flow is the hydrodynamically and thermally developing.
Oyumi, S.M. [٢٦]	Unsteady	Laminar	Two Parallel Plate Channel	Solve the continuity, momentum and energy equations simultaneously by used explicit procedure.
Muzychka and **Yovanovich** [٢٧]	Steady	Laminar	Non-Circular Ducts	Hydrodynamically fully developed, thermally developing flow under isothermal and isoflux boundary conditions.
Hooman K., Ranjbar-Kani, and **Hooman F.**	Steady	Laminar	Two Parallel Plate Channel	flow in a porous saturated channel bounded by two

[٢٨]				isothermal parallel plates. fully developed velocity distribution.
Haddad, Abuzaid, and **Al-Nimr** [٢٩]	Steady	Laminar	Parallel Plate microchannel	Used non-dimensional techniques.
Demartini, Vielmo, and **Moller** [٣٠]	Steady	Turbulent	Rectangular Duct	The numeric and experimental analysis. Used Finite Volumes Method, in two dimensions.
Ibrahim, A.N. [٣١]	Steady	Turbulent	Circular and Rectangular Ducts	Two cases of thermal boundary conditions were studied C.W.T and C.H.F. Two values of Reynolds number (Re = ٦٠,٠٠٠ & Re = ١٢٠,٠٠٠)

Chapter Three

MATHEMATICAL MODEL

In this chapter, the mathematical analysis is presented for the Partial Differential Equations (PDE's) which describe developing laminar fluid flow and heat transfer in parallel plate channel. Incompressible and constant property flow is assumed for developing velocity and temperature profile in the entrance region of the two parallel plates channel. The parallel plate channel has been chosen for initial consideration because the formulation illustrates the techniques used for confined flows without the complicating geometrical and three-dimensional factors of other configurations. The parallel plate channel geometry is shown in figure (٣-١). This channel is an approximation to a rectangular channel of large aspect ratio.

٣.١ ASSUMPTIONS AND GOVERNING EQUATIONS

The following study deals with developing laminar fluid flow and heat transfer through parallel plate channel as shown in figure (١-٣). The parallel plate channel will be expressed in Cartesian Coordinates System. This study will be achieved for two cases, Constant Wall Temperature and Constant Heat Flux respectively.

The development of laminar flow in the entrance of a channel bears a considerable resemblance to the boundary layer growth on a flat plate. Accordingly, the most commonly employed model for this problem is a boundary layer model near the channel walls with a potential core toward the center of the channel which accelerates as the boundary layer grows. This model does an entirely an adequate job in most respects, it is questionable only near the channel inlet where transverse momentum effects are important and hence the boundary layer mod eaks down, and in the core region where viscous effects may actually be present. One other aspect of this type of model is that the velocity distribution at the inlet to the channel is assumed to

be uniform. In actuality, the effect of the channel propagates upstream into the reservoir, causing the inlet profile to be rounded as shown in Wang, Y.L. (mentioned by Hornbeck, R.W., [٣٢]). In this reference Wang and Longwell obtained a numerical solution to the complete Navier-Stokes equations with all terms included for the two-dimensional problem of flow through an infinite stack of parallel plate channels. This upstream propagation effect did not influence the results strongly except for low Reynolds numbers.

The model for the velocity entrance region which has been chosen to be employed here is the same as the one used by Bodoia and Osterle (mentioned by Hornbeck, R.W., [٣٢]), and is very similar to the one discussed previously except that equations of the boundary layer type are assumed to apply over the entire flow field. This permits the viscous effects in the "core" region to be included. The transverse momentum effects which are important very near the inlet are again ignored, as any upstream propagation effects. However, the velocity profile at the inlet to the channel may have any shape desired, including the uniform profile customarily employed [٣٢].

For two dimensional developing, steady state, incompressible laminar flow in parallel plate channel the effects of heat conduction, body force, free convection, heat generation and viscous dissipation within the fluid are neglected.

The primary resistance to heat transfer by convection is normally controlled within a thin layer of fluid, adjacent to the immersed body in which viscous effects are important. The quantity of heat transferred is highly dependent upon the fluid motion within this boundary layer, being determined mainly by the thickness of the layer while greatly effecting heat transfer. The boundary layer and the general velocity field can be treated independently of the boundary layer thickness, provided the fluid properties do not change with temperature.

The following formulation is based largely on the work of Bodoia and Osterle (mentioned by Hornbeck, R.W., [٣٢]) and Incropera, F.P., [١]. The equations of motion are assumed to be

Continuity equation:

$$\frac{\partial(\rho.u)}{\partial x}+\frac{\partial(\rho.v)}{\partial y}=0$$

…(٣.١)

For incompressible flow, ρ = constant, and the continuity equation reduces to: $\frac{\partial u}{\partial x}+\frac{\partial v}{\partial y}=0$

… (٣.٢)

x-momentum equation:

$$\rho.u\frac{\partial u}{\partial x}+\rho.v\frac{\partial u}{\partial y}=-\frac{dp}{dx}+\frac{\partial}{\partial y}\left(\mu\frac{\partial u}{\partial y}\right) \qquad \text{... (٣.٣)}$$

For constant dynamic viscosity, equation (٣.٣) becomes:

$$u\frac{\partial u}{\partial x}+v\frac{\partial u}{\partial y}=-\frac{1}{\rho}\frac{dp}{dx}+\nu\frac{\partial^2 u}{\partial y^2} \qquad \text{...(٣.٤)}$$

Equation (٣.٤) is the x-component of momentum equation for a steady, two dimensional, laminar, constant-property boundary-layer flow of a Newtonian fluid in forced convection. The two terms on the left hand side are the nonlinear convection terms. The two terms on the right hand side arise from inertial forces and viscous shearing forces, respectively.

Assuming ∂v/∂x << ∂u/∂x and ∂v/∂y << ∂u/∂y, the y component of the momentum equation reduces [٣٣].

$$\frac{dp}{dy} = 0 \qquad \ldots(٣.٥)$$

The energy equation for incompressible, constant property flow is uncoupled from the momentum equation once the velocity distribution is known. When viscous dissipation is neglected, the energy equation may be written as

***Energy equation*:**

$$u\frac{\partial T}{\partial x} + v\frac{\partial T}{\partial y} = \alpha\frac{\partial^2 T}{\partial y^2} \qquad \ldots (٣.٦)$$

The two most commonly considered thermal boundary conditions for confined flows are constant wall temperature and constant wall heat flux per unit length in the flow direction. Both of these conditions are considered in this formulation.

The solution to the energy equation, for the entry region is more difficult to obtain, since velocity and temperature now depend on (x) as well as (y). The simplest solution for the thermal entry length problem is based on assuming that thermal conditions develop in the presence of a fully developed velocity profile [١].

٣.٢ BOUNDARY CONDITIONS

The requirement that the dependent variable or its derivative must be satisfied on the boundary of the partial differential equation is called the

boundary condition. The boundary conditions represent the statements of physical facts at specified values of the independent variable. Any fluid moves over a surface whose temperature differs from it, will lead to transfer of heat by convection. Hence, the thermal and hydrodynamic boundary layer considerations will be encountered. These considerations should be precisely treated especially when laminar boundary layer is faced. In order to achieve this purpose, suitable boundary conditions should be applied on the selected problem. Therefore; the boundary conditions according to the geometry will be written as follows [٣٢]:

Entrance region Boundary Conditions:

Uniform temperature and velocity profile at the entrance region of parallel plate channel is assumed. All entrance boundary conditions can be written as follows:

$$\left.\begin{aligned} u(0,y) &= u_o \\ v(0,y) &= 0 \\ p(0) &= p_o \\ T(0,y) &= T_o \end{aligned}\right\} \quad \ldots (٣.٧)$$

Note: $u(0,y) = u_o$ (Assumed constant here, although a function of y is also permissible).

Wall Boundary Conditions:

All velocity components are zero at the walls, hence:-

$$\left.\begin{aligned} u(x,a) &= 0 \\ v(x,a) &= 0 \end{aligned}\right\} \quad \ldots (٣.٨)$$

A number of temperature boundary conditions at the wall are possible. Two commonly employed conditions will be considered here constant wall temperature or constant wall heat flux. The complete boundary conditions for the problem are :-

$$T(x,a) = T_w \qquad (\textit{constant wall temperature}) \qquad \ldots(٣.٩)$$

$$k\frac{\partial T}{\partial y}(x,a) = q \qquad (\textit{constant wall heat flux}) \qquad \ldots(٣.١٠)$$

Centerline of duct Boundary Conditions:

At centerline of duct the boundary conditions are:

$$\left.\begin{aligned} \frac{\partial u}{\partial y}(x,0) &= 0 \\ v(x,0) &= 0 \\ \frac{\partial T}{\partial y}(x,0) &= 0 \end{aligned}\right\} \qquad \ldots(٣.١١)$$

٣.٣ THE DIMENSIONLESS QUANTITIES

Before undertaking a numerical solution, the first step should invariably place the equations to be solved in a dimensionless form having as few parameters as possible. This may be accomplished for equations (٣.٢), (٣.٤) and (٣.٦) by employing the following dimensionless variables :-

$$\left.\begin{aligned} U &= \frac{u}{u_o} \\ V &= \frac{v}{u_o} \\ X &= \frac{x}{d} \\ Y &= \frac{y}{d} \\ P &= \frac{p}{\rho u_o^2} \end{aligned}\right\} \qquad \ldots(٣.١٢)$$

where the characteristic velocity u_o will usually be chosen as the upstream velocity from the body, and a typical length d is measured between two parallel plate in the y-direction. For the parallel plate channel case $u(0) = u_o$.

The choice of the dimensionless temperature variable is dependent on the thermal boundary condition which is to be considered. The remaining dimensionless variables are the same for both boundary conditions. The dimensionless variables chosen are :-

For the Constant wall temperature, the thermal boundary condition will be:

$$\theta = \frac{T - T_w}{T_o - T_w} \qquad \ldots(٣.١٣)$$

For the Constant wall heat flux, the thermal boundary condition will be:

$$\theta = \frac{k}{qd}\left(T - T_o\right) \qquad \ldots(٣.١٤)$$

The following dimensionless quantities will be used in the present work:

Reynolds number:

$$\mathrm{Re} = \frac{\rho . u_o . d}{\mu} \qquad \ldots(٣.١٥)$$

Prandtl number:

$$\mathrm{Pr} = \frac{c_p \mu}{k} = \frac{\nu}{\alpha} \qquad \ldots(٣.١٦)$$

Nusselt number:

$$Nu = \frac{h.d}{k} \qquad \ldots(٣.١٧)$$

٣.٤ DIMENSIONLESS BOUNDARY CONDITIONS

The boundary conditions may be made dimensionless by the choice of the dimensionless variables (٣.١٢), (٣.١٣) and (٣.١٤):

Entrance region Dimensionless Boundary Conditions:

Uniform temperature and velocity profile at the entrance region of parallel plate channel is assumed. All entrance boundary conditions can be written as follows [٣٢]:

$$\left.\begin{aligned} U(0,Y) &= 1 \\ V(0,Y) &= 0 \\ P(0) &= 1 \end{aligned}\right\} \qquad \ldots (٣.١٨)$$

For the Constant wall temperature, the thermal boundary condition will be:

$$\theta(0,Y)=1 \qquad \ldots(٣.١٩)$$

For the Constant wall heat flux, the thermal boundary condition will be:

$$\theta(0,Y)=0 \qquad \ldots(٣.٢٠)$$

Wall Dimensionless Boundary Conditions:

All dimensionless velocity components are zero at walls, hence:

$$\left.\begin{aligned} U(X,1)&=0\\ V(X,1)&=0 \end{aligned}\right\} \qquad \ldots (٣.٢١)$$

A number of dimensionless temperature boundary conditions at the wall are possible:

For the Constant wall temperature, the thermal boundary condition will be:

$$\theta(X,1)=0 \qquad \ldots(٣.٢٢)$$

For the Constant wall heat flux, the thermal boundary condition will be:

$$\frac{\partial\theta}{\partial Y}(X,1)=1 \qquad \ldots(٣.٢٣)$$

Centerline of duct dimensionless Boundary Conditions:

At centerline of the duct the dimensionless boundary conditions are:

$$\left.\begin{aligned} \frac{\partial U}{\partial Y}(X,0)&=0\\ V(X,0)&=0\\ \frac{\partial\theta}{\partial Y}(X,0)&=0 \end{aligned}\right\} \qquad \ldots(٣.٢٤)$$

٣.٥ DIMENSIONLESS GOVERNING EQUATIONS

The dimensionless form is often more convenient to express the equations where each term is dimensionless. It is developed to simplify the solution of many engineering problems and to avoid large quantities in calculation.

The continuity equation may be made dimensionless by the choice of the dimensionless variables shown in equation (٣.١٢):

$$\frac{\partial(U.u_o)}{\partial(X.d)}+\frac{\partial(V.u_o)}{\partial(Y.d)}=0 \qquad \ldots(٣.٢٥)$$

where (u_o) and (d) are constant:

$$\frac{u_o}{d}\frac{\partial U}{\partial X}+\frac{u_o}{d}\frac{\partial V}{\partial Y}=0 \qquad \ldots(٣.٢٦)$$

Now multiply equation (٣.٢٦) by $\left(\frac{d}{u_o}\right)$:

Continuity equation*:*

$$\frac{\partial U}{\partial X}+\frac{\partial V}{\partial Y}=0 \qquad \ldots(٣.٢٧)$$

The x-momentum equation may be made dimensionless by the choice of the dimensionless variables of (٣.١٢) and (٣.١٥):

$$Uu_0\frac{\partial(Uu_0)}{\partial(Xd)}+Vu_0\frac{\partial(Uu_0)}{\partial(Yd)}=-\frac{1}{\rho}\frac{\partial(P\rho.u_0^2)}{\partial(Xd)}+\frac{\mu}{\rho}\frac{\partial^2(Uu_0)}{(\partial(Yd))^2} \qquad \ldots(٣.٢٨)$$

where (u_o),(d) and (ρ) are constant:

$$U\frac{\partial U}{\partial X}\left[\frac{u_0^2}{d}\right]+V\frac{\partial U}{\partial Y}\left[\frac{u_0^2}{d}\right]=-\frac{\partial P}{\partial X}\left[\frac{\rho.u_0^2}{\rho.d}\right]+\frac{\partial^2 U}{\partial Y^2}\left[\frac{\mu.u_0}{\rho.d^2}\right] \qquad \text{...(٣.٢٩)}$$

Now multiply equation (٣.٢٩) by $\left(\frac{d}{u_o^2}\right)$:

$$U\frac{\partial U}{\partial X}+V\frac{\partial U}{\partial Y}=-\frac{\partial P}{\partial X}+\frac{\partial^2 U}{\partial Y^2}\left[\frac{\mu}{\rho.d.u_0}\right] \qquad \text{...(٣.٣٠)}$$

where $\mathrm{Re}=\frac{\rho.u_0.d}{\mu}$

***X-momentum equation*:**

$$U\frac{\partial U}{\partial X}+V\frac{\partial U}{\partial Y}=-\frac{\partial P}{\partial X}+\frac{1}{\mathrm{Re}}\frac{\partial^2 U}{\partial Y^2} \qquad \text{...(٣.٣١)}$$

The energy equation for constant wall temperature may be made dimensionless by the choice of the dimensionless variables of (٣.١٢), (٣.١٣), (٣.١٥) and (٣.١٦):

$$Uu_0\frac{\partial\left(\theta\left(T_0-T_w\right)+T_w\right)}{\partial\left(Xd\right)}+Vu_0\frac{\partial\left(\theta\left(T_0-T_w\right)+T_w\right)}{\partial\left(Yd\right)}=\frac{k}{\rho.cp}\frac{\partial^2\left(\theta\left(T_0-T_w\right)+T_w\right)}{\partial\left(Yd\right)^2}$$

...(٣.٣٢)

where $(T_o\text{-}T_w)$,(T_w) *and (d) are constant:*

$$U\frac{\partial\theta}{\partial X}\left[\frac{u_0\left(\left(T_0-T_w\right)+T_w\right)}{d}\right]+V\frac{\partial\theta}{\partial Y}\left[\frac{u_0\left(\left(T_0-T_w\right)+T_w\right)}{d}\right]=\frac{k\left(\left(T_0-T_w\right)+T_w\right)}{\rho.cp.d^2}\frac{\partial^2\theta}{\partial Y^2}$$

...(٣.٣٣)

Now multiply equation (٣.٣٣) by $\left(\frac{d}{u_o((T_o-T_w)+T_w)}\right)$:

$$U\frac{\partial\theta}{\partial X}+V\frac{\partial\theta}{\partial Y}=\frac{k}{\rho.cp.d.u_0}\frac{\partial^2\theta}{\partial Y^2} \qquad \ldots(٣.٣٤)$$

Now multiply equation (٣.٣٤) by $\left(\frac{\mu}{\mu}\right)$:

where $\Pr=\frac{cp.\mu}{k}$, $\mathrm{Re}=\frac{\rho.u_0.d}{\mu}$

***<u>Energy equation for constant wall temperature</u>*:**

$$U\frac{\partial\theta}{\partial X}+V\frac{\partial\theta}{\partial Y}=\frac{1}{\Pr.\mathrm{Re}}\frac{\partial^2\theta}{\partial Y^2} \qquad \ldots(٣.٣٥)$$

The energy equation for constant wall heat flux may be made dimensionless by the choice of the dimensionless variables (٣.١٢), (٣.١٤), (٣.١٥) and (٣.١٦):

$$Uu_0\frac{\partial\left(\frac{\theta.q.d}{k}+T_0\right)}{\partial(Xd)}+Vu_0\frac{\partial\left(\frac{\theta.q.d}{k}+T_0\right)}{\partial(Yd)}=\frac{k}{\rho.cp}\frac{\partial^2\left(\frac{\theta.q.d}{k}+T_0\right)}{\partial(Yd)^2} \qquad \ldots(٣.٣٦)$$

where (q),(d),(T_o) and (k) are constant:

$$U\frac{\partial\theta}{\partial X}\left[\frac{u_0\left(\frac{q.d}{k}+T_0\right)}{d}\right]+V\frac{\partial\theta}{\partial Y}\left[\frac{u_0\left(\frac{q.d}{k}+T_0\right)}{d}\right]=\frac{k\left(\frac{q.a}{k}+T_0\right)}{\rho.cp.d^2}\frac{\partial^2\theta}{\partial Y^2} \qquad \ldots(٣.٣٧)$$

Now multiply equation (٣.٣٧) by $\left(\frac{d}{u_o\left(\frac{q.d}{k}+T_o\right)}\right)$:

$$U\frac{\partial\theta}{\partial X}+V\frac{\partial\theta}{\partial Y}=\frac{k}{\rho.cp.d.u_0}\frac{\partial^2\theta}{\partial Y^2} \qquad \ldots(٣.٣٨)$$

Now multiply equation (٣.٣٨) by $\left(\frac{\mu}{\mu}\right)$:

where $\Pr=\frac{cp.\mu}{k}$, $\mathrm{Re}=\frac{\rho.u_0.d}{\mu}$

***Energy equation for constant wall heat flux*:**

$$U\frac{\partial\theta}{\partial X}+V\frac{\partial\theta}{\partial Y}=\frac{1}{\Pr.\mathrm{Re}}\frac{\partial^2\theta}{\partial Y^2} \qquad \ldots(٣.٣٩)$$

٣.٦ INCOMPRESSIBLE CONSTANT PROPERTY FLOW-HEAT TRANSFER SOLUTION

In order to solve for the heat transfer in confined flow situation, it is first necessary to find the bulk (mixed-mean) temperature. This quantity is defined for the parallel plate channel as

$$T_b\equiv\frac{\int_0^a u.T.dy}{\int_0^a u.dy} \qquad \ldots(٣.٤٠)$$

The dimensionless variables for constant wall temperature boundary condition are:

$$\left.\begin{aligned} U &= \frac{u}{u_o} \\ \theta &= \frac{T - T_w}{T_o - T_w} \\ Y &= \frac{y}{a} \\ dY &= \frac{dy}{a} \end{aligned}\right\} \qquad \ldots(٣.٤١)$$

The bulk temperature for constant wall temperature boundary condition may be made dimensionless by the choice of the dimensionless variables (٣.٤١):

$$T_b \equiv \frac{\int_0^a U.u_o.\theta(T_o - T_w) + T_w.dY}{\int_0^a U.u_o.dY} \qquad \ldots(٣.٤٢)$$

The dimensionless bulk temperature for constant wall temperature boundary condition is:

$$\theta_b \equiv \frac{\int_0^1 U.\theta.dY}{\int_0^1 U.dY} \qquad \ldots(٣.٤٣)$$

where

$$\theta_b = \frac{T_b - T_w}{T_o - T_w}$$

The dimensionless variables for constant wall heat flux boundary condition are:

$$\left.\begin{aligned} U &= \frac{u}{u_o} \\ \theta &= \frac{k}{q.a}(T - T_o) \\ Y &= \frac{y}{a} \\ dY &= \frac{dy}{a} \end{aligned}\right\} \qquad \ldots(٣.٤٤)$$

The bulk temperature for constant wall heat flux boundary condition may be made dimensionless by the choice of the dimensionless variables (٣.٤٤):

$$T_{b\equiv}\frac{\int_0^a U.u_o\left(\frac{\theta.q.a}{k}+T_o\right)dY}{\int_0^a U.u_o.dY} \qquad \ldots(٣.٤٥)$$

The dimensionless bulk temperature for constant wall heat flux boundary condition is:

$$\theta_{b\equiv}\frac{\int_0^1 U.\theta.dY}{\int_0^1 U.dY} \qquad \ldots(٣.٤٦)$$

where

$$\theta_b = \frac{k}{q.a}(T_b - T_o)$$

<u>Dimensionless Bulk Temperature:</u>

$$\theta_b = \frac{\int_0^1 U.\theta.dY}{\int_0^1 U.dY} = \int_0^1 U.\theta.dY \qquad \ldots(٣.٤٧)$$

where $\int_0^1 U.dY = 1$

<u>The local Nusselt number is given by:</u>

$$N_{ux} = \frac{2ha}{k} \qquad \ldots(٣.٤٨)$$

where

$$h(T_w - T_b) = k\left.\frac{\partial T}{\partial y}\right|_{y=a} \qquad \ldots(٣.٤٩)$$

so

$$N_{ux} = \frac{-\left.\frac{\partial T}{\partial y}\right|_{y=a}(2a)}{T_b - T_w} \qquad \ldots(٣.٥٠)$$

The dimensionless variables for constant wall temperature boundary condition are:

$$\left.\begin{aligned}\theta &= \frac{T - T_w}{T_o - T_w}\\ Y &= \frac{y}{a}\end{aligned}\right\} \qquad \ldots(٣.٥١)$$

The local Nusselt number for constant wall temperature boundary condition is obtained by the choice of the dimensionless variables (٣.٥١):

$$N_{ux} = \frac{-2a \left. \frac{\partial(\theta(T_o - T_w) + T_w)}{\partial(Ya)} \right|_{y=a}}{T_b - T_w} \qquad \ldots(٣.٥٢)$$

where (T_o-T_w), (T_w) and (a) are constant

$$N_{ux} = \frac{-2a \frac{\partial\theta}{\partial Y} \frac{(T_o - T_w)}{a}}{T_b - T_w} \qquad \ldots(٣.٥٣)$$

where $\theta_b = \frac{T_b - T_w}{T_o - T_w}$

<u>The dimensionless local Nusselt Number for constant wall temperature:</u>

$$N_{ux} = \frac{-2 \left. \frac{\partial\theta}{\partial Y} \right|_{Y=1}}{\theta_b} \qquad \ldots(٣.٥٤)$$

The dimensionless variables for constant wall heat flux boundary condition are:

$$\left.\begin{aligned} \theta &= \frac{k}{q.a}(T - T_o) \\ Y &= \frac{y}{a} \end{aligned}\right\} \qquad \ldots(٣.٥٥)$$

The local Nusselt number for constant wall heat flux boundary condition is obtained by the choice of the dimensionless variables (٣.٥٥):

$$N_{ux} = \frac{-2a \left. \frac{\partial\left(\frac{\theta.q.a}{k} + T_o\right)}{\partial(Ya)} \right|_{y=a}}{T_b - T_w} \qquad \ldots(٣.٥٦)$$

where $\left(\frac{q.a}{k}\right)$*, (*$T_o$*) and (a) are constant*

$$N_{ux} = \frac{-2a \frac{\partial\theta}{\partial Y} \frac{q.a}{k.a}}{T_b - T_w} \qquad \ldots(٣.٥٧)$$

where $\left(\frac{\partial\theta}{\partial Y} = 1\right)$ *at wall for constant wall heat flux*

$$N_{ux} = \frac{-2a \frac{q}{k}}{T_b - T_w} \qquad \ldots(٣.٥٨)$$

Now adding and subtracting (t_o*) from the denominator of equation (٣.٥٨):*

$$N_{ux} = \frac{-2}{\frac{k}{q.a}(T_b - T_w + T_o - T_o)} \qquad \ldots(٣.٥٩)$$

$$N_{ux} = \frac{-2}{\frac{k}{q.a}(T_b - T_o) - \frac{k}{q.a}(T_w - T_o)} \qquad \ldots(٣.٦٠)$$

where

$$\theta_b = \frac{k}{q.a}(T_b - T_o)$$

$$\theta_w = \frac{k}{q.a}(T_w - T_o)$$

<u>The dimensionless local Nusselt Number for constant wall heat flux:</u>

$$N_{ux} = \frac{-2}{\theta_b - \theta_w} \qquad \text{...(٣.٦١)}$$

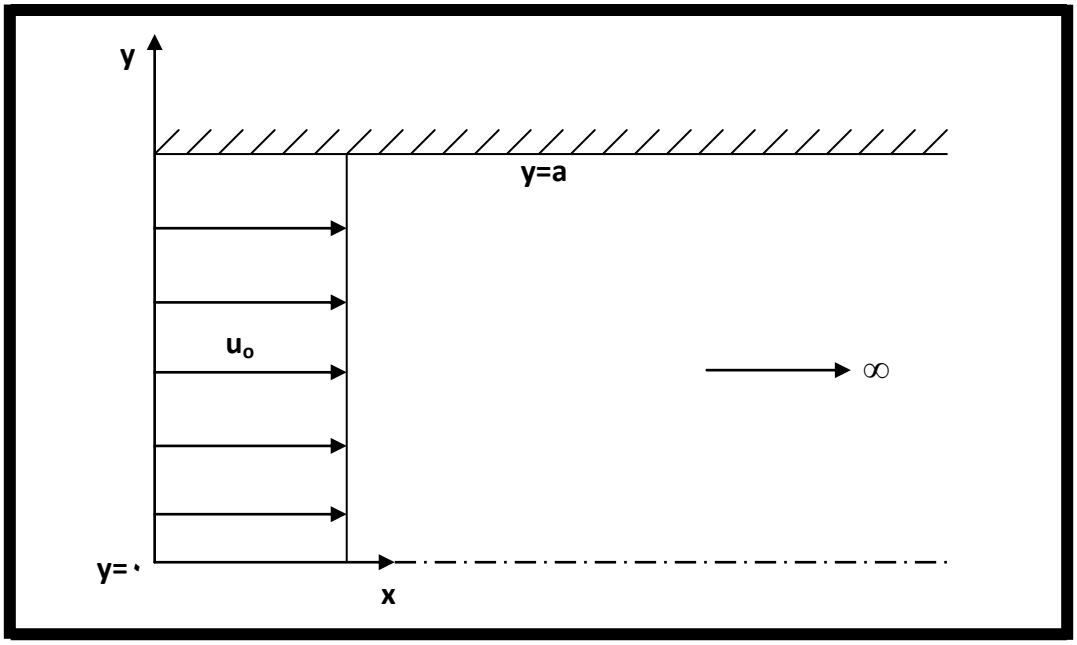

FIGURE (٣-١): Problem Configuration and Coordinate System for Parallel Plate Channel.

Chapter Four

NUMERICAL SOLUTION

٤.١ INTRODUCTION

The numerical solution procedures for governing differential equation which are described in chapter three are given in this chapter. The transformation of governing non-linear partial differential equations to the algebraic equations is achieved by using finite difference method.

The governing equations for the present study will be solved by using the special Finite Differences Method. The calculation region shown in figure (٤-١) for parallel plate channel, the nodal points are specified by using the two indexes, (*i*) in the axial direction (*x*) and (*j*) in the vertical direction (*y*). For each node in parallel plate channel, the coordinates will be ($X = i \times \Delta X$, $Y = j \times \Delta Y$), where ($i = 0, m$, $j = 0, n+1$).

Highly implicit difference representation valid for small secondary velocities. A finite difference representation is chosen for equations (٣.٢٧) and (٣.٣١). The finite difference grid is shown in figure (٤-٢). The difference form selected for equation (٣.٣١) is highly implicit since not only all Y-derivatives evaluated at (*i+* ١), the coefficients of the nonlinear convective terms are also evaluated at (*i+* ١). This representation, which results in nonlinear algebraic equations for the unknowns ($U_{i+١,j}$) and ($V_{i+١,j}$), is necessary if zero and small secondary velocities are to be considered, since the usual implicit scheme with

the coefficients evaluated at (*i*) is inconsistent for these conditions. This inconsistency is not discussed in detail, but for zero secondary velocity the usual implicit form results in the (*U*) velocity profile decreasing linearly from the edge of the plate to whatever value of (*Y*) is chosen as infinity. This result is obviously incorrect. The usual implicit scheme, does give correct results if the secondary velocity is of the order of the primary velocity or larger.

Figure (٤-١) shows the mesh between centerline and upper wall of parallel plate channel only, because symmetric between upper and lower wall of parallel plate channel (symmetric in boundary conditions and dimensions).

The continuity, momentum, and energy equations which will be solved by using Gauss- Elimination method as indicated in this chapter. The resulting algebraic forms for all equations presented in this chapter are solved by using a computer program built in QuickBasic language.

٤.٢ NUMERICAL FORMULATION FOR MOMENTUM AND CONTINUITY EQUATIONS

The special Finite Difference Method will be used to solved the momentum equation for a steady, two-dimensional, laminar, constant-property boundary-layer flow of a Newtonian fluid in forced convection. The two terms on the left side are the nonlinear convection terms. The two terms on the right side arise from inertial forces and viscous shearing forces, respectively. The numerical formulation for x-momentum equation is [٣٢]

$$U_{i,j}\frac{U_{i+1,j}-U_{i,j}}{\Delta X}+V_{i,j}\frac{U_{i+1,j+1}-U_{i+1,j-1}}{2(\Delta Y)}=$$

$$-\frac{P_{i+1}-P_i}{\Delta X}+\frac{1}{\mathrm{Re}}\frac{U_{i+1,j+1}-2U_{i+1,j}+U_{i+1,j-1}}{(\Delta Y)^2} \qquad \ldots(٤.١)$$

A somewhat unusual representation of equation (٣.٢٧) is chosen for a reason which will become clear shortly. The form is

$$\frac{U_{i+1,j+1}-U_{i,j+1}+U_{i+1,j}-U_{i,j}}{2(\Delta X)}+\frac{V_{i+1,j+1}-V_{i+1,j}}{\Delta Y}=0 \qquad \ldots(٤.٢)$$

Equations (٤.١) and (٤.٢) are written for j=٠(١)n constitute (٢*n*+ ٢) equations in the (٢*n*+ ٢) unknowns ($U_{i+١,٠}$,....,$U_{i+١,n}$; $V_{i+١,١}$,....,$V_{i+١,n}$); and ($P_{i+١}$). The number of unknowns can be reduced materially by writing the continuity equation (٤.٢) for j=٠(١)n and adding together all of these equations. The resulting equation is

$$U_{i+1,0}+2\sum_{j=1}^{n}U_{i+1,j}=U_{i,0}+2\sum_{j=1}^{n}U_{i,j} \qquad \ldots(٤.٣)$$

if both sides of equation (٤.٣) are multiplied by (ΔY/٢), it can be seen to be the trapezoidal rule integration form of the equation

$$\int_0^1 U\,dy\Big|_{i+1}=\int_0^1 U\,dy\Big|_i \qquad \ldots(٤.٤)$$

which is an integral form of the continuity equation. This equation is, of course, independent of any of those already given, but simply incorporates the boundary conditions on (*V*) at the channel centerline and walls by requiring that the axial flow rate must be constant. The use of this equation to simplify the solution of confined flow problems was first suggested by Bodoia, J.R., (mentioned by Hornbeck, R.W., [٣٢]) who called it an equation of constraint.

Since equation (٤.٣) does not involve (*V*), equation (٤.٣) together with equation (٤.١) written for j=٠(١)n now constitute (*n*+ ٢) equations in the (*n*+ ٢)

unknowns ($U_{i+1,0}$,....,$U_{i+1,n}$) and (P_{i+1}). To aid in obtaining a solution, it is convenient to rewrite equation (٤.١) as

$$\left[\frac{-V_{i,j}}{2(\Delta Y)}-\frac{1}{\mathrm{Re}(\Delta Y)^2}\right]U_{i+1,j-1}+\left[\frac{U_{i,j}}{\Delta X}+\frac{2}{\mathrm{Re}(\Delta Y)^2}\right]U_{i+1,j}$$

$$+\left[\frac{V_{i,j}}{2(\Delta Y)}-\frac{1}{\mathrm{Re}(\Delta Y)^2}\right]U_{i+1,j+1}+\left[\frac{1}{\Delta X}\right]P_{i+1}=\frac{U_{i,j}^2+P_i}{\Delta X} \qquad \text{...(٤.٥)}$$

Equations (٤.٥) [written for j=٠(١)n] and (٤.٣) may be written in matrix form as

$$\begin{vmatrix} 1 & 2 & 2 & 2 & 2 & - & - & 2 & 2 & 0 \\ \beta_0 & \Omega_0 & & & & & & & & 1/\Delta X \\ \varepsilon_1 & \beta_1 & \Omega_1 & & & & & & & 1/\Delta X \\ & \varepsilon_2 & \beta_2 & \Omega_2 & & & & & & 1/\Delta X \\ & & \varepsilon_3 & \beta_3 & \Omega_3 & & & & & 1/\Delta X \\ & & & - & - & - & & & & - \\ & & & & - & - & - & & & - \\ & & & & & - & - & - & & - \\ & & & & & & \varepsilon_{n-1} & \beta_{n-1} & \Omega_{n-1} & 1/\Delta X \\ & & & & & & & \varepsilon_n & \beta_n & 1/\Delta X \end{vmatrix} \times \begin{vmatrix} U_{i+1,0} \\ U_{i+1,1} \\ U_{i+1,2} \\ U_{i+1,3} \\ U_{i+1,4} \\ - \\ - \\ - \\ U_{i+1,n} \\ P_{i+1} \end{vmatrix} = \begin{vmatrix} S \\ \Phi_0 \\ \Phi_1 \\ \Phi_2 \\ \Phi_3 \\ - \\ - \\ - \\ \Phi_{n-1} \\ \Phi_n \end{vmatrix} \qquad \text{...(٤.٦)}$$

where

$$\Omega_0=-\frac{2}{\mathrm{Re}(\Delta Y)^2} \quad (\textit{incorporates symmetry at Y= ٠}) \qquad \text{...(٤.٧.a)}$$

$$S=U_{i,0}+2\sum_{j=1}^{n}U_{i,j} \qquad \text{...(٤.٧.b)}$$

and

$$\varepsilon_j=-\frac{V_{i,j}}{2(\Delta Y)}-\frac{1}{\mathrm{Re}(\Delta Y)^2} \qquad \text{...(٤.٧.c)}$$

$$\beta_j = \frac{U_{i,j}}{\Delta X} + \frac{2}{\mathrm{Re}(\Delta Y)^2} \qquad \text{...(٤.٧.d)}$$

$$\Omega_j = \frac{V_{i,j}}{2(\Delta Y)} - \frac{1}{\mathrm{Re}(\Delta Y)^2} \qquad (j > ٠) \qquad \text{...(٤.٧.e)}$$

$$\Phi_j = \frac{U_{i,j}^2 + P_i}{\Delta X} \qquad \text{...(٤.٧.f)}$$

for n=٥ the matrix becomes

$$\begin{vmatrix} 1 & 2 & 2 & 2 & 2 & 2 & 0 \\ \beta_0 & \Omega_0 & & & & & 1/\Delta X \\ \varepsilon_1 & \beta_1 & \Omega_1 & & & & 1/\Delta X \\ & \varepsilon_2 & \beta_2 & \Omega_2 & & & 1/\Delta X \\ & & \varepsilon_3 & \beta_3 & \Omega_3 & & 1/\Delta X \\ & & & \varepsilon_4 & \beta_4 & \Omega_4 & 1/\Delta X \\ & & & & \varepsilon_5 & \beta_5 & 1/\Delta X \end{vmatrix} \times \begin{vmatrix} U_{i+1,0} \\ U_{i+1,1} \\ U_{i+1,2} \\ U_{i+1,3} \\ U_{i+1,4} \\ U_{i+1,5} \\ P_{i+1} \end{vmatrix} = \begin{vmatrix} S \\ \Phi_0 \\ \Phi_1 \\ \Phi_2 \\ \Phi_3 \\ \Phi_4 \\ \Phi_5 \end{vmatrix} \qquad \text{...(٤.٨)}$$

The matrix of coefficients in equation (٤.٦) does not have the desirable tridiagonal character of the matrices. This matrix is, however, quite sparse. It would be possible to write a special computer program to solve the set (٤.٦) by taking full advantage of this sparseness. This would only be practical if a large number of production runs were contemplated and the savings in running time and storage space considered more important than the programming time required. As a general rule, it seems most practical to solve the set by using one of the standard routines for linear equations or matrix inversion which are available at any computer installation. A possible alternative is to solve the set by Gaussian elimination method. This method will work effectively except for equation (٤.٣) [top row of equation (٤.٦)], which must be drastically under relaxed.

After the set (٤.٦) has been solved for ($U_{i+١,٠}$,….,$U_{i+١,n}$) and ($P_{i+١}$), equation (٤.٢) may be employed in the form

$$V_{i+1,j+1} = V_{i+1,j} - \frac{\Delta Y}{2(\Delta X)}\left(U_{i+1,j+1} - U_{i,j+1} + U_{i+1,j} - U_{i,j}\right) \qquad \ldots(٤.٩)$$

which may be marched outward from the channel centerline to give the values of ($V_{i+١,١}$,….,$V_{i+١,n}$).

Another step (ΔX) downstream may now be taken and the process repeated. This may be continued as many times as necessary.

The proper choice of the (ΔX) mesh size at and near the channel entrance is a very important factor in obtaining an accurate solution. This region represents difficulties of two kinds: first, the equations of the boundary layer type used in this chapter are not valid there because transverse (Y) momentum and axial (X) second derivatives become important; and second, the entrance itself represents a mathematical difficulty in that it behaves like a singularity. The breakdown of the equations is not discussed here except to say that the boundary layer equations provide an excellent model except in a very small region close to the inlet. The mathematical singularity may be dealt with in the manner described in chapter three for the leading edge in the boundary layer development problem, by keeping (ΔX) very small and hence taking a large number of steps in the region close to the entrance. As in the boundary layer case, the spread of the effect of the singularity downstream is primarily a function of how many steps are taken to reach a given (X) position. If a large number of steps are taken to reach this value of (X), then the effect of the singularity there tends to disappear. The effect of the singularity may thus be confined to a region arbitrarily close to the entrance. After this singularity has been taken care of, the (ΔX) mesh size may be increased considerably.

As usual, the only sure way to decide on final mesh sizes is to obtain solutions with succeedingly smaller mesh sizes until the solutions obtained on two successive mesh reductions agree to within the desired accuracy.

The stability restrictions for this problem have been established by Bodoia, J.R., (mentioned by Hornbeck, R.W., [٣٢]) and the same as those given in chapter ٣ for the incompressible boundary layer problem. The formulation is universally stable for (U ≥ ٠), and if (U < ٠) , then

$$\frac{\Delta X}{|U|(\Delta Y)^2} \geq \frac{1}{2} \qquad \ldots(٤.١٠)$$

$$V \geq \sqrt{\frac{2|U|}{\Delta X}} \qquad \ldots(٤.١١)$$

which are generally satisfied only for very small values of $|U|$.

The truncation error of the momentum equation is of б(ΔX) and б((ΔY)٢) and that of continuity б(ΔX) and б(ΔY).

٤.٣ NUMERICAL FORMULATION FOR ENERGY EQUATION

Equation (٣.٣٥) or (٣.٣٩) may now be expressed in an implicit finite difference form similar to that used for the momentum equation in the preceding section. This difference form is

$$U_{i,j}\frac{\theta_{i+1,j}-\theta_{i,j}}{\Delta X}+V_{i,j}\frac{\theta_{i+1,j+1}-\theta_{i+1,j-1}}{2(\Delta Y)}$$

$$= \frac{1}{\mathrm{Pr.Re}} \frac{\theta_{i+1,j+1} - 2\theta_{i+1,j} + \theta_{i+1,j-1}}{(\Delta Y)^2} \qquad \ldots(٤.١٢)$$

Equation (٤.١٢) can be rewritten in a more useful form as

$$\left[\frac{-V_{i,j}}{2(\Delta Y)} - \frac{1}{\mathrm{Pr.Re}(\Delta Y)^2}\right]\theta_{i+1,j-1} + \left[\frac{U_{i,j}}{\Delta X} + \frac{2}{\mathrm{Pr.Re}(\Delta Y)^2}\right]\theta_{i+1,j}$$

$$+\left[\frac{V_{i,j}}{2(\Delta Y)} - \frac{1}{\mathrm{Pr.Re}(\Delta Y)^2}\right]\theta_{i+1,j+1} = \frac{U_{i,j}\theta_{i,j}}{\Delta X} \qquad \ldots(٤.١٣)$$

Equation (٤.١٣) is written for j=٠(١)n forms as a set of (*n+* ١) simultaneous linear equations in the values of ($\theta_{i+١,j}$). If the wall temperature is known (Constant Wall Temperature case), then these (*n+* ١) equations involve (*n+* ١) unknowns. The resulting matrix equation is

$$\begin{vmatrix} \beta_0' & \Omega_0' & & & & & & \\ \varepsilon_1' & \beta_1' & \Omega_1' & & & & & \\ & \varepsilon_2' & \beta_2' & \Omega_2' & & & & \\ & & - & - & - & & & \\ & & & - & - & - & & \\ & & & & - & - & - & \\ & & & & & \varepsilon_{n-1}' & \beta_{n-1}' & \Omega_{n-1}' \\ & & & & & & \varepsilon_n' & \beta_n' \end{vmatrix} \times \begin{vmatrix} \theta_{i+1,0} \\ \theta_{i+1,1} \\ \theta_{i+1,2} \\ - \\ - \\ - \\ \theta_{i+1,n-1} \\ \theta_{i+1,n} \end{vmatrix} = \begin{vmatrix} \Phi_0' \\ \Phi_1' \\ \Phi_2' \\ - \\ - \\ - \\ \Phi_{n-1}' \\ \Phi_n' \end{vmatrix} \qquad \ldots(٤.١٤)$$

where

$$\varepsilon_j' = \frac{-V_{i,j}}{2(\Delta Y)} - \frac{1}{\mathrm{Pr.Re}(\Delta Y)^2} \qquad \ldots(٤.١٥.a)$$

$$\beta_j' = \frac{U_{i,j}}{\Delta X} + \frac{2}{\mathrm{Pr.Re}(\Delta Y)^2} \qquad \ldots(٤.١٥.b)$$

$$\Omega_j' = \frac{V_{i,j}}{2(\Delta Y)} - \frac{1}{\mathrm{Pr.Re}(\Delta Y)^2} \qquad (j > ٠) \qquad \ldots(٤.١٥.c)$$

$$\Phi'_j = \frac{U_{i,j}\theta_{i,j}}{\Delta X} \qquad \text{...(٤.١٥.d)}$$

$$\Omega'_0 = \frac{-2}{\Pr.\mathrm{Re}(\Delta Y)^2} \qquad (j = ٠) \qquad \text{...(٤.١٥.e)}$$

for n=٥ the matrix becomes

$$\begin{vmatrix} \beta'_0 & \Omega'_0 & & & & \\ \varepsilon'_1 & \beta'_1 & \Omega'_1 & & & \\ & \varepsilon'_2 & \beta'_2 & \Omega'_2 & & \\ & & \varepsilon'_3 & \beta'_3 & \Omega'_3 & \\ & & & \varepsilon'_4 & \beta'_4 & \Omega'_4 \\ & & & & \varepsilon'_5 & \beta'_5 \end{vmatrix} \times \begin{vmatrix} \theta_{i+1,0} \\ \theta_{i+1,1} \\ \theta_{i+1,2} \\ \theta_{i+1,3} \\ \theta_{i+1,4} \\ \theta_{i+1,5} \end{vmatrix} = \begin{vmatrix} \Phi'_0 \\ \Phi'_1 \\ \Phi'_2 \\ \Phi'_3 \\ \Phi'_4 \\ \Phi'_5 \end{vmatrix} \qquad \text{...(٤.١٦)}$$

The matrix equation (٤.١٤) is tridiagonal and the method of appendix (A) is used to obtain a solution for the $\theta_{i+١,j}$'s.

For the Constant Heat Flux case, the wall temperature ($\theta_{i+١,n+١}$) is unknown, resulting in (*n+*٢) unknowns. The additional necessary equation (٣.٢٣), which expresses the heat flux at the wall, may be written in difference form as

$$\frac{3\theta_{i+1,n+1} - 4\theta_{i+1,n} + \theta_{i+1,n-1}}{2(\Delta Y)} = 1 \qquad \text{...(٤.١٧)}$$

By using the backward difference in appendix (B).

The matrix equation (٤.١٤) may be modified to include the additional unknown and equation by adding on an additional row and column.

$$\begin{vmatrix} \beta_0' & \Omega_0' & & & & & & & \\ \varepsilon_1' & \beta_1' & \Omega_1' & & & & & & \\ & \varepsilon_2' & \beta_2' & \Omega_2' & & & & & \\ & & - & - & - & & & & \\ & & & - & - & - & & & \\ & & & & - & - & - & & \\ & & & & & \varepsilon_{n-1}' & \beta_{n-1}' & \Omega_{n-1}' & \\ & & & & & & \varepsilon_n' & \beta_n' & \Omega_n' \\ & & & & & & 1/2(\Delta Y) & -4/2(\Delta Y) & 3/2(\Delta Y) \end{vmatrix} \times \begin{vmatrix} \theta_{i+1,0} \\ \theta_{i+1,1} \\ \theta_{i+1,2} \\ - \\ - \\ - \\ \theta_{i+1,n-1} \\ \theta_{i+1,n} \\ \theta_{i+1,n+1} \end{vmatrix} = \begin{vmatrix} \Phi_0' \\ \Phi_1' \\ \Phi_2' \\ - \\ - \\ - \\ \Phi_{n-1}' \\ \Phi_n' \\ 1 \end{vmatrix}$$

...(٤.١٨)

where the elements are defined as in (٤.١٤).

The element ١/٢(ΔY) in the last row makes the matrix in (٤.١٨) nontridiagonal. However, the matrix may be made tridiagonal by eliminating this element. This can be accomplished by dividing the last equation by ١/٢(ΔY), multiplying it by (ε_n), and subtracting the next to the last equation from it. The results are

$$\begin{vmatrix} \beta_0' & \Omega_0' & & & & & & & \\ \varepsilon_1' & \beta_1' & \Omega_1' & & & & & & \\ & \varepsilon_2' & \beta_2' & \Omega_2' & & & & & \\ & & - & - & - & & & & \\ & & & - & - & - & & & \\ & & & & - & - & - & & \\ & & & & & \varepsilon_{n-1}' & \beta_{n-1}' & \Omega_{n-1}' & \\ & & & & & & \varepsilon_n' & \beta_n' & \Omega_n' \\ & & & & & & 0 & \left(-4\varepsilon_n' - \beta_n'\right) & \left(3\varepsilon_n' - \Omega_n'\right) \end{vmatrix} \times \begin{vmatrix} \theta_{i+1,0} \\ \theta_{i+1,1} \\ \theta_{i+1,2} \\ - \\ - \\ - \\ \theta_{i+1,n-1} \\ \theta_{i+1,n} \\ \theta_{i+1,n+1} \end{vmatrix} = \begin{vmatrix} \Phi_0' \\ \Phi_1' \\ \Phi_2' \\ - \\ - \\ - \\ \Phi_{n-1}' \\ \Phi_n' \\ 2(\Delta Y)\varepsilon_n' - \Phi_n' \end{vmatrix}$$

...(٤.١٩)

for n=٥ the matrix becomes

$$\begin{vmatrix} \beta_0' & \Omega_0' & & & & & \\ \varepsilon_1' & \beta_1' & \Omega_1' & & & & \\ & \varepsilon_2' & \beta_2' & \Omega_2' & & & \\ & & \varepsilon_3' & \beta_3' & \Omega_3' & & \\ & & & \varepsilon_4' & \beta_4' & \Omega_4' & \\ & & & & \varepsilon_5' & \beta_5' & \Omega_5' \\ & & & & 0 & \left(-4\varepsilon_5' - \beta_5'\right) & \left(3\varepsilon_5' - \Omega_5'\right) \end{vmatrix} \times \begin{vmatrix} \theta_{i+1,0} \\ \theta_{i+1,1} \\ \theta_{i+1,2} \\ \theta_{i+1,3} \\ \theta_{i+1,4} \\ \theta_{i+1,5} \\ \theta_{i+1,6} \end{vmatrix} = \begin{vmatrix} \Phi_0' \\ \Phi_1' \\ \Phi_2' \\ \Phi_3' \\ \Phi_4' \\ \Phi_5' \\ 2(\Delta Y)\varepsilon_5' - \Phi_5' \end{vmatrix} \qquad \ldots(٤.٢٠)$$

Equation (٤.١٩) has a tridiagonal matrix of coefficients and the method of appendix (A) is used.

The mesh sizes used for the velocity and temperature solutions should be the same for convenience. The fineness of the ΔY mesh will be determined by the velocity solution for moderate to low Prandtl numbers and by the temperature solution for large Prandtl numbers. Of course , numerical experimentation (including refining the originally chosen mesh size) is necessary to verify any choice of the mesh size.

The solution can be carried downstream in the usual manner, solving first for the velocity distribution and then for the temperatures at each axial station.

٤.٤ CALCULATION OF BULK TEMPERATURE

The dimensionless bulk temperature (θ_b) is calculated numerically by employing Simpson's rule:

$$\theta_b\big|_{i+1} = \frac{\Delta Y}{3}\left(U_{i+1,0}\theta_{i+1,0} + 4\sum_{j=1,3,5,7,\ldots}^{n} U_{i+1,j}\theta_{i+1,j} + 2\sum_{j=2,4,6,8,\ldots.}^{n-1} U_{i+1,j}\theta_{i+1,j}\right) \qquad \ldots(٤.٢١)$$

Equation (٤.٢١) requires an even number of spaces across the half channel (n must be odd).

for n=٥ equation (٤. ٢١) becomes

$$\theta_b\big|_{i+1} = \frac{\Delta Y}{3}(U_{i+1,0}\theta_{i+1,0} + 4\sum_{j=1,3,}^{5} U_{i+1,j}\theta_{i+1,j} + 2\sum_{j=2,}^{4} U_{i+1,j}\theta_{i+1,j}) \qquad \ldots(٤.٢٢)$$

٤.٥ CALCULATION OF LOCAL NUSSELT NUMBER

The Nusselt number is given by equation (٣.٤٨). The local Nusselt number for Constant Wall Temperature boundary condition is given by equation (٣.٥٤), which is written in a finite difference form as,

$$N_{ux} = -2\frac{\left(3\theta_{i+1,n+1} - 4\theta_{i+1,n} + \theta_{i+1,n-1}\right)}{2(\Delta Y)\theta_b\big|_{i+1}} \qquad \ldots(٤.٢٣)$$

for n=٥ the equation (٤. ٢٣) becomes

$$N_{ux} = -2\frac{\left(3\theta_{i+1,6} - 4\theta_{i+1,5} + \theta_{i+1,4}\right)}{2(\Delta Y)\theta_b\big|_{i+1}} \qquad \ldots(٤.٢٤)$$

The local Nusselt number for Constant Heat Flux boundary condition is given by equation (٣.٦١), which is written in a finite difference form as,

$$N_{ux} = \frac{-2}{\theta_b\big|_{i+1} - \theta_w\big|_{i+1}} \qquad \ldots(٤.٢٥)$$

٤.٦ STEPS OF NUMERICAL SOLUTION

The numerical solution steps for all equations of this chapter can be summarized as follows:-

١. The calculation of x-momentum equation coefficients are obtained by using equations (٤.٧.a),.....,(٤.٧.f).
٢. The calculation of pressure difference in the axial direction and the axial velocity component for one column are obtained by using solve equation (٤.٦). The nodal Gaussian-elimination method was used for doing this calculation.
٣. The calculation of vertical velocity component for on column is obtained by using equation (٤.٩).
٤. Steps from ١ to ٣ should be repeated until reaching the fully developed region. To ensure the reaching of the fully developed region must be constant axial velocity in x-direction.
٥. The calculation of energy equation coefficients are obtained by using equations (٤.١٥.a),.....,(٤.١٥.e).
٦. The calculation of temperature component for one column is obtained by using equation (٤.١٤) for Constant Wall Temperature or equation (٤.١٩) for Constant Heat Flux. The nodal Gaussian-elimination method was used for doing this calculation.
٧. The calculation of the bulk temperature from equation (٤.٢١) is reached.
٨. The calculation of the local Nusselt number for Constant Wall Temperature boundary condition is obtained by using equation (٤.٢٣),

and the local Nusselt number for Constant Heat Flux boundary condition is obtained by using equation (٤.٢٥).

٤.٧ COMPUTER PROGRAM

The computer program is developed to calculate the velocity profile, temperature distribution, bulk temperature, and local Nusselt number. These calculations are based on the theoretical analysis presented in this chapter.

The computer program is written in QuickBasic language.

In order to **RUN** the program the following data is required:

-Reynolds number.

-Prandtl number.

-Number of node in y-direction (n).

-Thermal boundary condition Constant Wall Temperature or Constant Heat flux.

The computational procedure is as follows:

١. The program calculates number of nodes, grid generation.

٢. It reads the boundary conditions for velocity, pressure and temperature from equations (٣.٧), (٣.٨), (٣.٩), (٣.١٠) and (٣.١١).

٣. It calculates the x-momentum equation coefficients from equation (٤.٧.a), (٤.٧.b), (٤.٧.c), (٤.٧.d), (٤.٧.e) and (٤.٧.f).

٤. It creates, initializes and solves the matrix (٤.٦).

٥. It calculates the pressure difference in the axial direction and velocity profile.

٦. It calculates the energy equation coefficients from equation (٤.١٥.a),...,(٤.١٥.e).

٧. It creates, initializes and solves the matrix (٤.١٤) for Constant Wall Temperature boundary condition or (٤.١٩) for Constant Heat Flux boundary condition.

٨. It calculates the temperature distribution.

٩. It calculates the bulk temperature from equation (٤.٢١).

١٠. It calculates the local Nusselt number for Constant Wall Temperature from equation (٤.٢٣), and for Constant Heat Flux from equation (٤.٢٥).

١١. It opens a data file to save the program results in each step of program calculations.

١٢. It prints the results for each step of calculations.

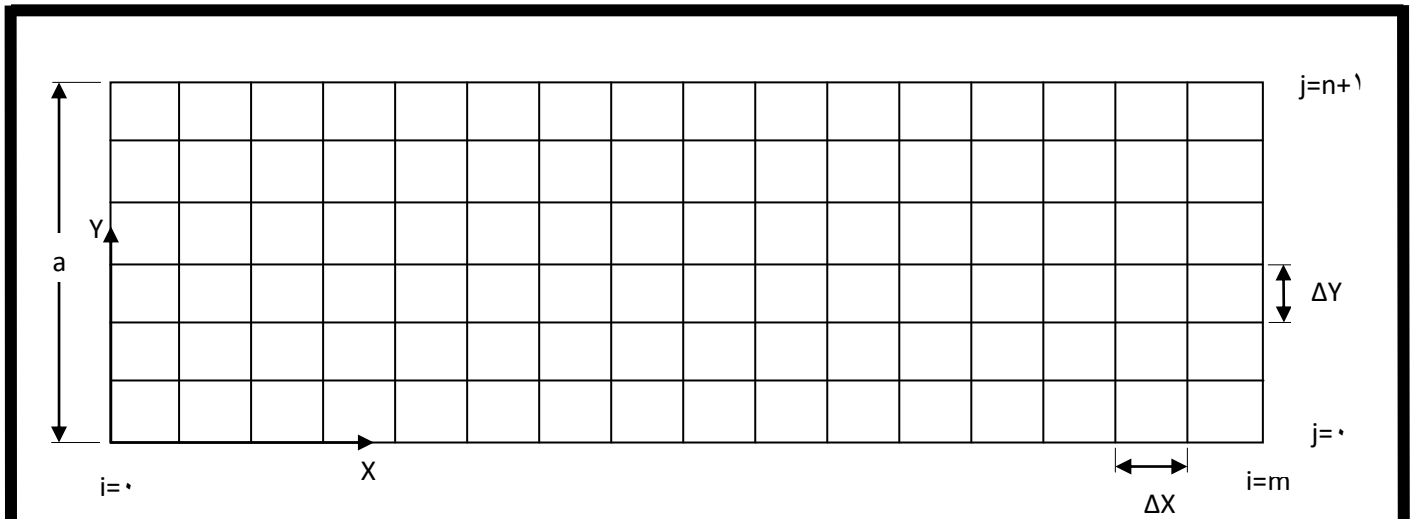

FIGURE (٤-١): Nodal Grid for Parallel Plate Channel

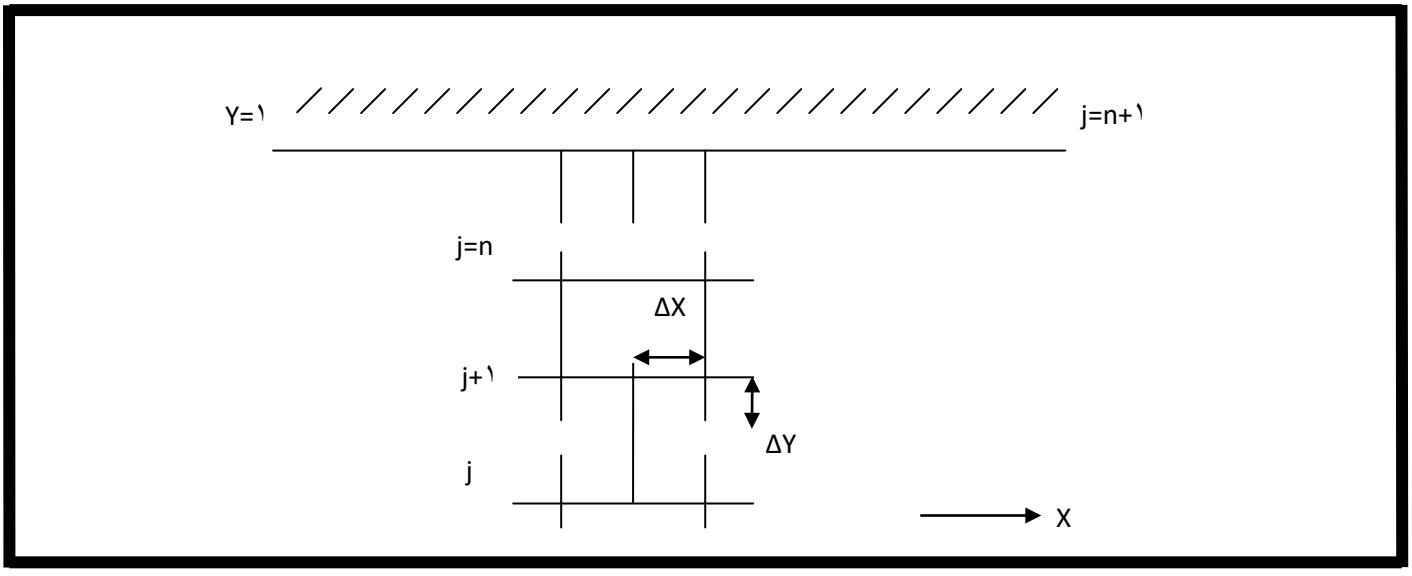

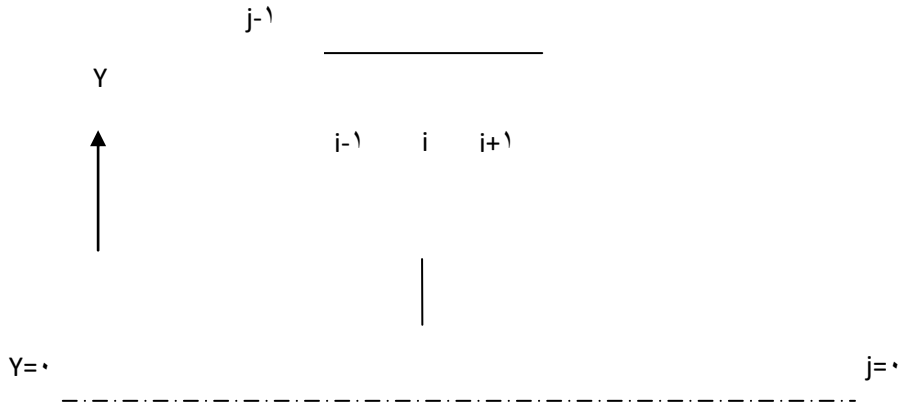

FIGURE (٤-٢): Finite Difference Grid For Parallel Plate Channel

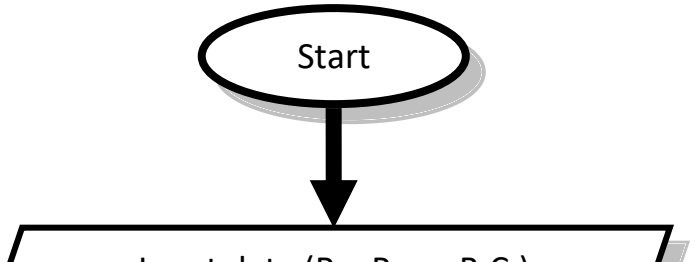

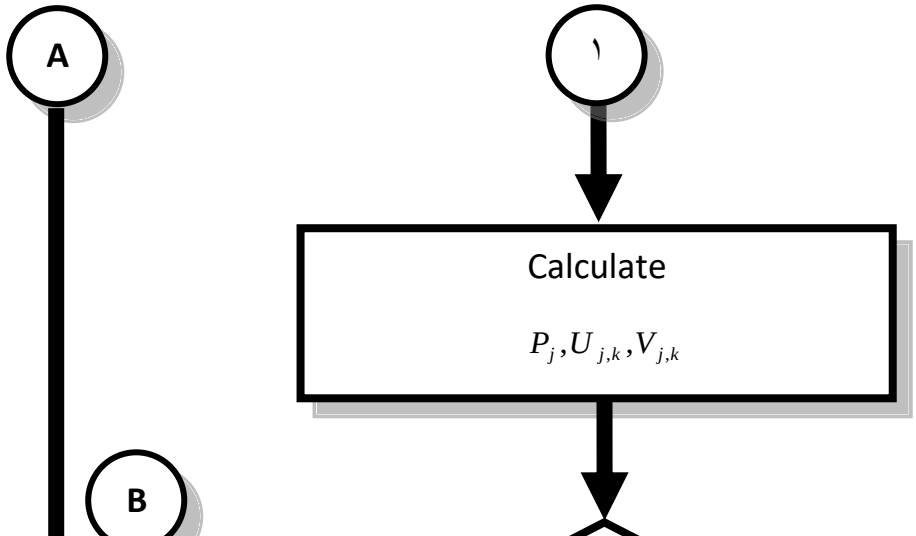
A
١
Calculate
$P_j, U_{j,k}, V_{j,k}$
B

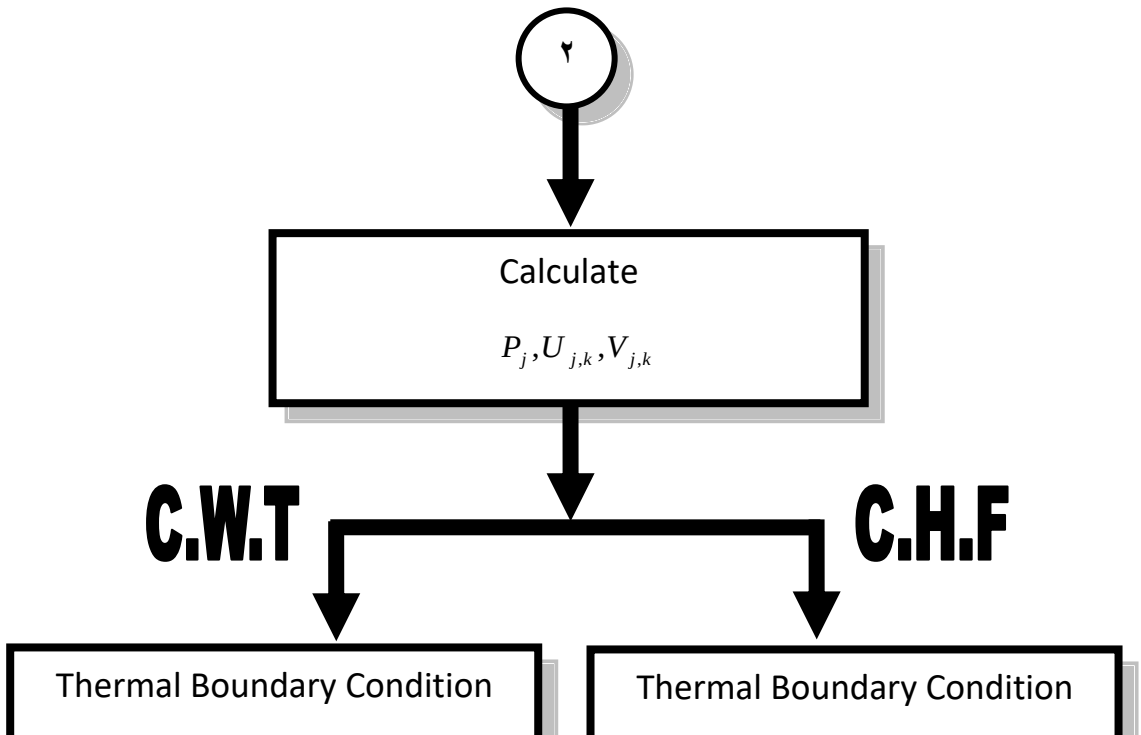
٢
Calculate
$P_j, U_{j,k}, V_{j,k}$
C.W.T
C.H.F
Thermal Boundary Condition
Thermal Boundary Condition

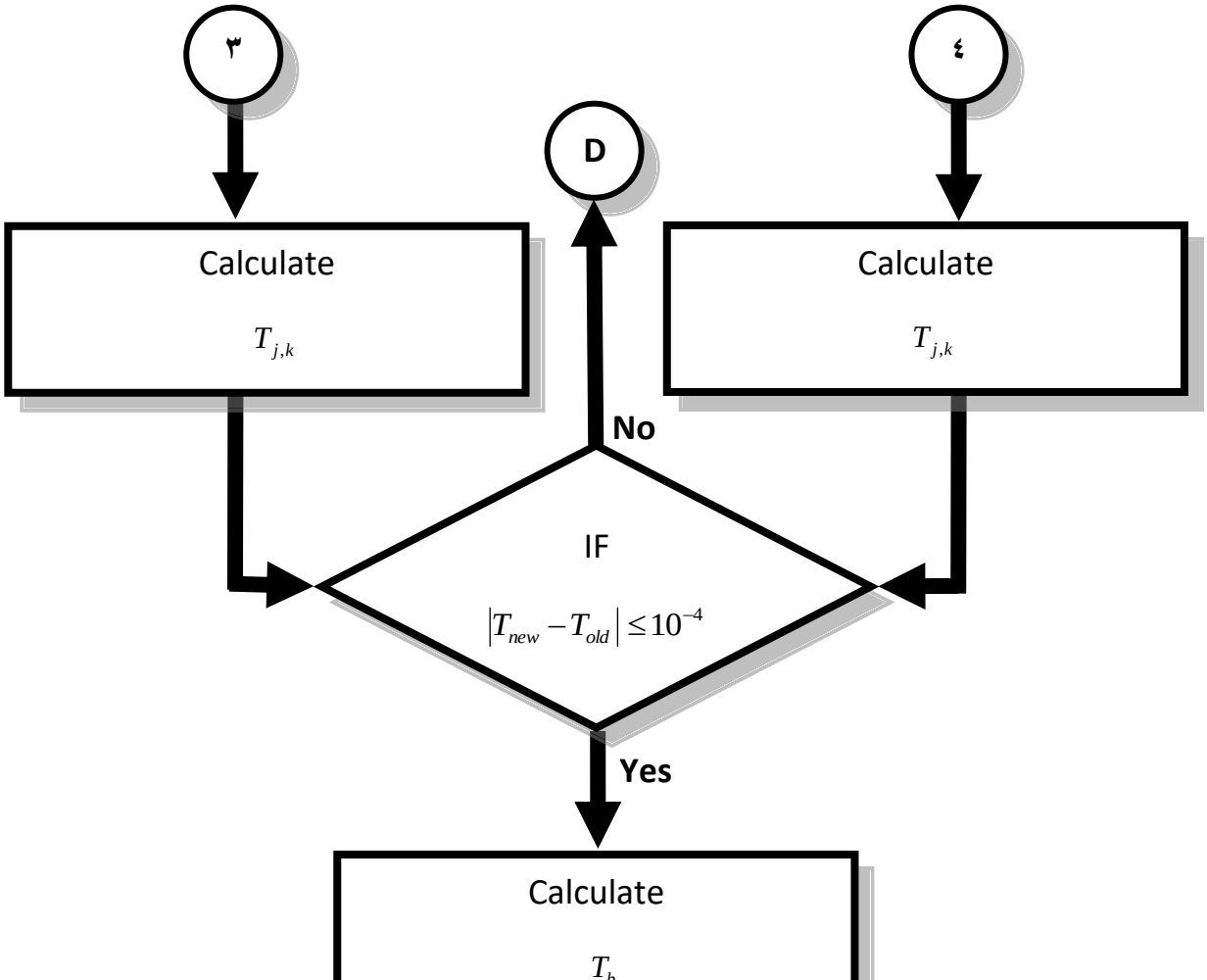
٣
٤
D
Calculate
$T_{j,k}$
Calculate
$T_{j,k}$
No
IF
$|T_{new} - T_{old}| \leq 10^{-4}$
Yes
Calculate
T_b

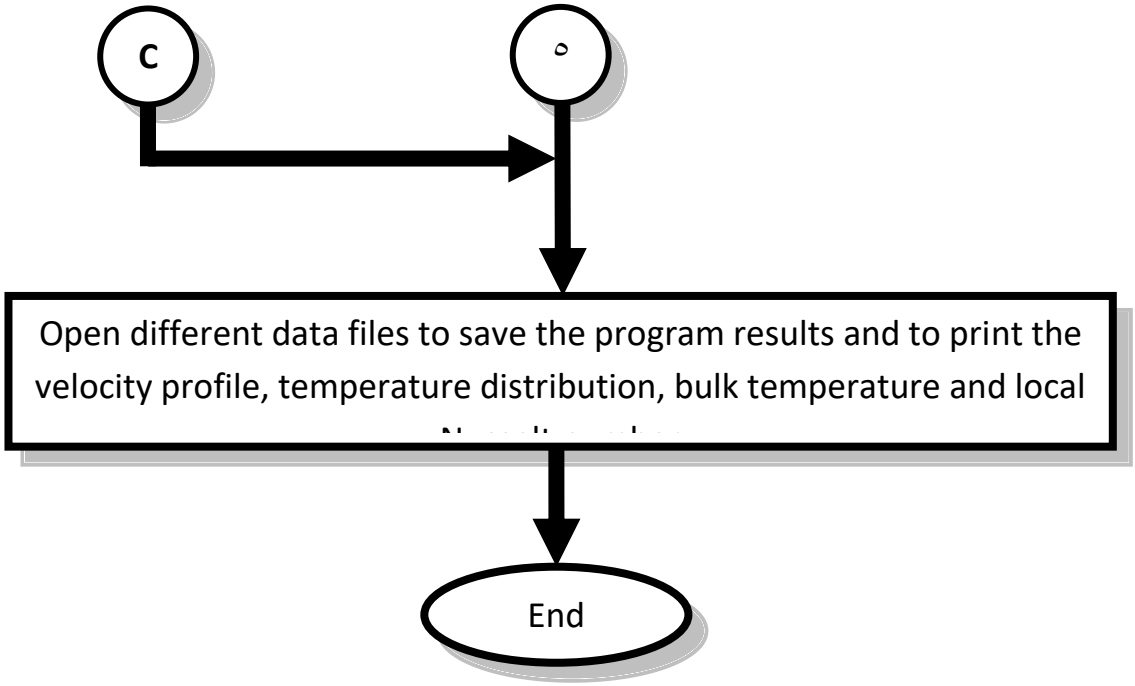

FIGURE (٤-٣): Continued

RESULTS AND DISCUSSION

٥.١ INTRODUCTION

The numerical results are presented and discussed in this chapter for the parallel plate channel. Five values are selected for Reynolds number (Re=١٠٠), (Re=٥٠٠), (Re=١٠٠٠), (Re=١٥٠٠) and (Re=٢٠٠٠) and four values are selected for Prandtl number (Pr=٠.٧), (Pr=١), (Pr=١.٢) and (Pr=٦) for two cases of heating, Constant Wall Temperature and Constant Heat Flux. Results include velocity profile, temperature distribution, bulk temperature, local Nusselt number for both cases. The results of the present work are compared with the previous works by Incropera [١] and Holman [٣٦] present in Table (٥-١), (٥-٢) and (٥-٣).

٥.٢ NUMERICAL SOLUTION LIMITATIONS

The results in this chapter were obtained from the numerical solution (which was explained in chapter four) by using the computer program which was prepared for this purpose. The nodal spacing is constant across the axial direction and vertical direction. (m*(٢*(n+١)+١)) represents the number of nodal points for parallel plate channel. The parallel plate channel problem was solved with (n=٥), but (m) varied corresponding on Reynolds number and Prandtl number (i.e., when the Reynolds number is ١٠٠٠ and Prandtl number is ١, m=٦٠٠).

٥.٣ DEVELOPMENT OF VELOCITY PROFILES

Figures (٥-١.a), (٥-١.b), (٥-١.c), (٥-١.d) and (٥-١.e) show the velocity profiles which manifest stages of developing the hydrodynamic boundary layer for Reynolds numbers (Re=١٠٠), (Re=٥٠٠), (Re=١٠٠٠), (Re=١٥٠٠) and (Re=٢٠٠٠) at different sections of parallel plate channel.

The velocity in the inlet section is uniformly distributed over its width and that its magnitude is ($U=U_o=١$). The velocity at wall equals zero but with an increase distance in y-direction from the surface, the x-direction velocity component of fluid (U), must then increasing until it approaches maximum in centerline of channel. In the fully developed region the vertical velocity component (V) is zero and the gradient of the axial velocity component $\left(\frac{\partial U}{\partial X}\right)$ are everywhere zero. Hence the axial velocity component depends only on (Y), U(X,Y)=U(Y).

The shape of the boundary layer becomes constant after a certain distance from the entrance, which is the so-called “The Hydrodynamic Entry length”. It is noted that the hydrodynamic entrance length increases with the increasing of Reynolds number. It can be seen that the boundary layer is developed faster for the lower Reynolds number, however the flow field is similar for all studied cases. At a large distance from the inlet the velocity distribution becomes parabolic over the width of the channel. The velocity profiles become fully developed at approximately

$$\frac{L_e}{2a} = 0.05\,\mathrm{Re}$$

The resulting velocity profile consist of two boundary layer profiles on the two walls joined in the center by a line of constant velocity. Since the volume of flow the same for every section, the decrease in the rate of flow near the walls which is due to friction must be compensated by a corresponding increase near the axis.

Figure (٥-٢) shows the velocity profiles in the developing and fully developed region for Reynolds number (Re=١٠٠), (Re=٥٠٠), (Re=١٠٠٠), (Re=١٥٠٠) and (Re=٢٠٠٠). In developing region the velocity at the wall equals zero and increases with increasing distance in y-direction from the wall until the maximum velocity at the centerline of the channel, the maximum velocity increases with decreasing Reynolds number but the velocity near the wall increases with increasing Reynolds number. In the fully developed region the velocity at the wall equals zero and increases with increasing distance in y-direction from the wall until maximum velocity at the centerline of the channel, all values of Reynolds number have the same velocity profile in the fully developed region (the velocity profiles in fully developed is independent of Reynolds number).

٥.٤ TEMPERATURE DISTRIBUTION

All figures from (٥-٣.a) to (٥-٧.d) show the dimensionless temperature distribution for Constant Wall Temperature boundary condition which manifests stages of developing of the thermal boundary layer for different Reynolds numbers (Re=١٠٠), (Re=٥٠٠), (Re=١٠٠٠), (Re=١٥٠٠) and (Re=٢٠٠٠),

and different Prandtl numbers (Pr=٠.٧), (Pr=١), (Pr=١.٢) and (Pr=٦), at different sections of parallel plate channel.

The dimensionless temperature in the inlet section is uniformly distributed over its width and that its magnitude is ($\theta=\theta_o=١$). The dimensionless temperature at the walls equals zero but increases with increasing distance in y-direction from the surface, until it approaches the maximum in the centerline of the channel.

The shape of the thermal boundary layer will be fixed after a certain distance from the entrance, which is called "The Thermal Entry Length". It is noted that the thermal entrance length increases with increasing of Reynolds and Prandtl numbers. It can be seen that the thermal boundary layer developed faster for lower Reynolds and Prandtl numbers, however, the flow field is similar for all studied cases. The temperature distribution becomes fully developed at approximately

$$\frac{L_{et}}{2a} = 0.05\,\mathrm{Re}\,.\,\mathrm{Pr}$$

In the fully developed region the gradient of the dimensionless temperature $\left(\frac{\partial\theta}{\partial X}\right)$, is everywhere zero because of the reaching of the fluid temperature to a value close to the wall temperature.

All figures from (٥-٨.a) to (٥-١٢.d) show the dimensionless temperature distribution for Constant Heat Flux boundary condition which manifests stages of developing of the thermal boundary layer for different Reynolds numbers (Re=١٠٠), (Re=٥٠٠), (Re=١٠٠٠), (Re=١٥٠٠) and (Re=٢٠٠٠), and different Prandtl numbers (Pr=٠.٧), (Pr=١), (Pr=١.٢) and (Pr=٦), at different sections of parallel plate channel.

The dimensionless temperature in the inlet section is zero over its width. The dimensionless temperature at the walls equals maximum value but decreases with increasing distance in y-direction from the surface, then it decreases until it approaches minimum in centerline of channel.

The shape of the thermal boundary layer will be fixed after a certain distance from the entrance, which is called “The Thermal Entry Length”. It is noted that the thermal entrance length increases with increasing of Reynolds and Prandtl numbers. It can be seen that the thermal boundary layer is developed faster for lower Reynolds and Prandtl numbers, however the flow field is similar for all studied cases. The temperature distribution becomes fully developed at approximately

$$\frac{L_{et}}{2a} = 0.05\,\mathrm{Re}.\mathrm{Pr}$$

In the fully developed region the gradient of the dimensionless temperature $\left(\frac{\partial\theta}{\partial X}\right)$, is everywhere zero because of the reaching of the fluid temperature to a value close to the wall temperature.

If Prandtl number is greater than one, the hydrodynamic boundary layer develops more rapidly than the thermal boundary layer ($L_e < L_{et}$), while the inverse is true, if Prandtl number less is than one, the thermal boundary layer develops more rapidly than the hydrodynamic boundary layer ($L_{et} < L_e$), but if Prandtl number equals one the hydrodynamic and thermal boundary layer the same ($L_e = L_{et}$).

Figures (٥-١٣), (٥-١٤), (٥-١٥), (٥-١٦) and (٥-١٧) show the developing and fully developed dimensionless temperature distribution in parallel plate channel for Constant Wall Temperature boundary condition and different

Prandtl numbers (Pr=٠.٧), (Pr=١), (Pr=١.٢) and (Pr=٦), figure (٥-١٣) at Reynolds number (Re=١٠٠), figure (٥-١٤) at Reynolds number (Re=٥٠٠), figure (٥-١٥) at Reynolds number (Re=١٠٠٠), figure (٥-١٦) at Reynolds number (Re=١٥٠٠), and figure (٥-١٧) at Reynolds number (Re=٢٠٠٠). In developing region the dimensionless temperature at the walls equals zero and increases with increasing distance in y-direction from the surface until the maximum dimensionless temperature at the centerline of the channel. The maximum dimensionless temperature increases with increasing Prandtl number (maximum dimensionless temperature is one). The dimensionless temperature near the wall increases with increasing Prandtl and Reynolds numbers. For lower Reynolds and Prandtl numbers the dimensionless temperature distribution is parabolic for constant wall temperature, but for high Reynolds (must Re < ٢٣٠٠ for laminar flow) and Prandtl numbers the dimensionless temperature distribution is flatter for Constant Wall Temperature.

In fully developed region the dimensionless temperature at the wall equals zero and increases with increasing distance in y-direction from the wall until the maximum dimensionless temperature at the centerline of the channel, dimensionless temperature distribution is parabolic for Constant Wall Temperature, all values of Reynolds and Prandtl numbers have the same dimensionless temperature distribution in fully developed region (the temperature distribution in fully developed is independent of Reynolds and Prandtl numbers).

Figures (٥-١٨), (٥-١٩), (٥-٢٠) and (٥-٢١) show the developing and fully developed dimensionless temperature distribution in parallel plate channel for Constant Wall Temperature boundary condition and different Reynolds number (Re=١٠٠), (Re=٥٠٠), (Re=١٠٠٠), (Re=١٥٠٠) and (Re=٢٠٠٠), figure (٥-

١٨) at Prandtl number (Pr=٠.٧), figure (٥-١٩) at Prandtl number (Pr=١), figure (٥-٢٠) at Prandtl number (Re=١.٢), figure (٥-٢١) at Prandtl number (Pr=٦). In developing region the dimensionless temperature at the walls equals zero and increases with increasing distance in y-direction from the surface until the maximum dimensionless temperature at the centerline of the channel, the maximum dimensionless temperature depend on Reynolds and Prandtl numbers (maximum dimensionless temperature is one). Effect of Prandtl number higher than effect of Reynolds number through comparison between these figures (from (٥-١٨) to (٥-٢١)) and the previous figures (from (٥-١٣) to (٥-١٧)). The dimensionless temperature near the wall increases with increasing Prandtl and Reynolds numbers. For lower Reynolds and Prandtl numbers the dimensionless temperature distribution is parabolic for Constant Wall Temperature, but for high Reynolds (must Re < ٢٣٠٠ for laminar flow) and Prandtl numbers the dimensionless temperature distribution is flatter for Constant Wall Temperature.

Prandtl number effected on the shape of the dimensionless temperature distribution. The Prandtl number is given by $\Pr = \frac{\nu}{\alpha}$. It is a ratio of kinematic viscosity to thermal diffusivity. Physically, it relates the viscous effects to the thermal effects. When (Pr > ١.٠) then (v > α) and a momentum disturbance propagates farther into the free stream than a thermal disturbance.

In fully developed region the dimensionless temperature at the wall equals zero and increases with increasing distance in y-direction from the wall until the maximum dimensionless temperature at the centerline of the channel, dimensionless temperature distribution is parabolic for Constant Wall Temperature, all values of Reynolds and Prandtl numbers have the same dimensionless temperature distribution in fully developed region (the

temperature distribution in fully developed undepend on Reynolds and Prandtl numbers).

Figures (٥-٢٢), (٥-٢٣), (٥-٢٤), (٥-٢٥) and (٥-٢٦) show the developing and fully developed dimensionless temperature distribution in parallel plate channel for Constant Heat Flux boundary condition and different Prandtl numbers (Pr=٠.٧), (Pr=١), (Pr=١.٢) and (Pr=٦), figure (٥-٢٢) at Reynolds number (Re=١٠٠), figure (٥-٢٣) at Reynolds number (Re=٥٠٠), figure (٥-٢٤) at Reynolds number (Re=١٠٠٠), figure (٥-٢٥) at Reynolds number (Re=١٥٠٠), and figure (٥-٢٦) at Reynolds number (Re=٢٠٠٠). In developing region the dimensionless temperature at the walls equals maximum value and decreases with increasing distance in y-direction from the surface until the minimum dimensionless temperature at centerline of channel, the minimum value of dimensionless temperature approach to zero. In Constant Heat Flux case and for developing region the change of dimensionless temperature usually occurs near the wall, but in the fully developed region the dimensionless temperature start maximum value at the wall and decreases with increasing distance in y-direction from the surface until the minimum value of dimensionless temperature at the centerline of the channel, in the fully developed region all figures have same dimensionless temperature distribution (the dimensionless temperature distribution in fully developed is independent of Reynolds and Prandtl numbers).

Figures (٥-٢٧), (٥-٢٨), (٥-٢٩) and (٥-٣٠) show the developing and fully developed dimensionless temperature distribution in parallel plate channel for Constant Heat Flux boundary condition and different Reynolds number (Re=١٠٠), (Re=٥٠٠), (Re=١٠٠٠), (Re=١٥٠٠) and (Re=٢٠٠٠), figure (٥-٢٧) at Prandtl number (Pr=٠.٧), figure (٥-٢٨) at Prandtl number (Pr=١), figure (٥-٢٩)

at Prandtl number (Re=١.٢), figure (٥-٣٠) at Prandtl number (Pr=٦). In developing region the dimensionless temperature at the walls equals maximum value and decreases with increasing distance in y-direction from the surface until the minimum dimensionless temperature at the centerline of the channel, the minimum value of dimensionless temperature approach to zero. In Constant Heat Flux case and for developing region the change of dimensionless temperature usually occurs near the wall, but in the fully developed region the dimensionless temperature start maximum value at wall and decreases with increasing distance in y-direction from the surface until minimum value of dimensionless temperature at the centerline of the channel. In the fully developed region all figures have same dimensionless temperature distribution (the dimensionless temperature distribution in fully developed region is independent of Reynolds and Prandtl numbers). Effect of Prandtl number is higher than effect of Reynolds number through comparison between these figures (from (٥-٢٧) to (٥-٣٠)) and the previous figures (from (٥-٢٢) to (٥-٢٦)). The shape of the fully developed dimensionless temperature distribution θ(X,Y) differs according to whether a uniform surface temperature or heat flux is maintained.

٥.٥ OVERALL HEATING

Figures (٥-٣١), (٥-٣٢), (٥-٣٣), (٥-٣٤) and (٥-٣٥) show the dimensionless bulk temperature in developing region for Constant Wall Temperature boundary condition and different Prandtl numbers (Pr=٠.٧), (Pr=١), (Pr=١.٢) and (Pr=٦), figure (٥-٣١) at Reynolds number (Re=١٠٠), figure (٥-٣٢) at Reynolds number (Re=٥٠٠), figure (٥-٣٣) at Reynolds number (Re=١٠٠٠),

figure (٥-٣٤) at Reynolds number (Re=١٥٠٠), and figure (٥-٣٥) at Reynolds number (Re=٢٠٠٠). Maximum dimensionless bulk temperature equals to (٠.٩٤) at the first step and decreases this value with increasing the axial distance from inlet. For low Prandtl number the dimensionless bulk temperature is faster the reach to the minimum value (approximately ٠.٦٧) because small thermal entry length and the reverse is true for high Prandtl number. The dimensionless bulk temperature (dimensionless mean temperature) depends on Prandtl, Reynolds number, and the axial distance (X).

Figures (٥-٣٦), (٥-٣٧), (٥-٣٨), (٥-٣٩) and (٥-٤٠) show the dimensionless bulk temperature in developing region for Constant Heat Flux boundary condition and different Prandtl numbers (Pr=٠.٧), (Pr=١), (Pr=١.٢) and (Pr=٦), figure (٥-٣٦) at Reynolds number (Re=١٠٠), figure (٥-٣٧) at Reynolds number (Re=٥٠٠), figure (٥-٣٨) at Reynolds number (Re=١٠٠٠), figure (٥-٣٩) at Reynolds number (Re=١٥٠٠), and figure (٥-٤٠) at Reynolds number (Re=٢٠٠٠). Minimum dimensionless bulk temperature approximately equals to zero in the first step and increases with increasing axial distance from inlet and reaches maximum value of approximately (٠.٠٩١). For low Prandtl number the dimensionless bulk temperature is faster reach to the maximum value (approximately ٠.٠٩١) because small thermal entry length and the reverse is true for high Prandtl number. The dimensionless bulk temperature (dimensionless mean temperature) depends on Prandtl, Reynolds number, and the axial distance (X). For Constant Heat Flux boundary condition the relation is linear as shown in the figures.

٥.٦ LOCAL NUSSULT NUMBER

Figures (٥-٤١), (٥-٤٢), (٥-٤٣) and (٥-٤٤) show the axial development of local Nusselt number of parallel plate channel with Reynolds numbers (Re=١٠٠), (Re=٥٠٠), (Re=١٠٠٠), (Re=١٥٠٠) and (Re=٢٠٠٠), for Constant Wall Temperature boundary condition. figure (٥-٤١) at Prandtl number (Pr=٠.٧), figure (٥-٤٢) at Prandtl number (Pr=١), figure (٥-٤٣) at Prandtl number (Re=١.٢), figure (٥-٤٤) at Prandtl number (Pr=٦). In these figures, Nusselt number has the maximum value at the start of entrance region (first step) and then decreases gradually until it will be close to thermal fully developed region. The boundary layer thickness is zero at the start of entrance region, hence, there is no resistance against heat transfer which leads to raise the heat transfer coefficient value to maximum. So the heat transfer coefficient decreases when the boundary layer begins the process of developing until it reaches a constant value. The length at which the thermal boundary layer is fully developed increases with increasing Reynolds and Prandtl numbers. For Constant Wall Temperature boundary condition, the maximum Nusselt number is (١٢.٧), but the minimum value of Nusselt number is (٤.٣) for all Reynolds and Prandtl numbers. For low Reynolds and Prandtl numbers the local Nusselt number reaches faster the minimum value (small thermal entry length $\frac{L_{et}}{2a} = 0.05\,\mathrm{Re}.\mathrm{Pr}$), and the reverse is true for high Reynolds and Prandtl numbers. The local Nusselt number depends on Prandtl number, Reynolds number, and the axial distance from inlet.

Figures (٥-٤٥), (٥-٤٦), (٥-٤٧) and (٥-٤٨) show the axial development of local Nusselt number of parallel plate channel with Reynolds numbers (Re=١٠٠), (Re=٥٠٠), (Re=١٠٠٠), (Re=١٥٠٠) and (Re=٢٠٠٠), for Constant Heat Flux boundary condition. Figure (٥-٤٥) at Prandtl number (Pr=٠.٧), figure (٥-٤٦) at Prandtl number (Pr=١), figure (٥-٤٧) at Prandtl number (Re=١.٢), figure

(٥-٤٨) at Prandtl number (Pr=٦). In these figures, Nusselt number has the maximum value at the start of entrance region (first step) and then decreases gradually until it will be close to thermal fully developed region. The boundary layer thickness is zero at the start of entrance region, hence, there is no resistance against heat transfer which leads to raise the heat transfer coefficient value to maximum. So the heat transfer coefficient decreases when the boundary layer begins the process of developing until it reaches a constant value. The length at which the thermal boundary layer is fully developed increases with increasing Reynolds and Prandtl numbers. For Constant Heat Flux boundary condition, the maximum Nusselt number is (١٨), but the minimum value of Nusselt number is (٥.٠) for all Reynolds and Prandtl numbers, for low Reynolds and Prandtl numbers the local Nusselt number is faster reach to the minimum value (small thermal entry length $\frac{L_{et}}{2a} = 0.05\,\mathrm{Re}.\mathrm{Pr}$), and the reverse is true for high Reynolds and Prandtl numbers. The local Nusselt number depends on Prandtl number, Reynolds number, and the axial distance from inlet.

It is noted that the local Nusselt number for the Constant Heat Flux case is greater than the local Nusselt number for Constant Wall Temperature case, however, the flow field is similar for all studied cases (same Reynolds and Prandtl numbers). The local Nusselt number changes along the length of the channel, this is confirmed by the result shown in figures (from (٥-٤١) to (٥-٤٨)). Results of this numerical procedure appear to be in a close agreement with the correlation related to it [١], [١٣], [٢٦], [٣٤], and [٣٦].

Table (٥-١) Comparison the hydrodynamic entry length with previous work

	hydrodynamic entry length (L_e)
Incropera [١]	L_e =٠.٠٥ D Re
Holman [٣٦]	L_e =٠.٠٥ D Re
Present work	L_e =٠.٠٥ d Re

Table (٥-٢) Comparison the thermal entry length with previous work

	thermal entry length (L_{et})
Incropera [١]	L_{et} =٠.٠٥ D Pr Re
Holman [٣٦]	L_{et} =٠.٠٥ D Pr Re
Present work	L_{et} =٠.٠٥ d Pr Re

Table (٥-٣) Comparison the Nusselt number with previous work

	Nusselt number (Nu)			
	Maximum value		Minimum value	
	C.W.T	C.H.F	C.W.T	C.H.F
Incropera [١]	١٣	١٤.٨	٣.٦٦	٤.٣٦
Holman [٣٦]	١٢.٨	١٤.٦	٣.٦٦	٤.٣٦٤
Present work	١٢.٨	١٨	٤.٣	٥.١

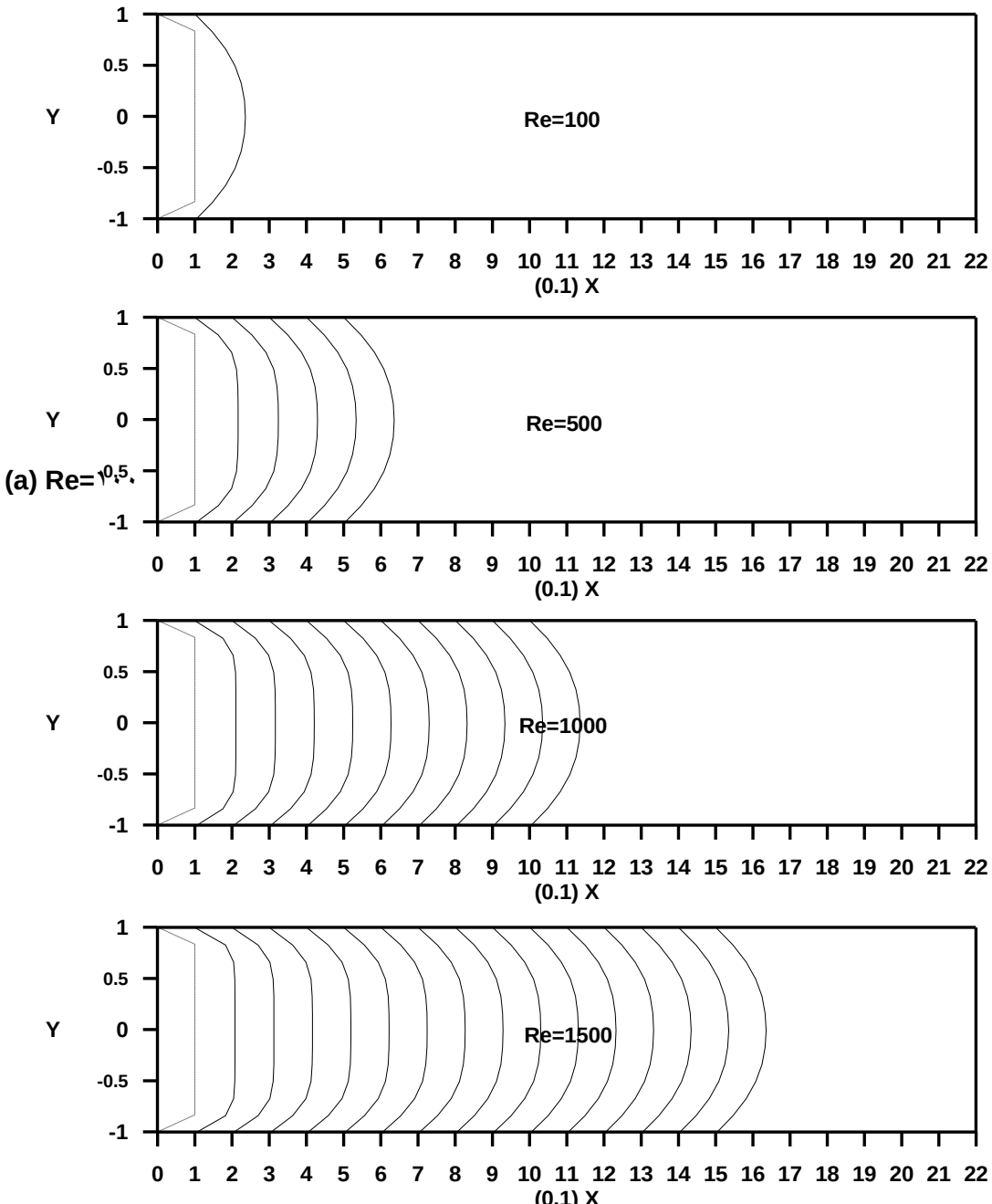

(a) Re=١٠٠،

(b) Re=٥٠٠

(c) Re=١٠٠٠

(d) Re=١٥٠٠

(e) Re=٢٠٠٠

Figure (٥-١) Laminar, hydrodynamic velocity profile development in a parallel plate channel for different Reynolds number

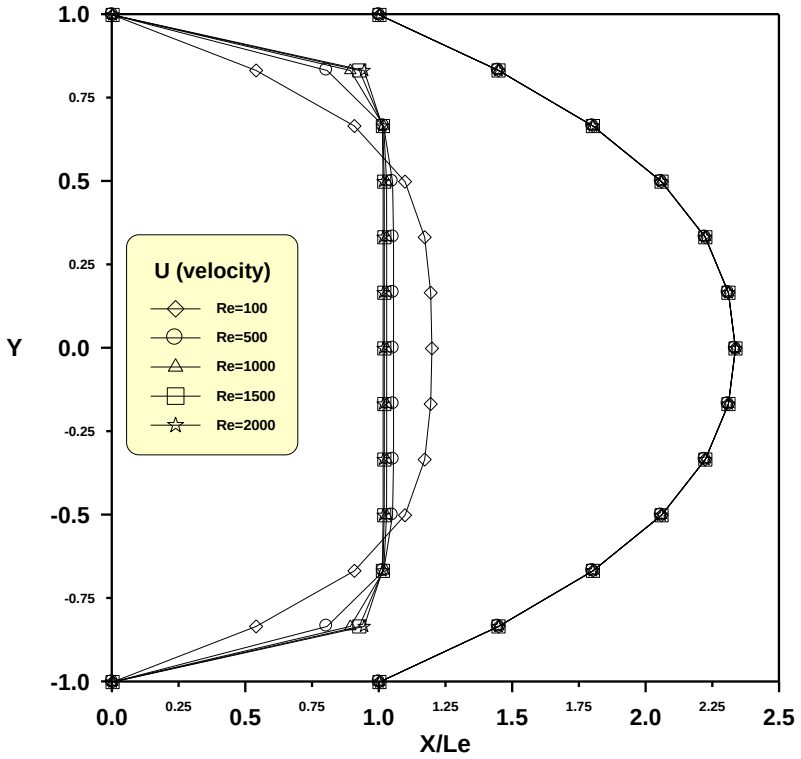

Figure (٥-٢) Developing and fully developed velocity profile in a parallel plate channel for different Reynolds number

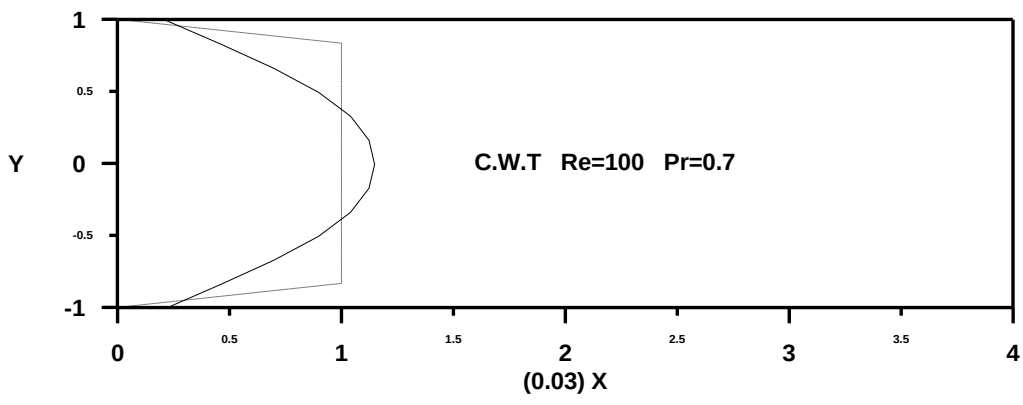
1
0.5
Y
0
-0.5
-1
C.W.T Re=100 Pr=0.7
0
0.5
1
1.5
2
2.5
3
3.5
4
(0.03) X

(a) Pr=٠.٧

(b) Pr=١

(c) Pr=١.٢

(d) Pr=٦

Figure (٥-٣) Laminar, thermal temperature distribution development in a parallel plate channel for constasnt wall temperature, Re=١٠٠, different Prandtl number

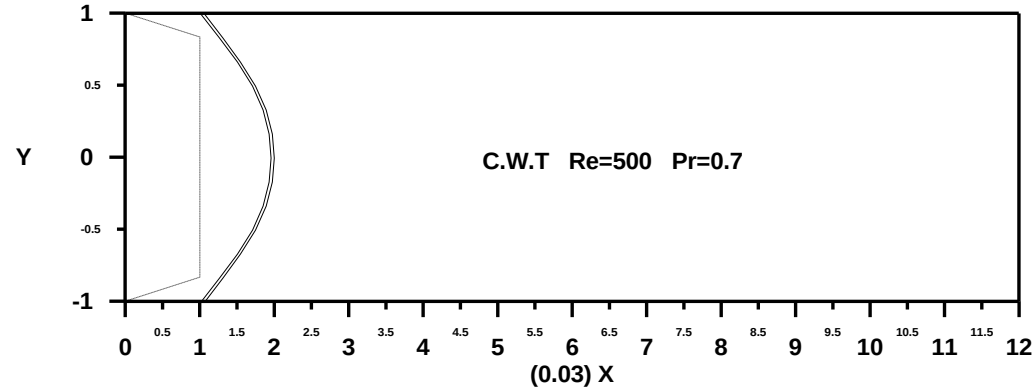

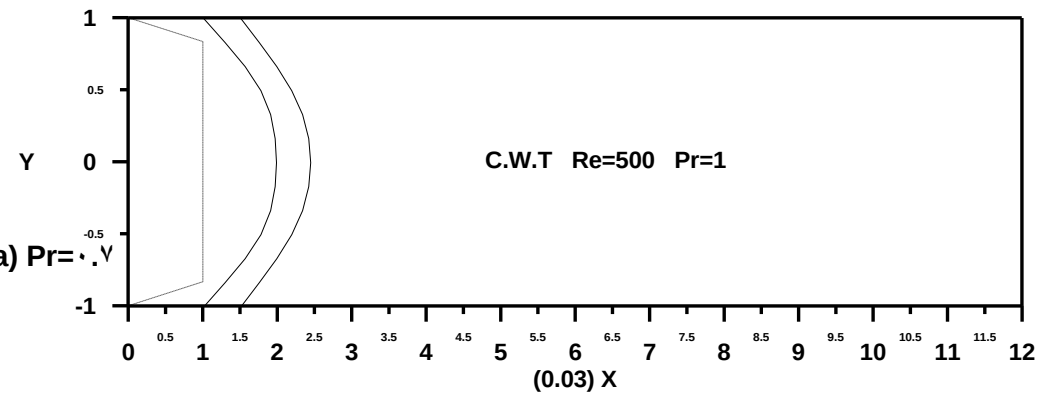

(a) Pr=٠.٧

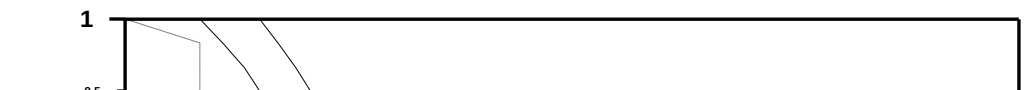

(b) Pr=١

(c) Pr=١.٢

(a) Pr=٠.٧

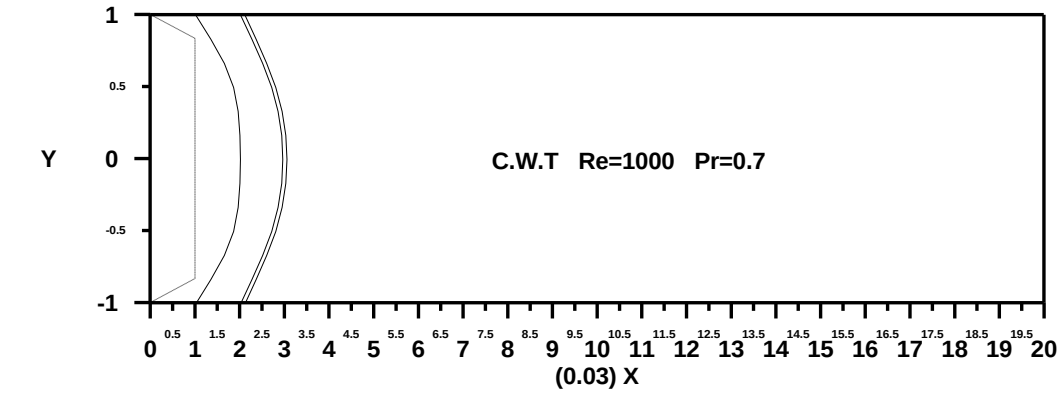

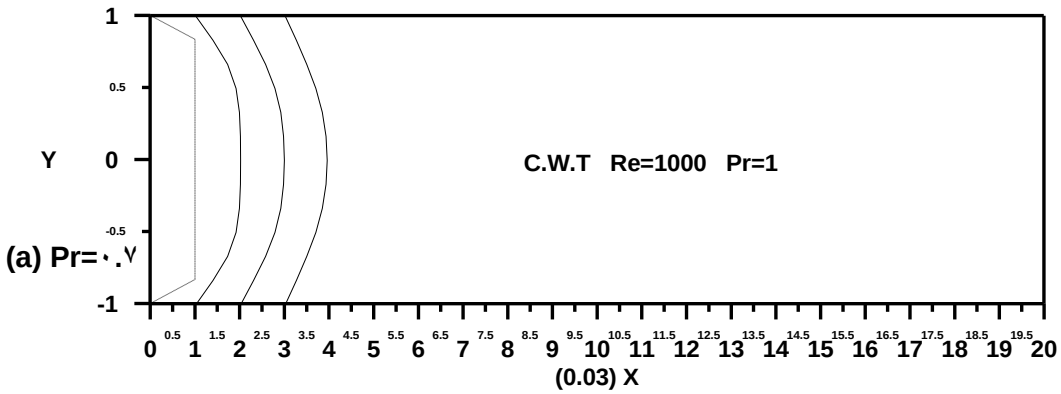

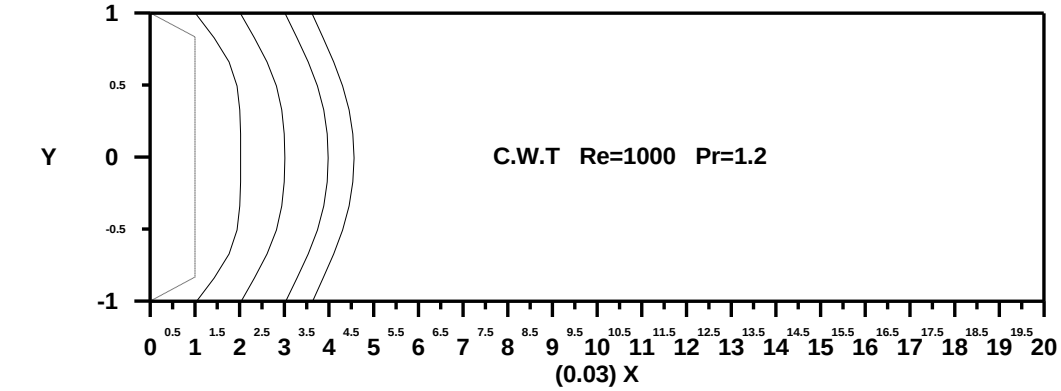

(d) Pr=٦

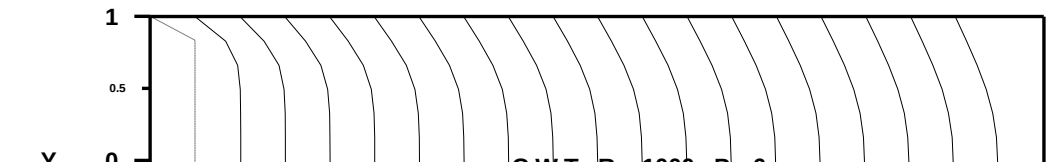

Figure (٥-٤) Laminar, thermal temperature distribution development in a parallel plate channel for constant wall temperature,Re=٥٠٠,different Prandtl number

(b) Pr=١

(c) Pr=١.٢

(d) Pr=٦

Figure (٥-٥) Laminar, thermal temperature distribution development in a parallel plate channel for constant wall temperature, Re=١٠٠٠, different Prandtl number

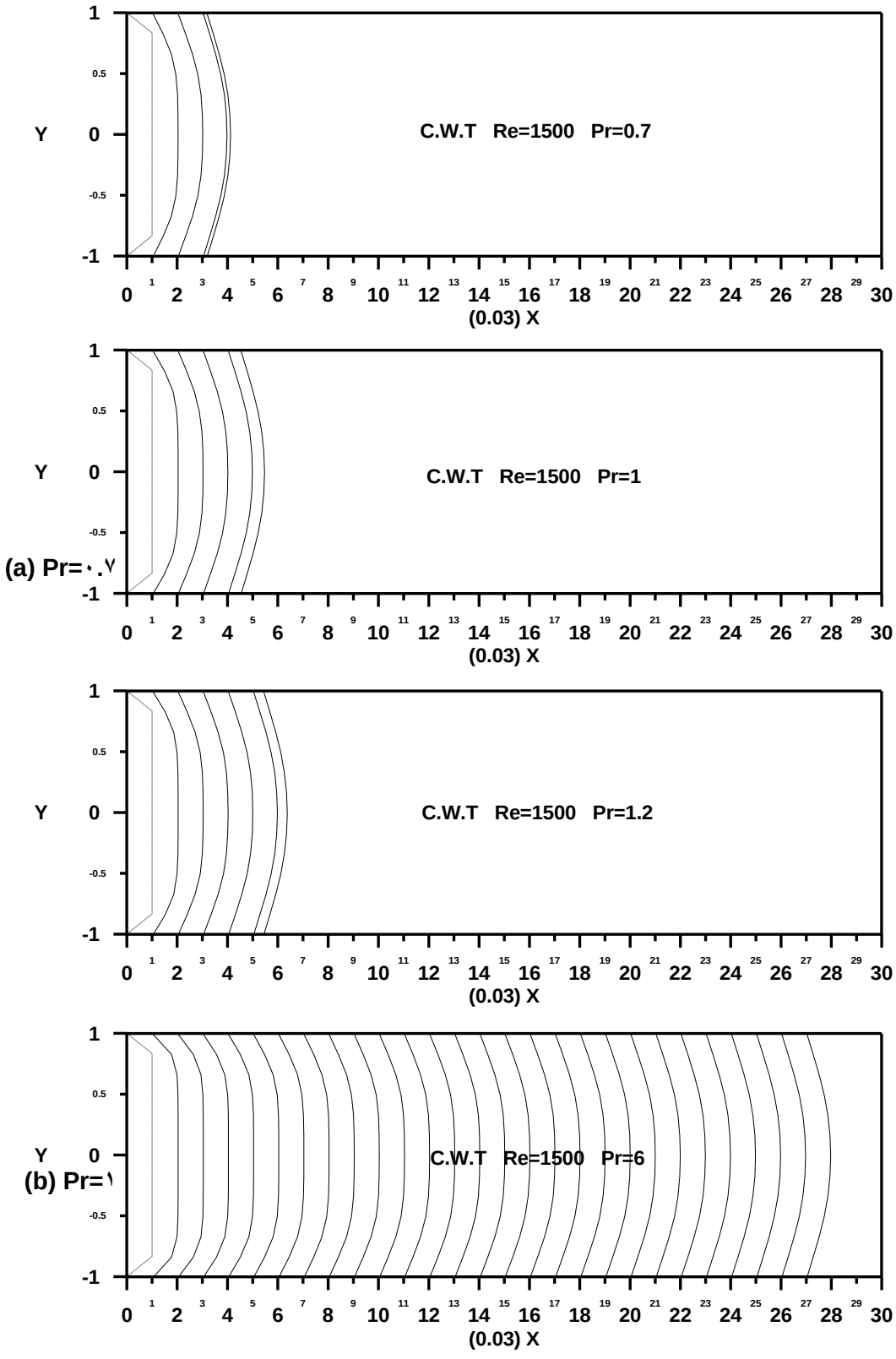

(c) Pr=١.٢

(d) Pr=٦

Figure (٥-٦) Laminar, thermal temperature distribution development in a parallel plate channel for constant wall temperature, Re=١٥٠٠, different Prandtl number

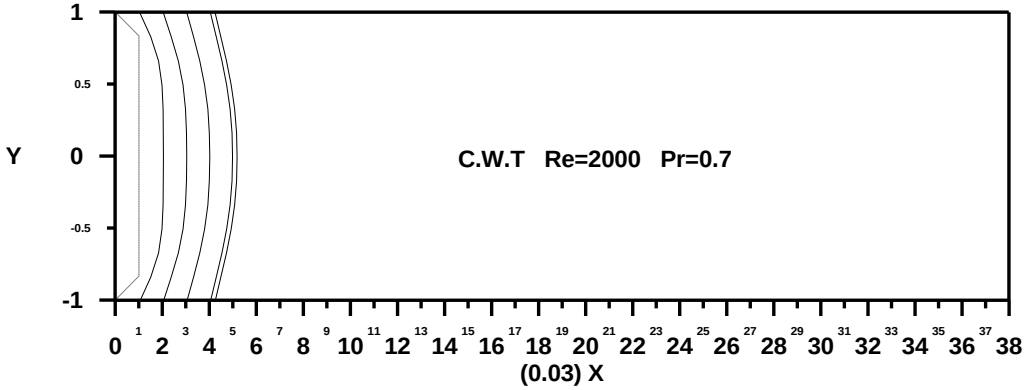

(a) Pr=٠.٧

(b) Pr=١

(a) Pr=٠.٧

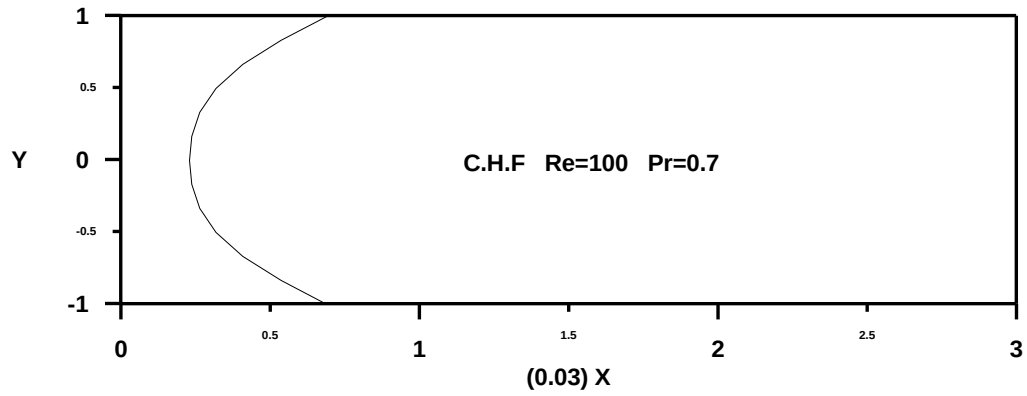

(b) Pr=١

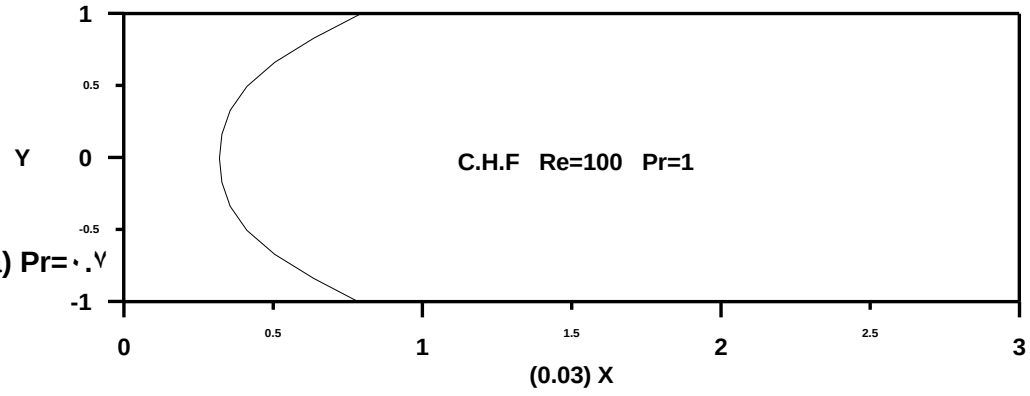

(c) Pr=١.٢

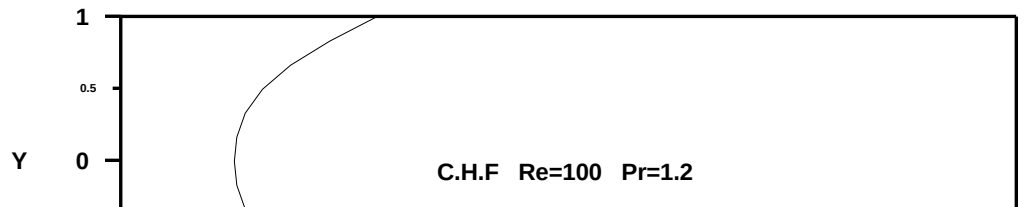

(d) Pr=٦

Figure (٥-٧) Laminar, thermal temperature distribution development in a parallel plate channel for constant wall temperature, Re=٢٠٠٠, different Prandtl number

(b) Pr=١

(c) Pr=١.٢

(d) Pr=٦

Figure (٥-٨) Laminar, thermal temperature distribution development in a parallel plate channel for constant heat flux, Re=١٠٠, different Prandtl number

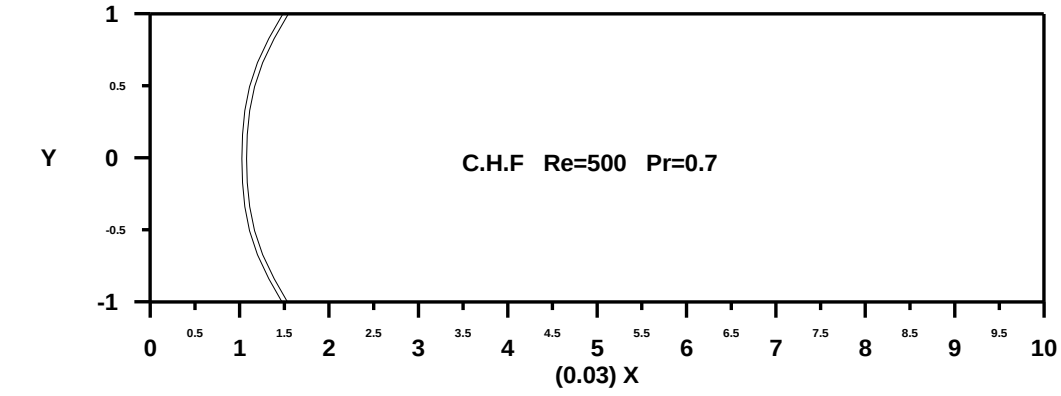

(a) Pr=٠.٧

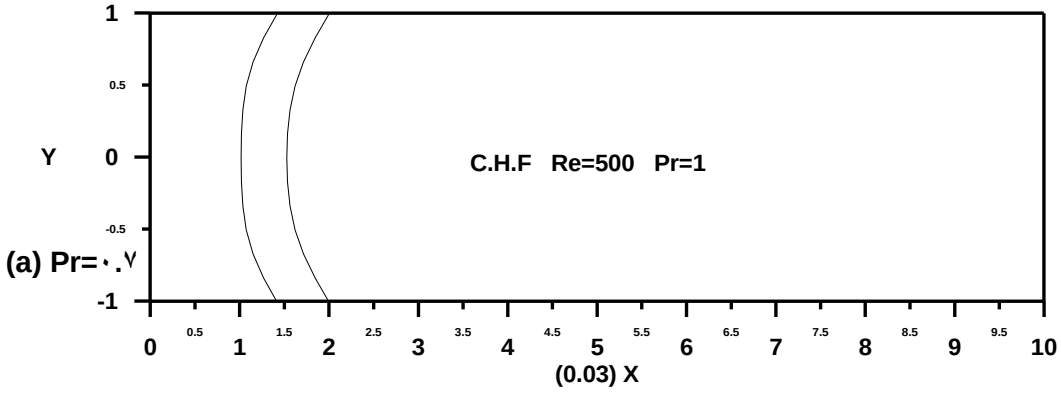

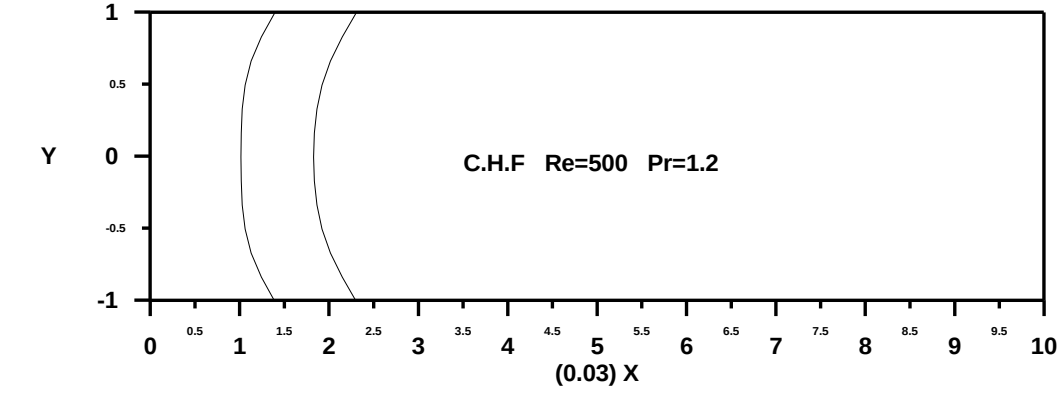

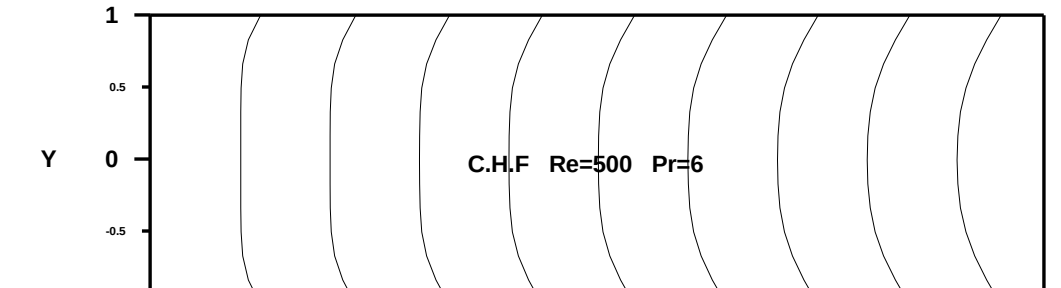

(b) Pr=١

(c) Pr=١.٢

(d) Pr=٦

Figure (٥-٩) Laminar, thermal temperature distribution development in a parallel plate channel for constant heat flux, Re=٥٠٠, different Prandtl number

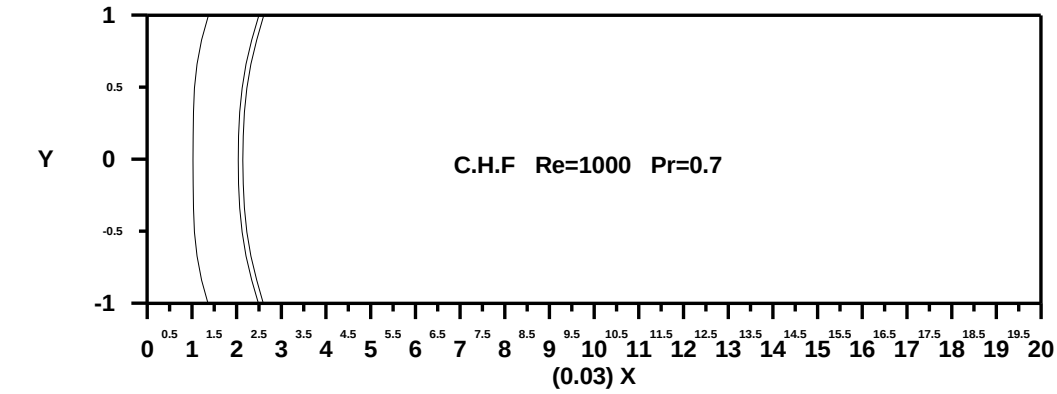
C.H.F Re=1000 Pr=0.7
Y
1
0.5
0
-0.5
-1
0 1 2 3 4 5 6 7 8 9 10 11 12 13 14 15 16 17 18 19 20
(0.03) X

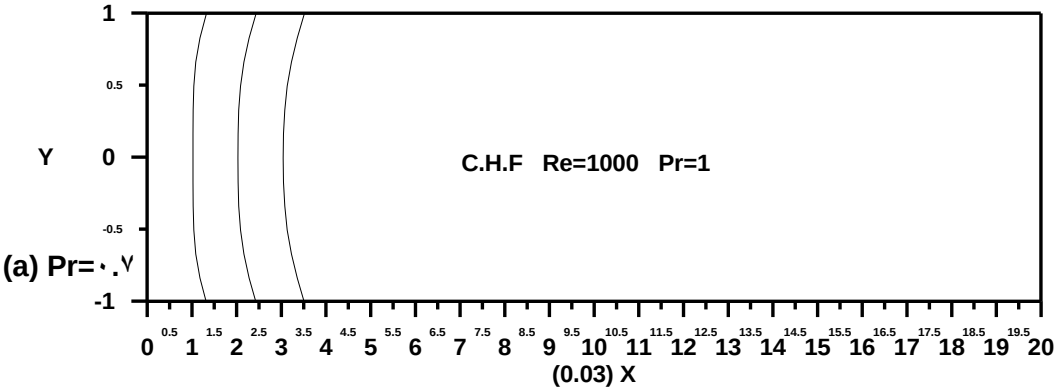
C.H.F Re=1000 Pr=1
Y
1
0.5
0
-0.5
-1
0 1 2 3 4 5 6 7 8 9 10 11 12 13 14 15 16 17 18 19 20
(0.03) X

(a) Pr=٠.٧

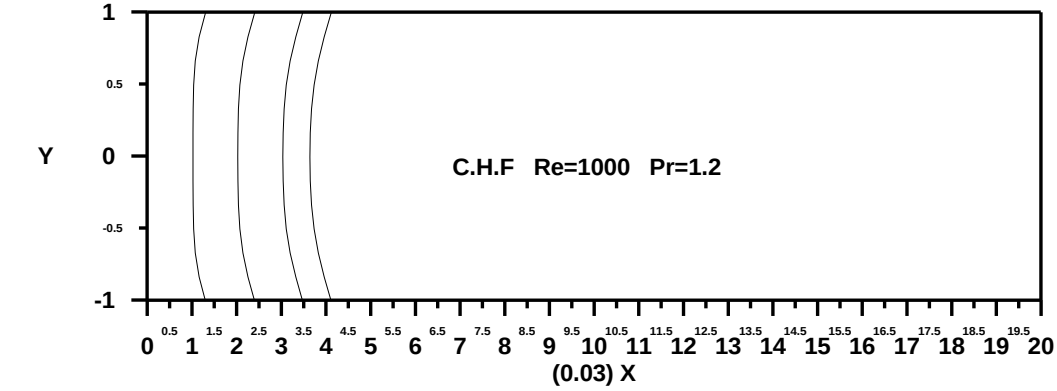
C.H.F Re=1000 Pr=1.2
Y
1
0.5
0
-0.5
-1
0 1 2 3 4 5 6 7 8 9 10 11 12 13 14 15 16 17 18 19 20
(0.03) X

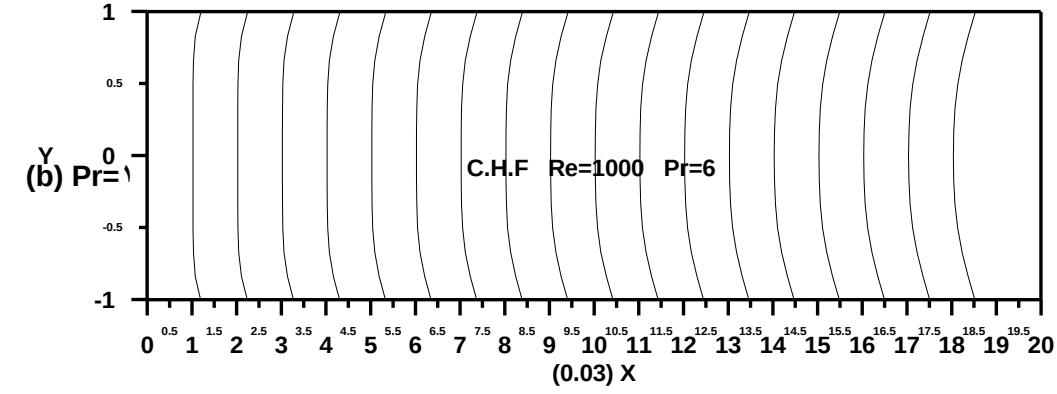
C.H.F Re=1000 Pr=6
Y
1
0.5
0
-0.5
-1
0 1 2 3 4 5 6 7 8 9 10 11 12 13 14 15 16 17 18 19 20
(0.03) X

(b) Pr=١

(c) Pr=١.٢

(d) Pr=٦

Figure (٥-١٠) Laminar, thermal temperature distribution development in a parallel plate channel for constant heat flux, Re=١٠٠٠, different Prandtl number

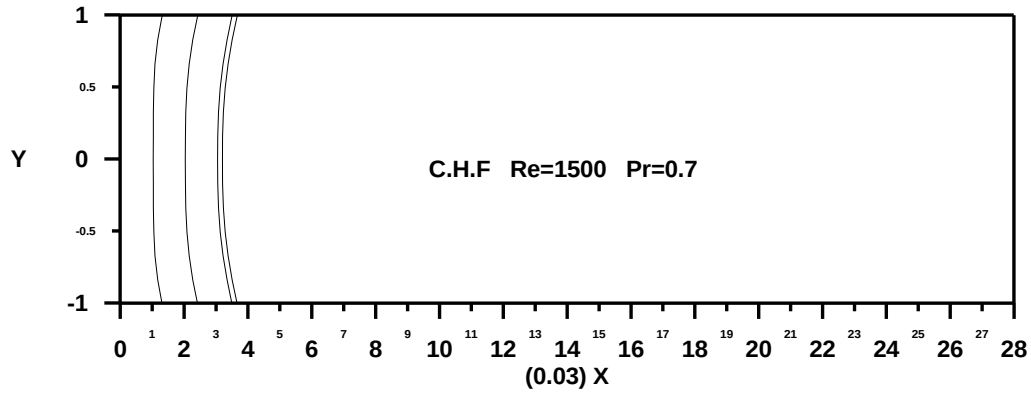

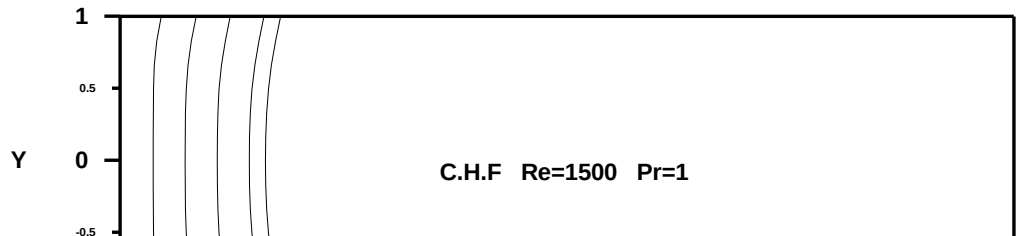

(a) Pr=٠.٧

(b) Pr=١

(c) Pr=١.٢

(d) Pr=٦

Figure (٥-١١) Laminar, thermal temperature distribution development in a parallel plate channel for constant heat flux, Re=١٥٠٠, different Prandtl number

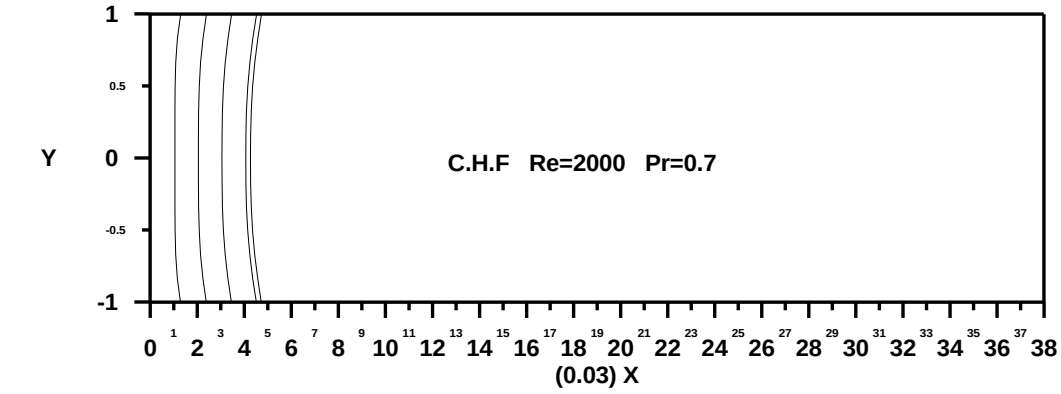

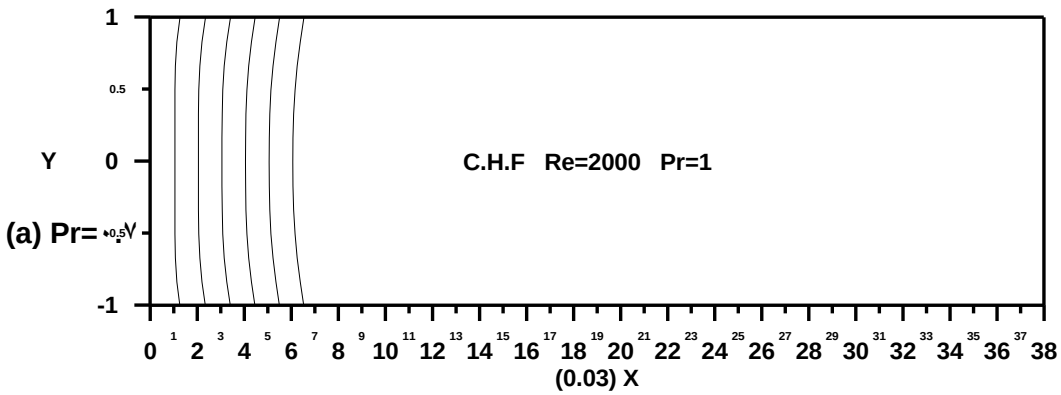

(a) Pr=٠٫٧

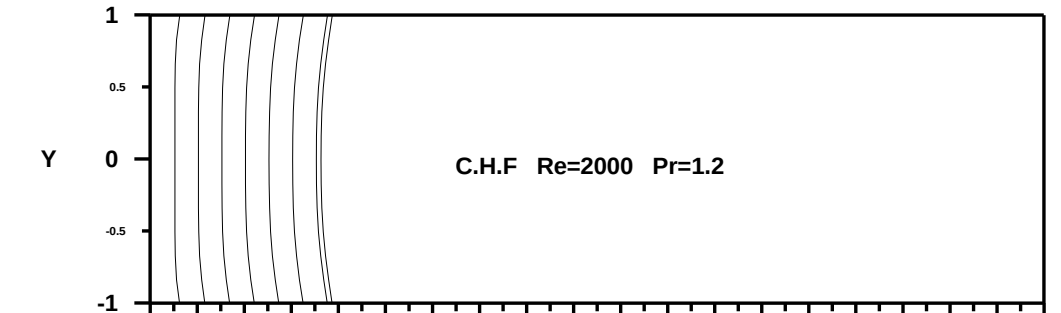

(b) Pr=١

(c) Pr=١.٢

(d) Pr=٦

Figure (٥-١٢) Laminar, thermal temperature distribution development in a parallel plate channel for constant heat flux, Re=٢٠٠٠, different Prandtl number

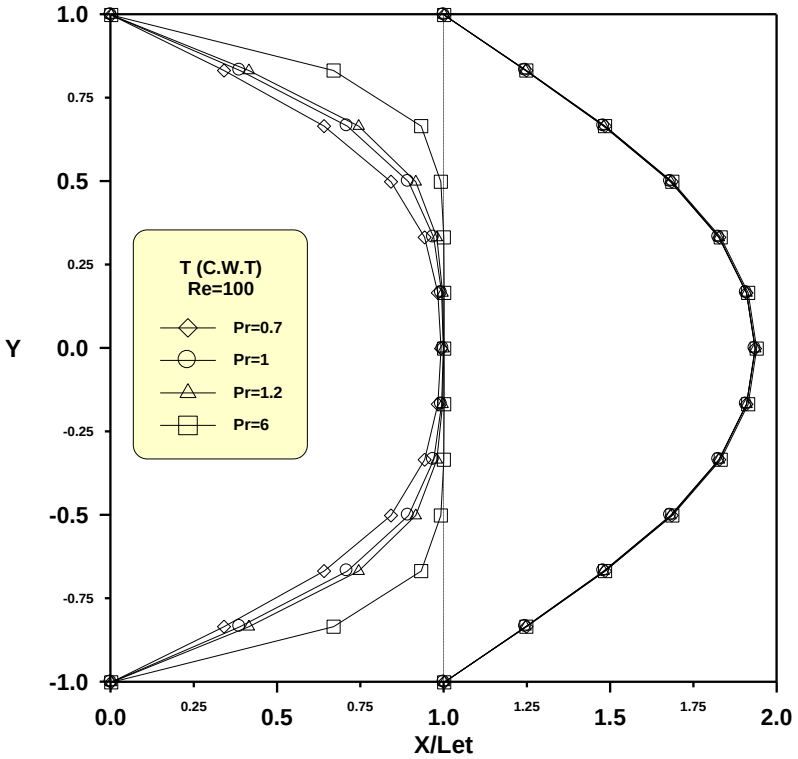

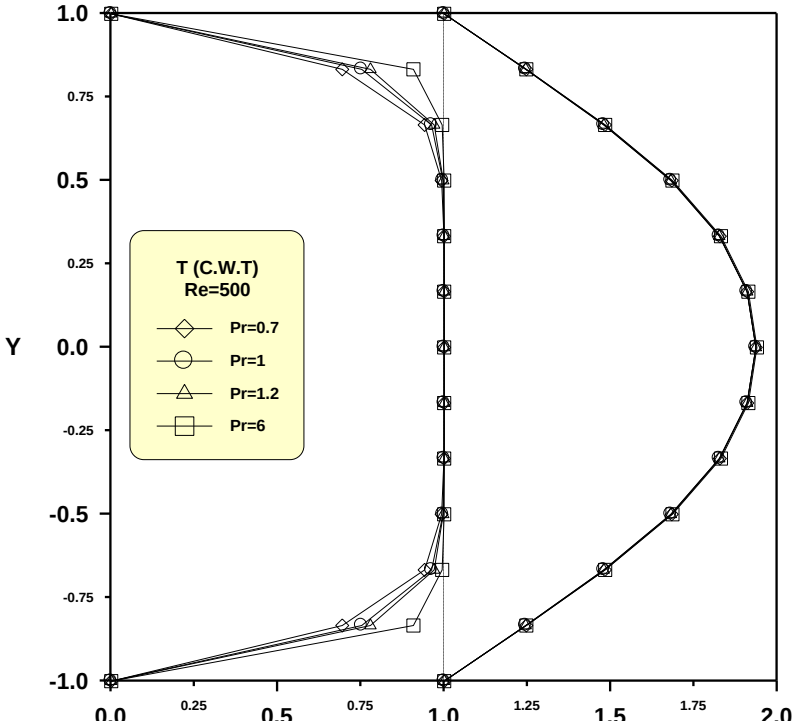

Figure (٥-١٣) Developing and fully developed temperature distribution in a parallel plate channel for constant wall temperature, Re=١٠٠, different Prandtl number

Figure (٥-١٤) Developing and fully developed temperature distribution in a parallel plate channel for constant wall temperature, Re=٥٠٠, different Prandtl number

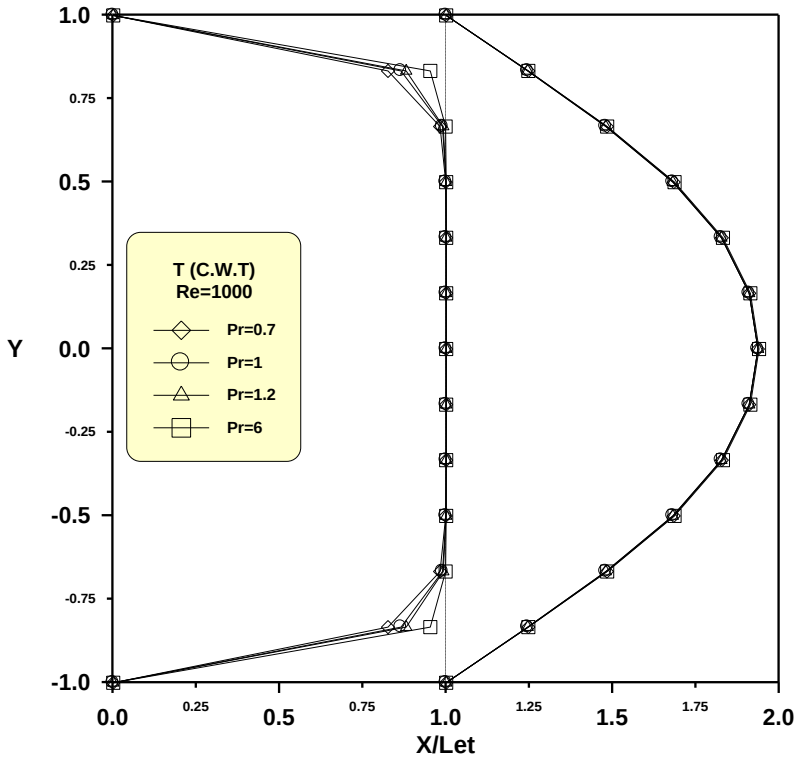

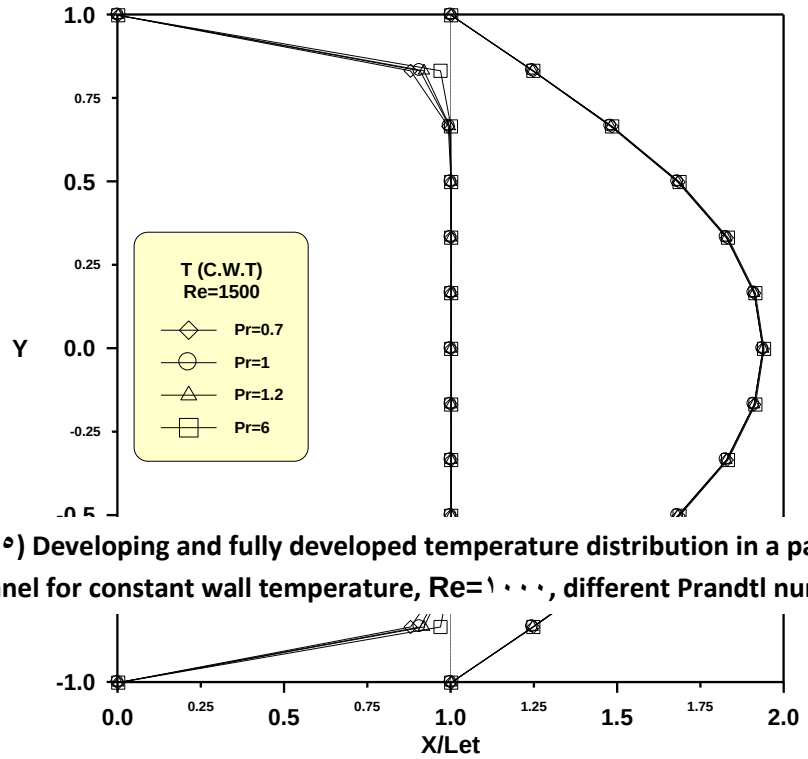

Figure (٥-١٥) Developing and fully developed temperature distribution in a parallel plate channel for constant wall temperature, Re=١٠٠٠, different Prandtl number

Figure (٥-١٦) Developing and fully developed temperature distribution in a parallel plate channel for constant wall temperature, Re=١٥٠٠, different Prandtl number

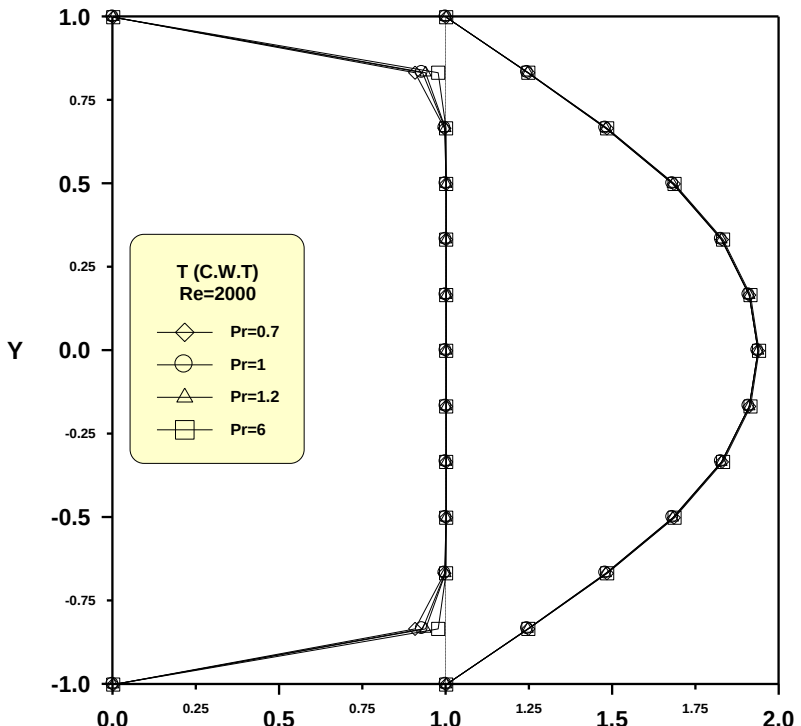

Figure (٥-١٧) Developing and fully developed temperature distribution in a parallel plate channel for constant wall temperature, Re=٢٠٠٠, different Prandtl number

Figure (٥-١٨) Developing and fully developed temperature distribution in a parallel plate channel for constant wall temperature, Pr=٠.٧, different Reynolds number

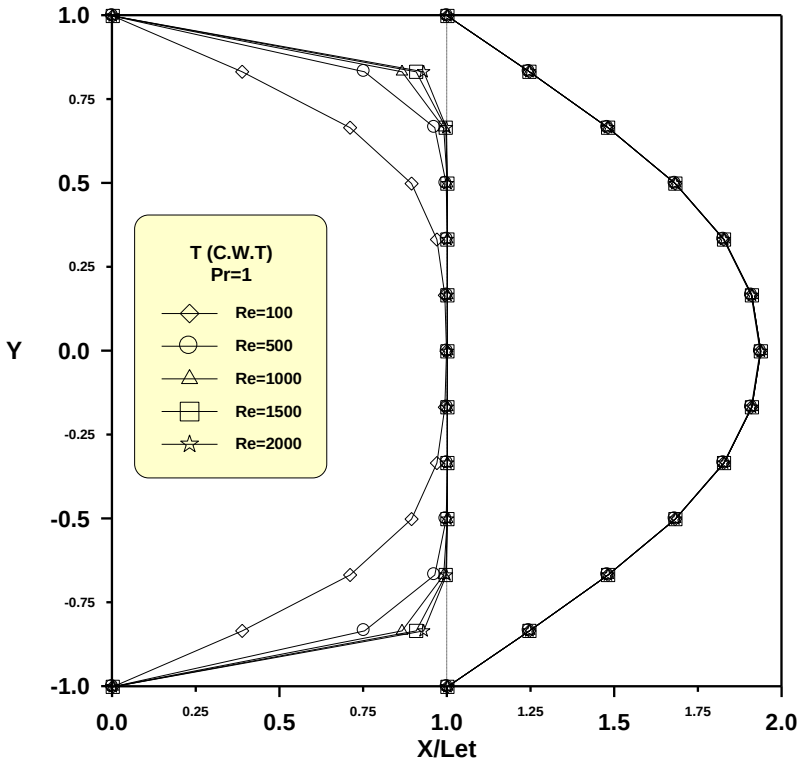

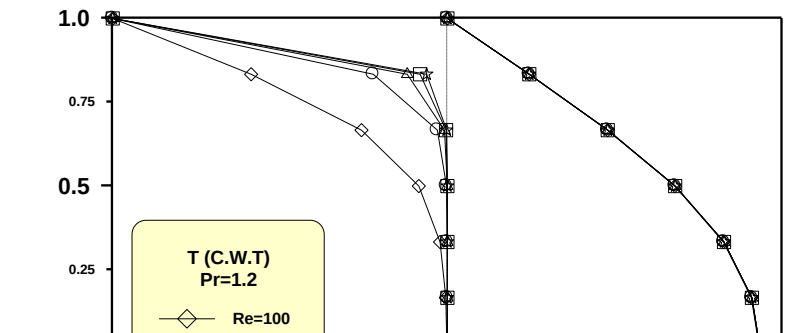

Figure (٥-١٩) Developing and fully developed temperature distribution in a parallel plate channel for constant wall temperature, Pr=١, different Reynolds number

Figure (٥-٢٠) Developing and fully developed temperature distribution in a parallel plate channel for constant wall temperature, Pr=١.٢, different Reynolds number

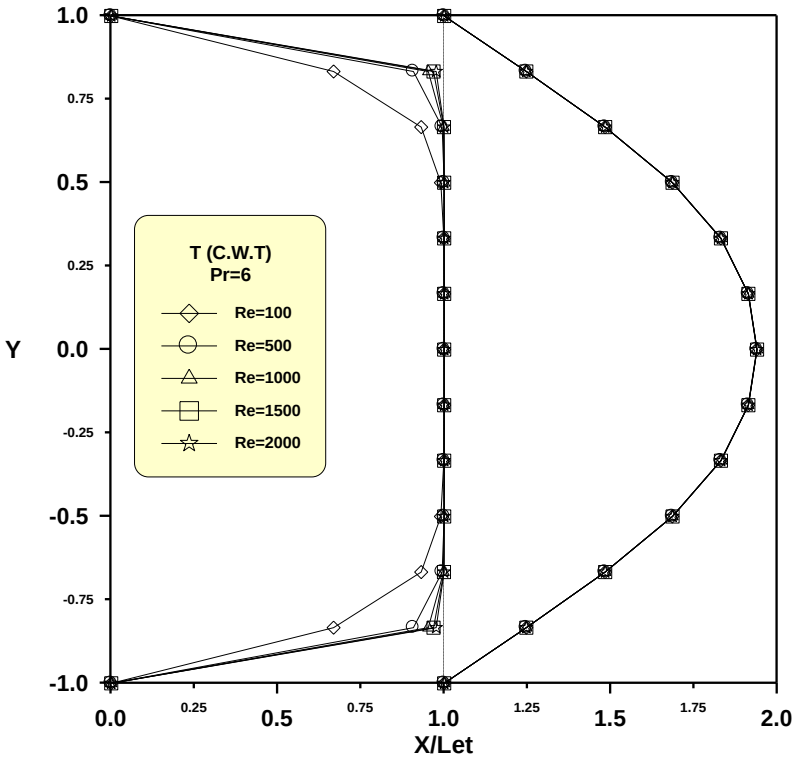

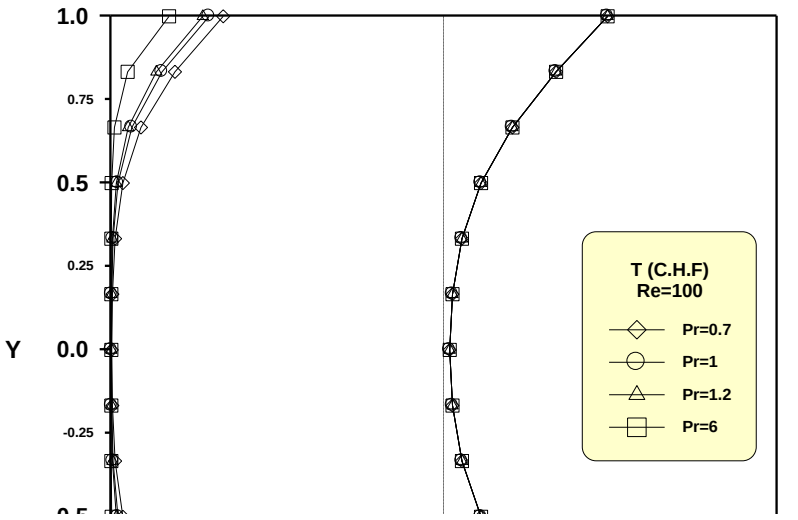

Figure (٥-٢١) Developing and fully developed temperature distribution in a parallel plate channel for constant wall temperature, Pr=٦, different Reynolds number

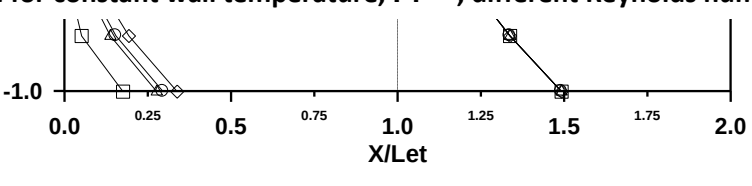

Figure (٥-٢٢) Developing and fully developed temperature distribution in a parallel plate channel for constant heat flux, Re=١٠٠, different Prandtl number

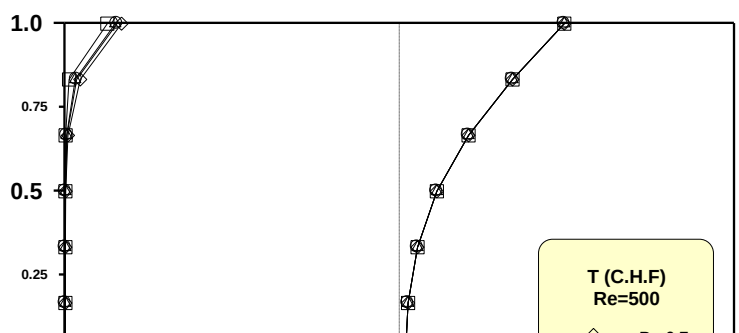

Figure (٥-٢٣) Developing and fully developed temperature distribution in a parallel plate channel for constant heat flux, Re=٥٠٠, different Prandtl number

Figure (٥-٢٤) Developing and fully developed temperature distribution in a parallel plate channel for constant heat flux, Re=١٠٠٠, different Prandtl number

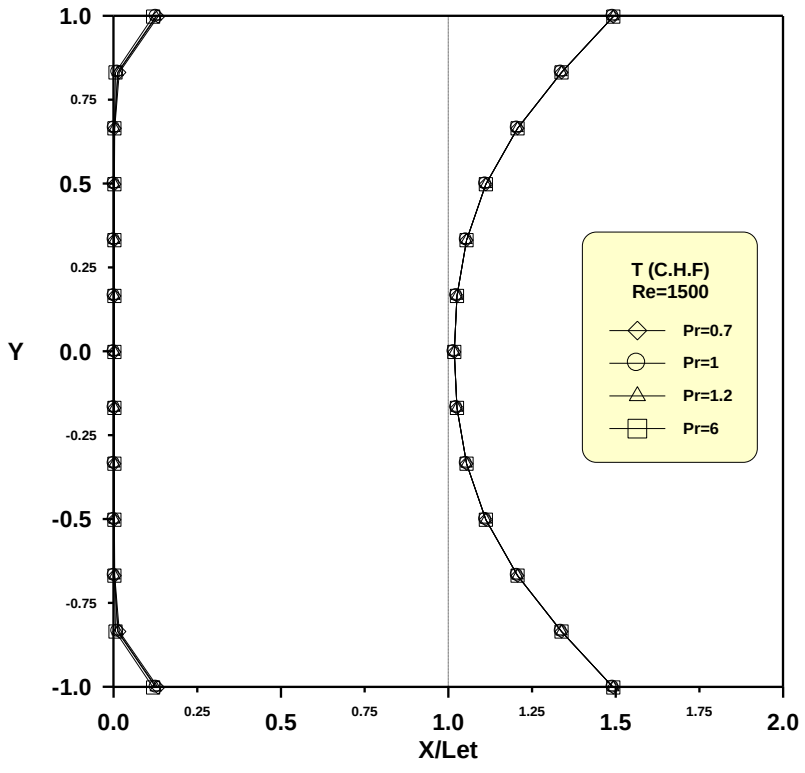

Figure (٥-٢٥) Developing and fully developed temperature distribution in a parallel plate channel for constant heat flux, Re=١٥٠٠, different Prandtl number

Figure (٥-٢٦) Developing and fully developed temperature distribution in a parallel plate channel for constant heat flux, Re=٢٠٠٠, different Prandtl number

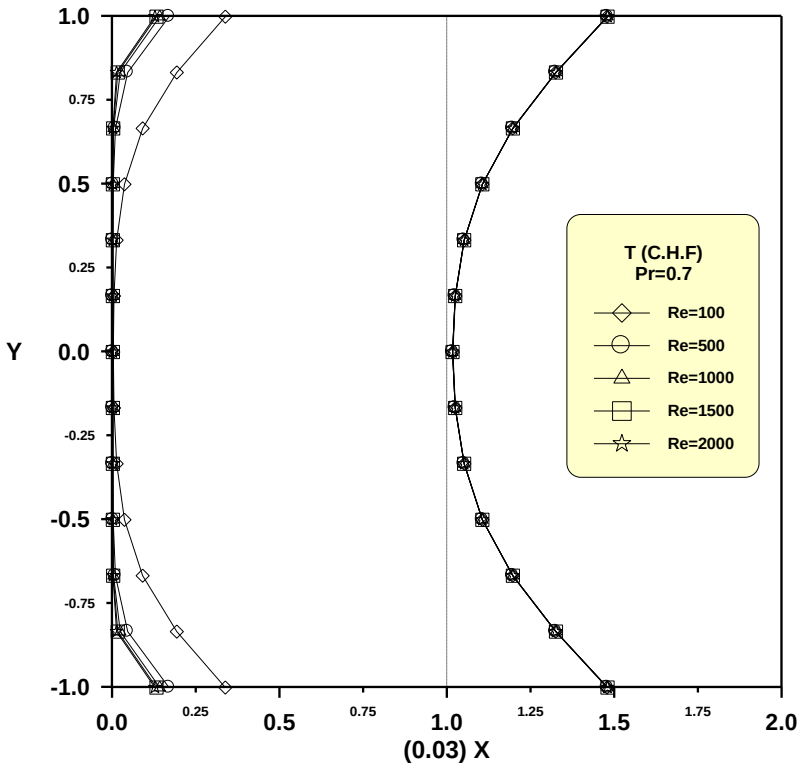

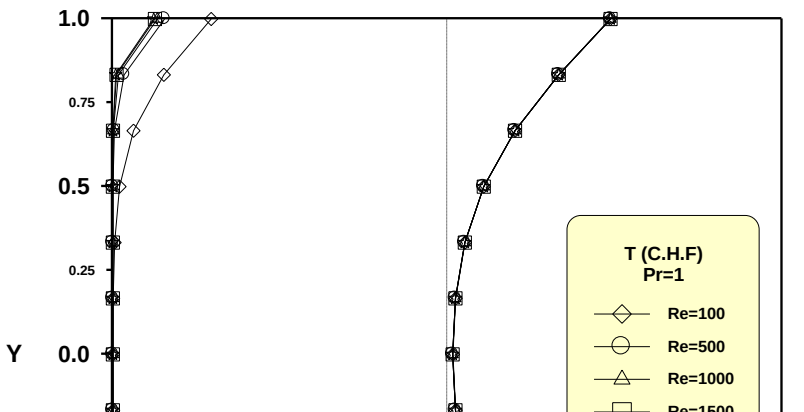

Figure (٥-٢٧) Developing and fully developed temperature distribution in a parallel plate channel for constant heat flux, Pr=٠.٧, different Reynolds number

Figure (٥-٢٨) Developing and fully developed temperature distribution in a parallel plate channel for constant heat flux, Pr=١, different Reynolds number

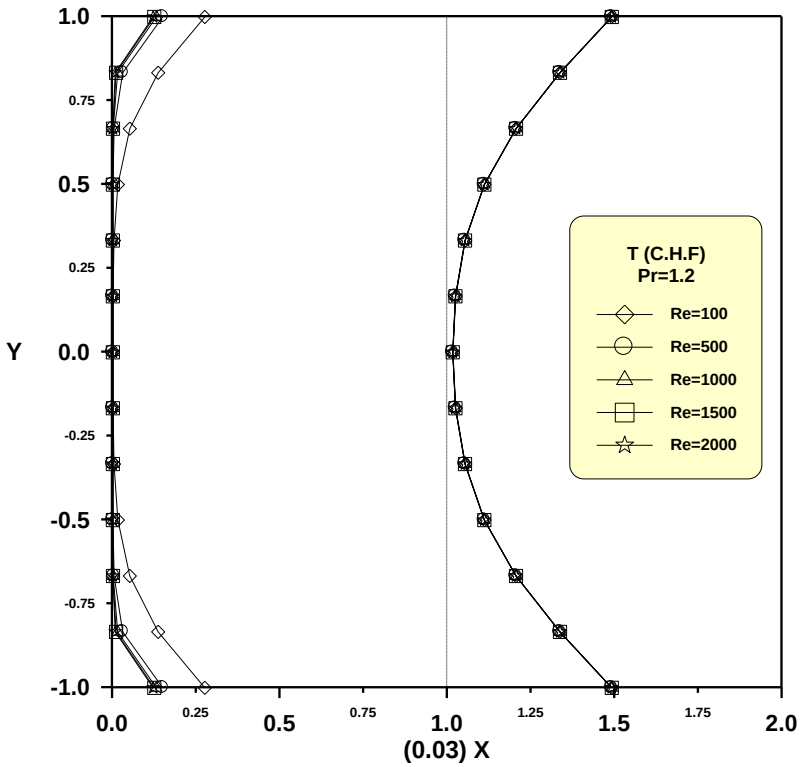

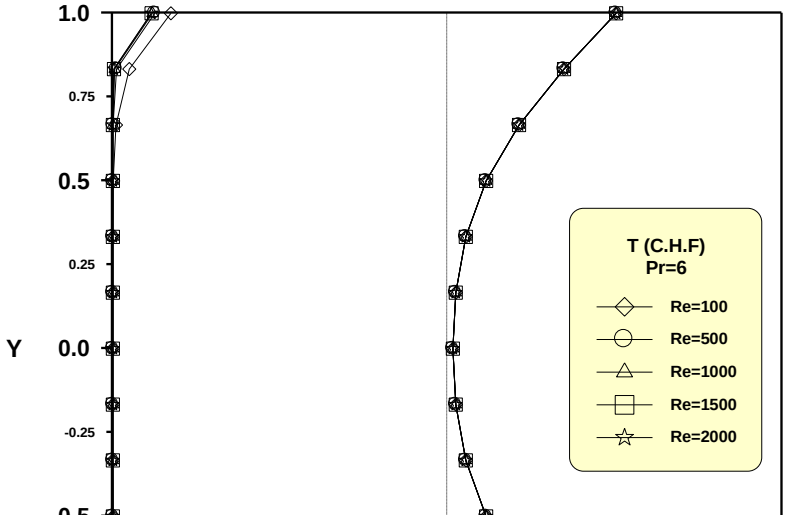

Figure (٥-٢٩) Developing and fully developed temperature distribution in a parallel plate channel for constant heat flux, Pr=١.٢, different Reynolds number

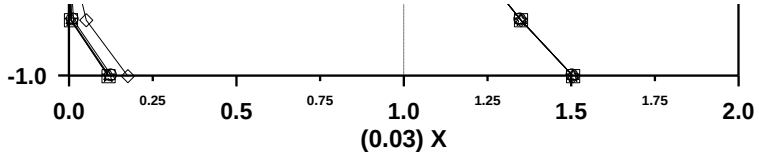

Figure (٥-٣٠) Developing and fully developed temperature distribution in a parallel plate channel for constant heat flux, Pr=٦, different Reynolds number

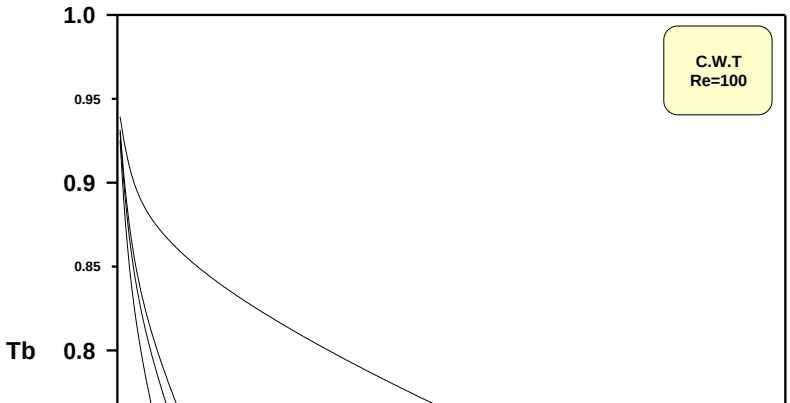

Figure (٥-٣١) Bulk temperature in a parallel plate channel for constant wall temperature, Re=١٠٠, different Prandtl number

Figure (٥-٣٢) Bulk temperature in a parallel plate channel for constant wall temperature, Re=٥٠٠, different Prandtl number

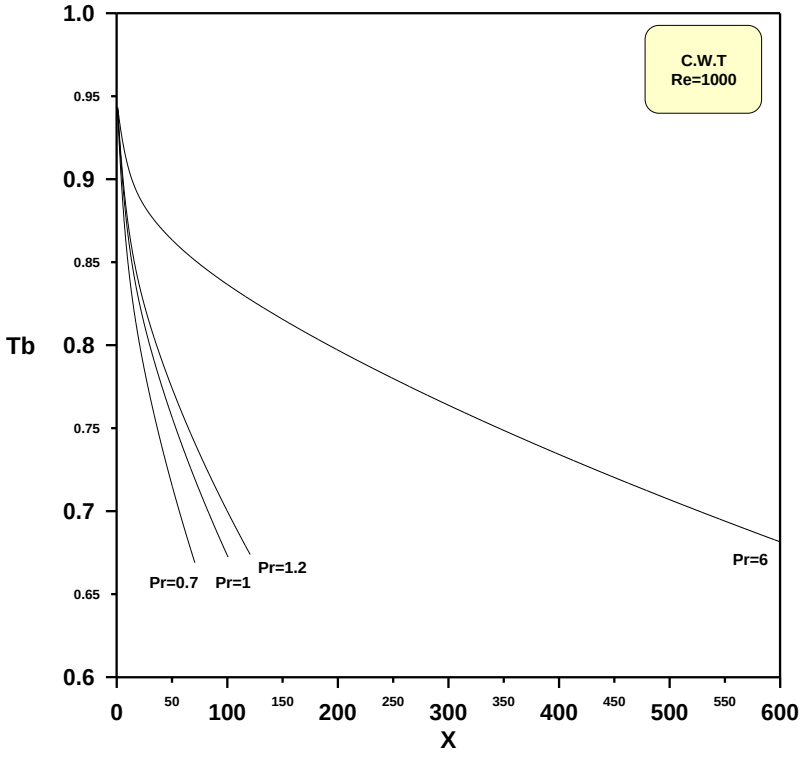

Figure (٥-٣٣) Bulk temperature in a parallel plate channel for constant wall temperature, Re=١٠٠٠, different Prandtl number

Figure (٥-٣٤) Bulk temperature in a parallel plate channel for constant wall temperature, Re=١٥٠٠, different Prandtl number

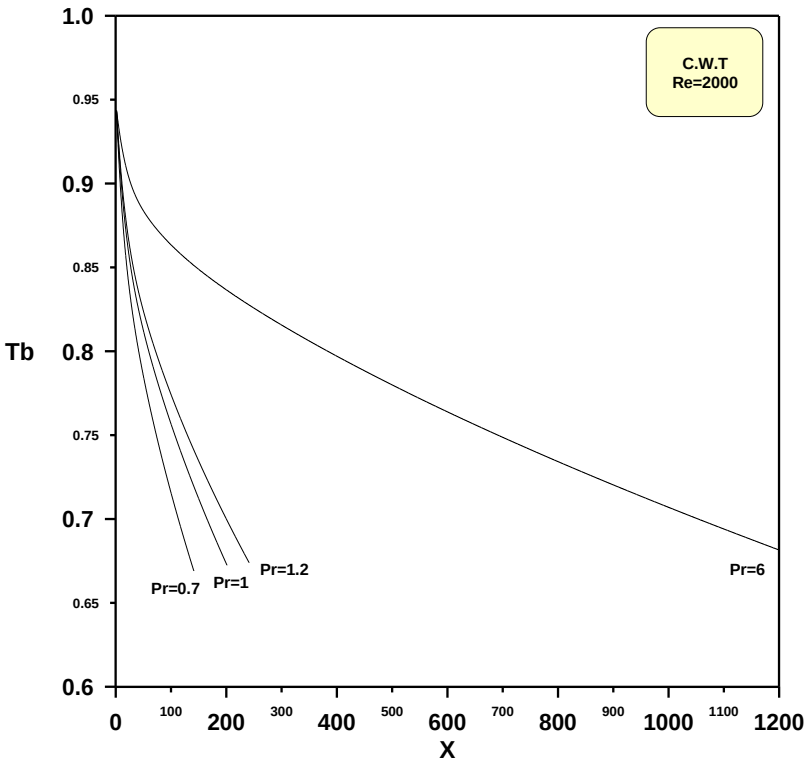

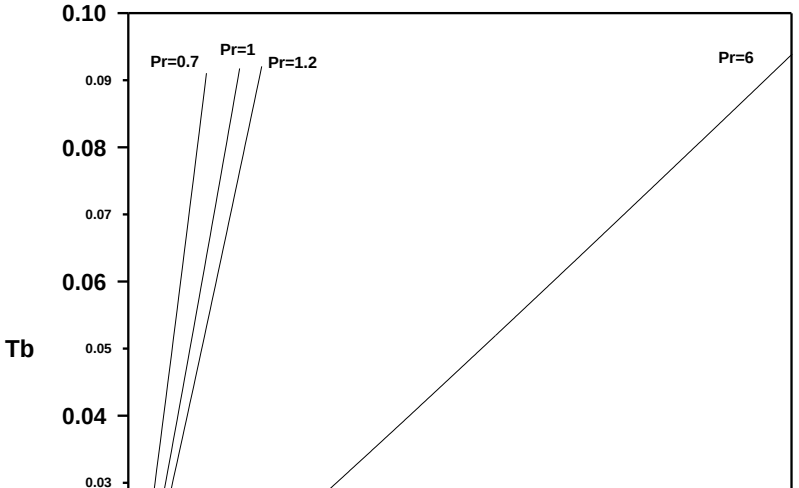

Figure (٥-٣٥) Bulk temperature in a parallel plate channel for constant wall temperature, Re=٢٠٠٠, different Prandtl number

Figure (٥-٣٦) Bulk temperature in a parallel plate channel for constant heat flux, Re=١٠٠, different Prandtl number

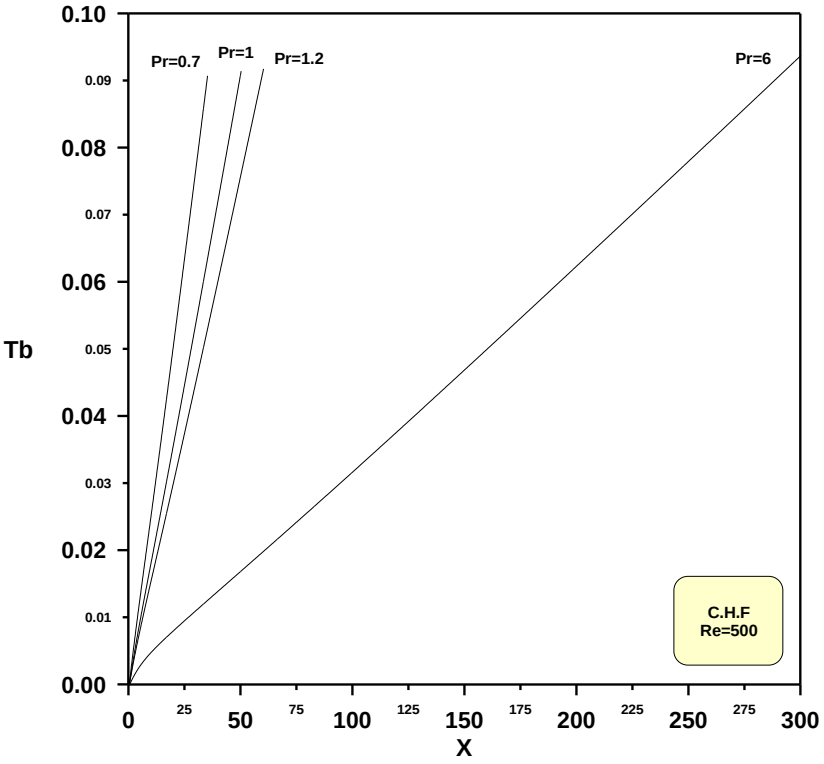

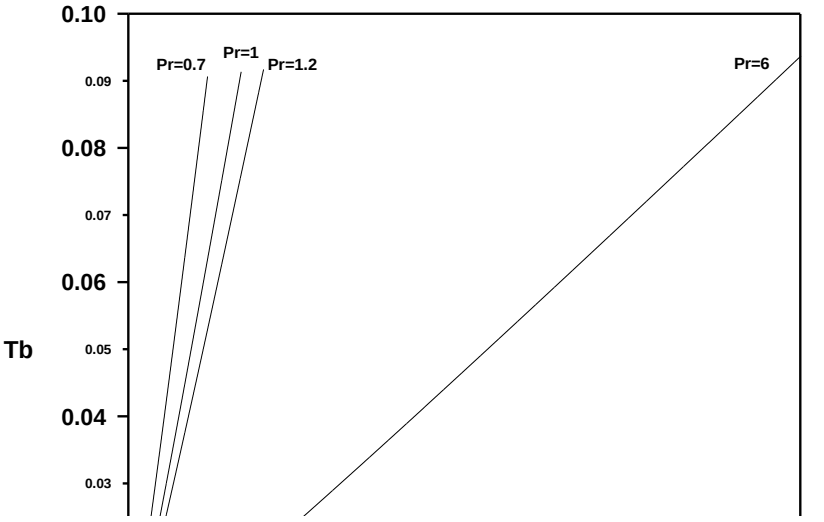

Figure (٥-٣٧) Bulk temperature in a parallel plate channel for constant heat flux, Re=٥٠٠, different Prandtl number

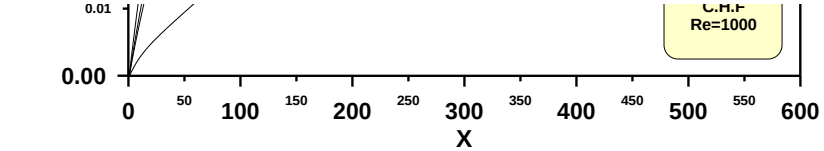

Figure (٥-٣٨) Bulk temperature in a parallel plate channel for constant heat flux, Re=١٠٠٠, different Prandtl number

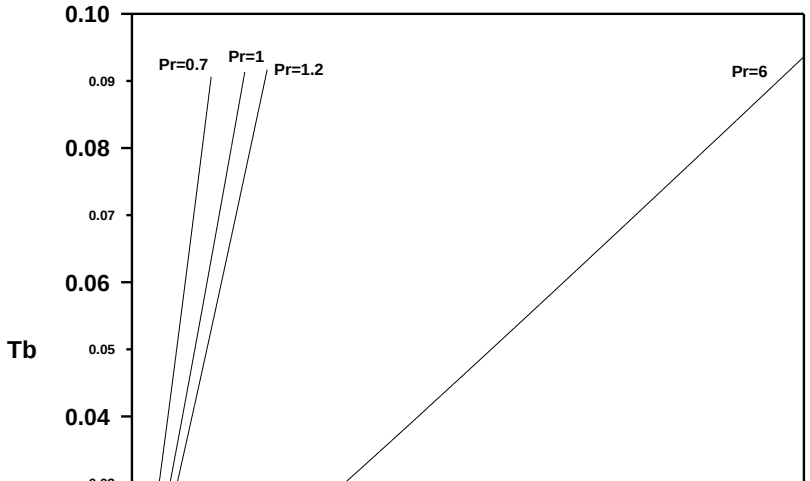

Figure (٥-٣٩) Bulk temperature in a parallel plate channel for constant heat flux, Re=١٥٠٠, different Prandtl number

Figure (٥-٤٠) Bulk temperature in a parallel plate channel for constant heat flux, Re=٢٠٠٠, different Prandtl number

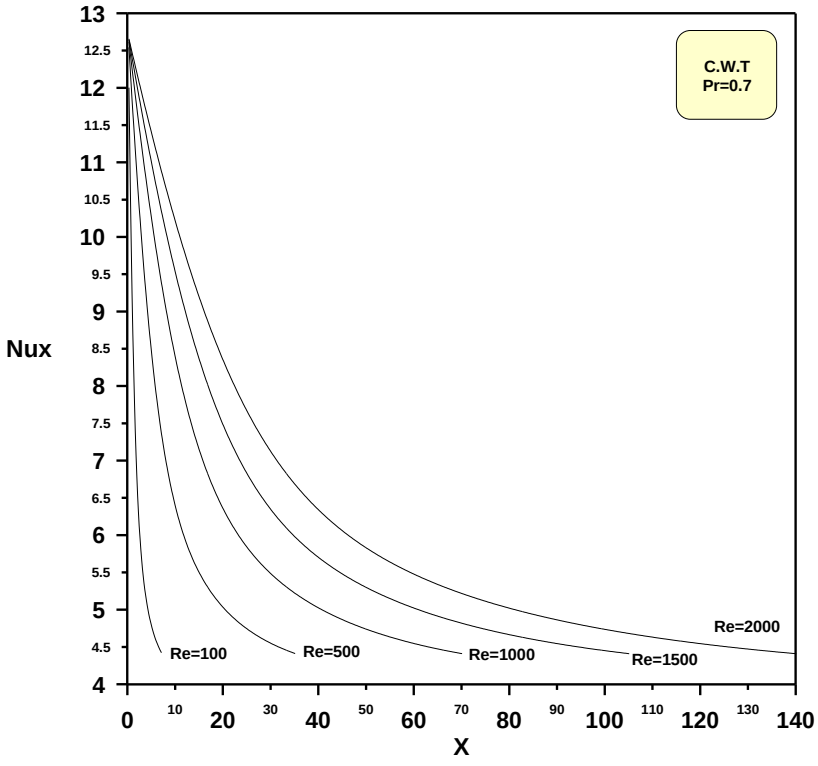

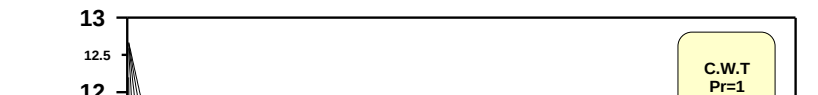

Figure (٥-٤١) Local Nusselt number in a parallel plate channel for constant wall temperature, Pr=٠.٧, different Reynolds number

Figure (٥-٤٢) Local Nusselt number in a parallel plate channel for constant wall temperature, Pr=١, different Reynolds number

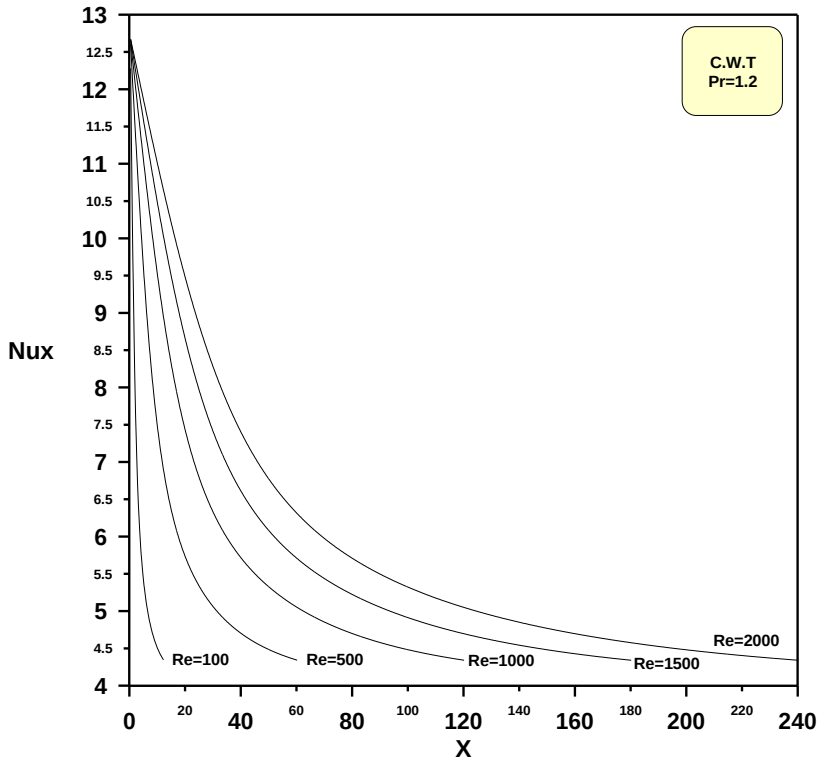

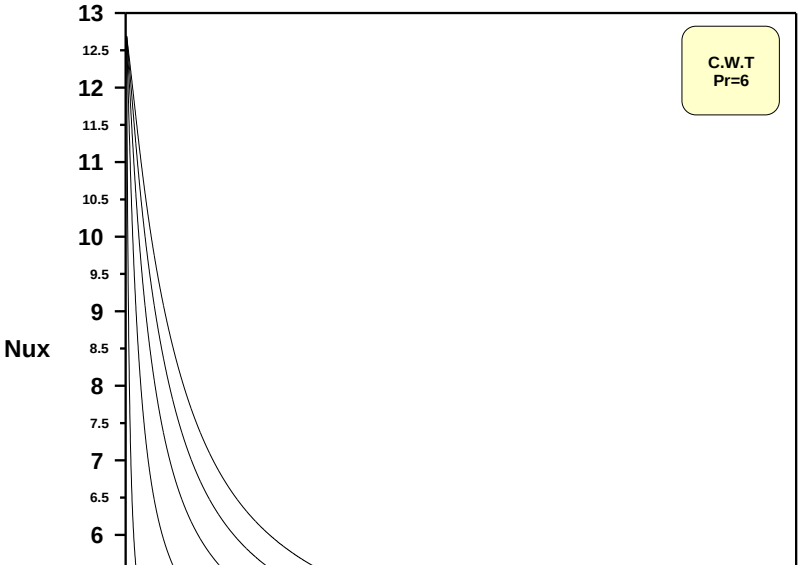

Figure (٥-٤٣) Local Nusselt number in a parallel plate channel for constant wall temperature, Pr=١.٢, different Reynolds number

Figure (٥-٤٤) Local Nusselt number in a parallel plate channel for constant wall temperature, Pr=٦, different Reynolds number

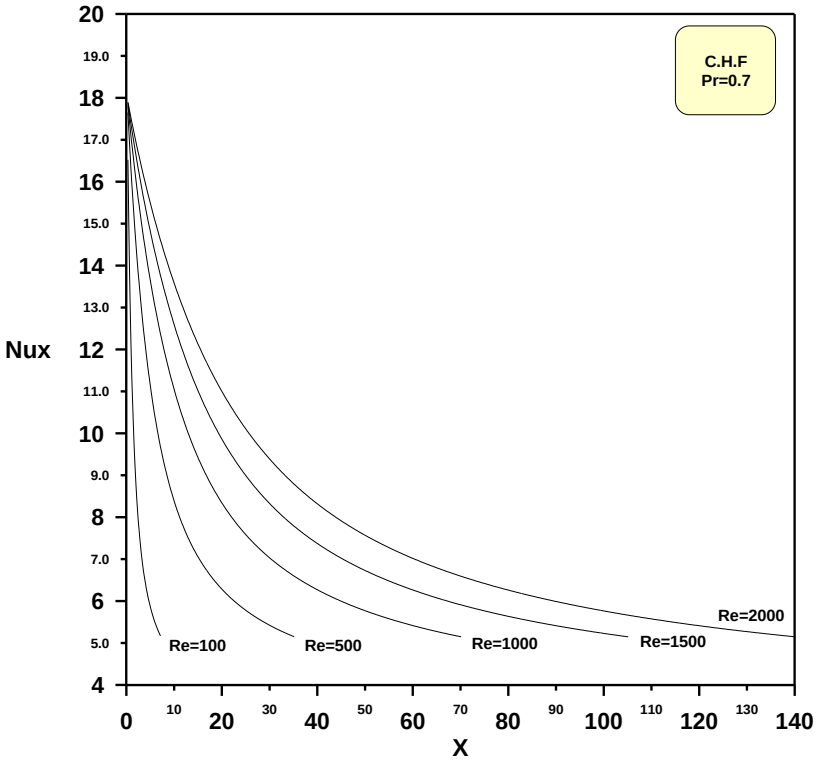

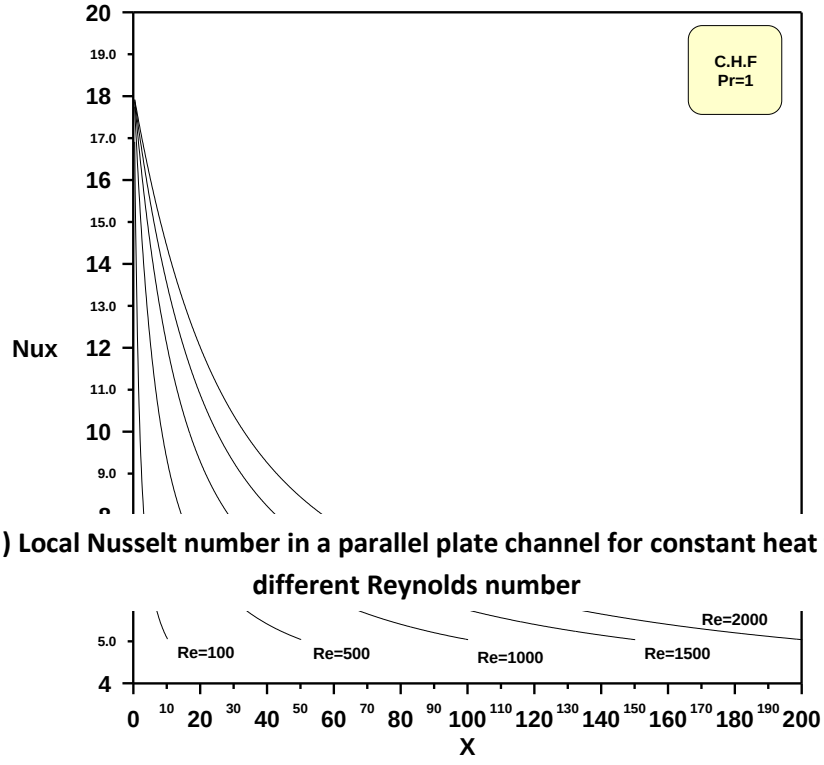

Figure (٥-٤٥) Local Nusselt number in a parallel plate channel for constant heat flux, Pr=٠.٧, different Reynolds number

Figure (٥-٤٦) Local Nusselt number in a parallel plate channel for constant heat flux, Pr=١, different Reynolds number

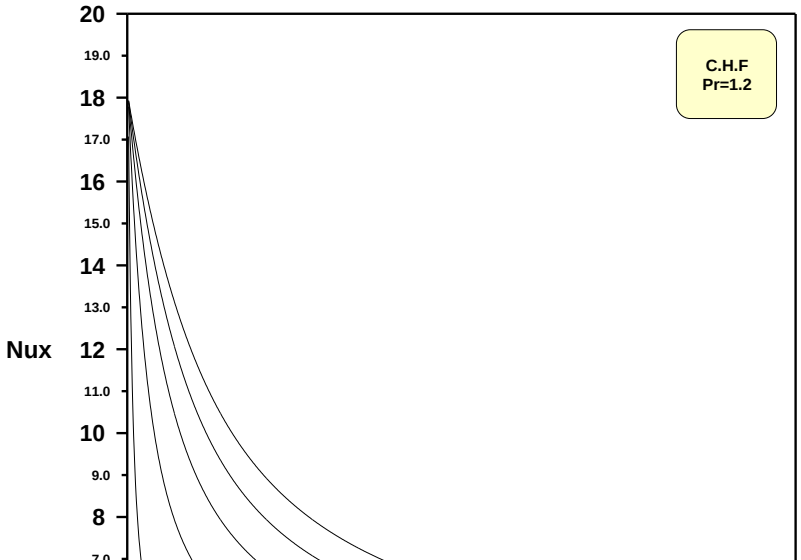

Figure (٥-٤٧) Local Nusselt number in a parallel plate channel for constant heat flux, Pr=١.٢, different Reynolds number

Figure (٥-٤٨) Local Nusselt number in a parallel plate channel for constant heat flux, Pr=٦, different Reynolds number

Chapter Six

CONCLUSIONS AND RECOMMENDATIONS

٦.١ CONCLUSIONS

From the results of the numerical solution of the present work for parallel plate channel with constant wall temperature and constant wall heat flux boundary conditions, the following conclusions are deduced:-

١. The Gaussian elimination method which is to be used, eliminates the need to assume the shape of the velocity and temperature profiles.

Furthermore, this approach provides a picture of the variation of the velocity and temperature within the entire channel.

٢. The maximum velocity at the centerline of the channel, in the fully developed region the vertical velocity component (V) is zero and the gradient of the axial velocity component (∂U/∂X) are everywhere zero, hence, the axial velocity component depends only on (Y). It can be seen that the boundary layer developed faster for the lower Reynolds number. However, the flow field is similar for all studied cases. At fully developed region the shape of velocity profile becomes parabolic over the width of the channel. The velocity profile becomes fully developed at approximately $\frac{L_e}{2a} = 0.05\,\mathrm{Re}$

٣. The maximum dimensionless temperature for constant wall temperature at the centerline of the channel but for constant wall heat flux boundary condition is at the walls. The thermal boundary layer developed faster for lower Reynolds and Prandtl numbers, however, the flow field is similar to the studied cases. The dimensionless temperature distribution becomes fully developed at approximately $\frac{L_{et}}{2a} = 0.05\,\mathrm{Re}.\mathrm{Pr}$

١٠١

.

٤. If (Pr > ١), the hydrodynamic boundary layer develops more rapidly than the thermal boundary layer ($L_e < L_{et}$), while inverse is true (Pr < ١), but if (Pr = ١) the hydrodynamic and thermal boundary layers are the same ($L_e = L_{et}$).

٥. The effect of the fluid flow features on the heat transfer behavior appears clearly in calculating bulk temperature, where the bulk temperature decreases in the developing region for Constant Wall Temperature boundary condition, and the bulk temperature increases

linearly in developing region for Constant Heat Flux boundary condition. The bulk temperature decreases for Constant Wall Temperature and increases for Constant Heat Flux until its slope becomes zero. The zero slope of bulk temperature means that there is no heat transfer ($\Delta T \approx ٠$) because of the reaching of the fluid temperature to a value close to the wall temperature.

٦. The Nusselt number has the maximum value at the start of entrance region (first step) and then decreases gradually until it will be close to thermal fully developed region, because of the high velocities near the walls at the entrance and decreases these velocities with an axial direction. The Nusselt number of constant wall heat flux boundary condition greater is than Nusselt number for constant wall temperature boundary condition case, however, the flow field is similar for all studied cases.

٦.٢ RECOMMENDATIONS FOR FUTURE WORK

١. Performing a laminar flow heat transfer for Newtonian fluids solving the thermal entry length problem for rectangular ducts by using the explicit finite difference method.

٢. Performing an entrance region heat transfer in rhombic ducts for a Newtonian fluid by algebraic coordinate transformation.

٣. Performing an entrance region non-isothermal flow and heat transfer to power-law fluids with rectangular coordinates transformed into new orthogonal coordinates and the finite difference technique for arbitrary cross-section ducts.

٤. Performing a fully developed laminar flow of power-law non-Newtonian fluid in a rectangular duct by the finite element method.

٥. Performing a laminar fluid flow and heat transfer in parallel plate channels with porous walls by using finite difference method.

٦. Performing a laminar forced convection heat transfer in combined entry region of two parallel plates channel solving boundary layer equations in stream function-only formulation.

٧. Performing an experimental study by using the hot wire measure for studying developing laminar flow for rectangular duct.

References

[١]. Incropera, F.P. and Dewitt, D.P., "Fundamentals of Heat and Mass Transfer", John Wiley & Sons, New York, ١٩٩٦.

[٢]. Schmidt, F.W. and Zeldin, B., "Laminar Heat Transfer in the Entrance Region of Ducts", Int. J. Heat Mass Transfer, Vol. ٢٣, No. ١, ١٩٧٠.

[٣]. Emery, A.F and Gessner, F.B., "The Numerical Prediction of Turbulent Flow and Heat transfer in The Entrance Region of a parallel plate Duct", ASME Journal of Heat Transfer, Vol. ٩٨, No. ٤, pp.٥٩٤-٦٠٠, ١٩٧٦.

[٤]. Babus'haq, R.F., "Heat transfer by forced convection in the entrance region of pipes", M.Sc. thesis, Mechanical Engineering Department University of Technology, ١٩٧٨.

[٥]. Emery, A.F., Neighbors, B.K., and Gessner, F.B., "The Numerical Prediction of Developing Turbulent Flow and Heat transfer in a Square Duct", ASME Journal of Heat Transfer, Vol. ١٠٢, pp.٥١-٥٧, ١٩٨٠.

[٦]. Ching, J.C., and Jenq, S.C., "Laminar and Turbulent Heat Transfer in the Pipe Entrance Region for Liquid Metals", Int. J. Heat Mass Transfer, Vol. ٢٤, pp.١١٧٩-١١٨٩, ١٩٨١.

[٧]. Emery, A.F, and Gessner, F.B., "The Numerical Prediction of Developing Turbulent Flow in Rectangular Ducts", ASME Journal of Fluid Engineering, Vol. ١٠٣, pp. ٤٤٥-٤٥٥, ١٩٨١.

[٨]. Lawal, A., "Mixed Convection Heat Transfer to Power Law Fluids in Arbitrary Cross-Sectional Ducts", J. Heat Transfer, Vol. ١١١, pp. ٣٩٩-٤٠٦, ١٩٨٩.

[٩]. Al-Ali, H.H. and Selim, M.S., "Momentum and Heat Transfer in the Entrance Region of a parallel plate channel: Developing Laminar Flow with constant wall temperature", Int. J. Heat Mass Transfer, Vol. ٥١, No. ٤, ١٩٩٢.

[١٠]. Szilagyi, B. and Susan-Resiga, R "Lattice Boltzmann Approach to Viscous Flows Between Parallel Plates", victor Sofonea Research Center for Hydrodynamics, Cavitation and Magnetic Fluids Technical University of Timisoara (Bd. Mihai Viteazul ١, RO-١٩٠٠ Timisoara, Romania),١٩٩٥.

[١١]. Lakovic, S., Stefanovic, V., Ilic, G., and Stojiljkovic, M., "Convective Heat and Mass Transfer under the Conditions of Hydrodynamic Stabilization of the Flow", Int. J. The Scientific Journal FACTA UNIVERSITATIS, Vol. ١, No. ٤, pp. ٣٩٧-٤٠٧, ١٩٩٧.

[١٢]. Inaoka, K., Yamamoto, J., and Suzki, K., "Heat Transfer Characteristics of a Flat Plate Laminar Boundary Layer Disturbed by a Square Rod", ١٩٩٧, E-mail: inaoka@htrans.mech.kyoto-u.ae.IP, .

[١٣]. Silva, E.F., Guerrero, J.S., and Cotta, R.M., "Integral transform solution of boundary layer equations in stream function-only formulation", Int. J. of NON-LINEAR MECHANICS, Vol. ٣٤, pp. ٥١-٦١, ١٩٩٩.

[١٤]. Benhamou, B., Galanis, N., and Laneville, A., "Transient effects of orthogonal pipe oscillations on laminar developing incompressible flow", Int. J. Heat and Mass Transfer, Vol. ٣٤, Issue ٧, pp. ٥٦١-٥٨٤, ٢٠٠٠.

[١٥]. Barber, R.W. and Emerson, D.R., "A numerical study of low Reynolds number slip flow in the hydrodynamic development region of circular and parallel plate ducts", ٢٠٠٠, E-mail: r.w.barber@dl.ac.uk, Web page: http://www.cse.clrc.ac.uk/Group/CSECEG.

[١٦]. Shariff, M.M. and Greywall, M.S., "Streamwise computation of parabolized axisymmetric laminar flows with heat transfer", ASME ٢٠٠٠ Fluids Engineering Division Summer Meeting, Boston, Massachusetts, June ١١-١٥, ٢٠٠٠.

[١٧]. Zhang, L.Z. and Niu, J.L., "A numerical study of laminar forced convection in sinusoidal ducts with arc lower boundaries under uniform wall temperature", Int. J. Heat and Mass Transfer, Vol. ٤٠, No. ١, pp. ٥٥-٧٢, ٢٠٠١.

[١٨]. Barber, R.W. and Emerson, D.R., "A numerical investigation of low Reynolds number gaseous slip flow at the entrance of circular and parallel plate micro-channels", ٢٠٠١, E-mail: r.w.barber@dl.ac.uk,

Web page: http://www.cse.clrc.ac.uk/Group/CSECEG.

[١٩]. Adachi, T. and Uehara, H., "Correlation between heat transfer and pressure drop in channels with periodically grooved parts", Int. J. Heat and Mass Transfer, Vol. ٤٤, pp. ٤٣٣٣-٤٣٤٣, ٢٠٠١.

[٢٠]. Patnaik, B.S., Gowda, Y.T., Ravisankar, M.S., Narayana, P.A., and Seetharamu, K.N., "Finite element simulation of internal flows with heat transfer using a velocity correction approach", ٢٠٠١, E-mail: {bsv_patnaik,knseetharamu}@hotmail.com.

[٢١]. Mahulikar, S.P. and Tso, C.P., "A new classification for thermal development of fluid flow in a circular tube under laminar forced convection", ISSN: ١٣٦٤-٥٠٢١(paper) ١٤٧١-٢٩٤٦ (online), Vol. ٤٥٨, No. ٢٠١٩, pp. ٦٦٩-٦٨٢, ٢٠٠٢, E-mail: mcptso@ntu.edu.sg.

[٢٢]. Uzun, I., "Heat Transfer to a Power-Law Fluid in Arbitrary Cross-Sectional Ducts", Turkish J. Eng. Env. Sci., Vol. ٢٦, pp. ٧-١٤, ٢٠٠٢.

[٢٣]. Barber, R.W. and Emerson, D.R., "The influence of Knudsen number on the hydrodynamic development length within parallel plate micro-channels", ٢٠٠٢, E-mail: r.w.barber@dl.ac.uk, Web page: http://www.cse.clrc.ac.uk/Group/CSECEG.

[٢٤]. Sahin, A.Z. and Ben-Mansour, R., "Entropy generation in laminar fluid flow through a circular pipe", Int. J. Entropy, Vol. ٥, pp. ٤٠٤-٤١٦, ٢٠٠٣, E-mail: azsahin@kfupm.edu.sa.

[٢٥]. Erbay, L.B., Ercan, M.S., Sulus, B., and Yalcin, M.M., "Entropy generation during fluid flow between two parallel plates with moving bottom plate", Int. J. Entropy, Vol. ٥, pp. ٥٠٦-٥١٨, ٢٠٠٣, E-mail: mercan@ford.com.tr.

[٢٦]. Oyumi, S.M., "Laminar fluid flow and heat transfer in channels", University of California, Department of Nuclear Engineering, Berkeley, CA ٩٤٧٢٠, ٢٠٠٤.

[٢٧]. Muzychka, Y.S. and Yovanovich, M.M., "Laminar Forced Convection Heat Transfer in the Combined Entry Region of Non-Circular Ducts", ASME Journal of Heat Transfer, Vol. ١٢٦, pp. ٥٤-٦١, ٢٠٠٤.

[٢٨]. Hooman, K., Ranjbar-Kani, A.A., and Hooman, F., "Forced Convection Through a Hyperporous Duct with Internal Heating/ Cooling Effects", Mechanical Engineering Department, Engineering Faculty, Persian Gulf University, Bushehr, Iran, ٢٠٠٤.

[٢٩]. Haddad, O., Abuzaid, M., and Al-Nimr, M., "Entropy Generation Due to Laminar Incompressible Forced Convection Flow Through Parallel-Plates Microchannel", Int. J. Entropy, Vol. ٥, pp. ٤١٣-٤٢٦, ٢٠٠٤, E-mail: haddad@just.edu.jo(O.M.HADDAD).

[٣٠]. Demartini, L.C., Vielmo, H.A., and Moller, S.V., "Numeric and Experimental Analysis of the Turbulent flow through a Channel with Baffle Plates", ٢٠٠٤, E-mail: vielmoh@mecanica.ufrgs.br.

[٣١]. Ibrahim, A.N., "Developing Turbulent Flow and Heat Transfer through Rectangular and Circular Duct Cross Section", M.Sc. thesis, Mechanical Engineering Department, University of Babylon, ٢٠٠٥.

[٣٢]. Hornbeck, R.W., "Numerical Marching Techniques for Fluid Flows with Heat Transfer", National Aeronautics and Space Administration, Washington, ١٩٧٣.

[٣٣]. Adams, J.A. and Rogers D.F., "Computer-Aided Heat Transfer Analysis", McGraw-Hill Book Company, New York, ١٩٧٣.

[٣٤]. Schlichting, H., "Boundary-Layer Theory", McGraw-Hill Book Company, New York, ١٩٦٨.

[٣٥]. Anderson, D.A., Tannehill, J.C., and Pletcher, R.H., "Computational Fluid Mechanics and Heat Transfer", McGraw-Hill Book Company, New York, ١٩٨٤.

[٣٦]. Holman, J.P., "Heat Transfer", McGraw-Hill Book Company, New York, ١٩٩٩.

Table (٢-١) summary of the Literature Survey

Steady or Unsteady	Type of Flow	Geometrical Shape	Notes
Steady	Laminar	Tube and Parallel Plate Channel	The velocity profile is fully developed.
Steady	Turbulent	Parallel Plate Channel	Three dimensional.
Unsteady	Turbulent	Circular Pipe	Experimental work.
steady	Turbulent	Square Duct	Flow under Constant Wall Temperature & Constant Heat Flux boundary condition.
Steady	Laminar & Turbulent	Circular Pipe	The flow is liquid metals.
Steady	Turbulent	Rectangular Duct	Comparisons between experimental data and numerical predictions.
Steady	Laminar	Rectangular Duct	Studied entrance region non-isothermal flow and heat transfer to power-law fluids.
Steady	Laminar	Parallel Plate Channel	Uniform surface temperature. Used a new integral method.
Steady	Laminar	Parallel Plate Channel	Used the Lattice Boltzmann Method.

Laminar	Parallel Plate Channel	The similarity method between this problem and corresponding potential flow is applied.	**Schmidt** and **Zeldin** [٢]
Laminar	Flat plate disturbed by a square rod	Used the Karman-like vortex.	**Emery** and **Gessner** [٣]
Laminar	Parallel Plate Channel	Incompressible flow, used integral transform method.	**Babus'haq** [٤]
Laminar	Straight horizontal pipe	Newtonian incompressible flow.	**Emery**, **Neighbors,** and **Gessner** [٥]
Laminar	Circular and Parallel Plate Ducts	Used **THOR-٢D**- a two- dimensional finite-volume Navier-Stokes solver developed by the Computational Engineering Group at **CLRC** Dares bury Laboratory.	**Ching** and **Jenq** [٦]
Laminar	Circular Pipe	Hydrodynamically fully developed flow condition.	**Emery** and **Gessner** [٧]
Laminar	Irregular Cross-Sectional Shapes	Hydrodynamically fully developed, thermally developing flow under uniform temperature conditions.	**Lawal** [٨]
Laminar	Circular and Parallel Plate micro-channels	Examines the role of the Reynolds number on the hydrodynamic development length	**Al-Ali** and **Selim [٩]**
			Szilagyi and **Susan-Resiga** [١٠]

The Reference

Parallel Plate Channel	Fully developed flow and temperature.	**Lakovic, Stefanovic, Ilic,** and **Stojiljkovic** [١١]	Steady
Circular, Square, and Elliptic	Solving full Navier-Stokes equations.	**Inaoka, Yamamoto,** and **Suzuki** [١٢]	Unsteady
Circular Tube	Used four different conditions.	**Silva, Guerrero,** and **Cotta** [١٣]	Steady
Triangular, Square, Sinusoidal ducts	Non-Newtonian fluid in the thermal entrance region under Constant Wall Temperature boundary condition	**Benhamou, Galanis,** and **Laneville** [١٤]	Steady
Parallel Plate micro-channels	Using continuum flow theory.	**Barber** and **Emerson** [١٥]	Steady
Circular Pipe	Uniform wall heat flux.	**Shariff** and **Greywall** [١٦]	Steady
Two Parallel Plate Channel	The fluid is incompressible and Newtonian and the flow is the hydrodynamically and thermally developing	**Zhang** and **Niu** [١٧]	Unsteady
Two Parallel Plate Channel	Solve the continuity, momentum and energy equations simultaneously by used	**Barber** and **Emerson** [١٨]	Steady

Hydrodynamically fully developed, thermally developing flow under isothermal and isoflux boundary conditions.	**Adachi** and **Uehara** [١٩]	Steady	Laminar
flow in a porous saturated channel bounded by two isothermal parallel plates. fully developed velocity distribution.	**Patnaik, Gowda, Ravisankar,**	Steady	Laminar &
	Mahulikar and **Tso** [٢١]	Steady	Laminar
Used non-dimensional techniques.	**Uzun** [٢٢]	Steady	Laminar
The numeric and experimental analysis. Used Finite Volumes Method, in two dimensions.	**Barber** and **Emerson** [٢٣]	Steady	Laminar
Two cases of thermal boundary conditions were studied Constant Wall Temperature and C.H.F. Two values of Reynolds number (Re = ٦٠,٠٠٠ & Re = ١٢٠,٠٠٠).	**Sahin** and **Ben-Mansour** [٢٤]	Unsteady	Laminar
	Erbay, Ercan, Sulus, and **Yalcin** [٢٥]	Steady	Laminar
	Oyumi, S.M. [٢٦]	Unsteady	Laminar

Muzychka and **Yovanovich** [٢٧]	Steady	Laminar	Non-Circular Ducts
Hooman K., Ranjbar-Kani, and **Hooman F.** [٢٨]	Steady	Laminar	Two Parallel Plate Channel
Haddad, Abuzaid, and **Al-Nimr** [٢٩]	Steady	Laminar	Parallel Plate microchannel
Demartini, Vielmo, and **Moller** [٣٠]	Steady	Turbulent	Rectangular Duct
Ibrahim, A.N. [٣١]	Steady	Turbulent	Circular and Rectangular Ducts